CZECH TECHNICAL UNIVERSITY IN PRAGUE

Faculty of Civil Engineering

K134 -- Department of Steel and Timber Structures

Design of composite steel and fibre-concrete columns at elevated temperature

DOCTORAL THESIS

MSc. ILLIA TKALENKO

Doctoral study programme: (P3604) Civil Engineering

Branch of study: (3607V009) Building and Structural Engineering

Doctoral thesis tutor: prof F. Wald

Prague, 2022

CZECH TECHNICAL UNIVERSITY IN PRAGUE
Faculty of Civil Engineering
Thákurova 7, 166 29 Praha 6

DECLARATION

Ph.D. student's name: MSc. Tkalenko Illia

Title of the doctoral thesis: Design of composite steel and fibre-concrete columns at elevated temperature

I hereby declare that this doctoral thesis is my own work and effort written under the guidance of the tutor prof. Ing. František Wald, CSc.
All sources and other materials used have been quoted in the list of references.

The doctoral thesis was written in connection with research on the project: GA15-19073S - "Models of steel and fibre concrete composite columns exposed to fire".

In Prague on 20.06.2022

signature

Acknowledgement

Throughout the writing of this thesis I have received a great deal of support and assistance.

I would first like to thank my supervisor, prof František Wald for his methodological and technical support, deep participation in solving emerging organizational and technical problems and invaluable support in the writing of this work.

Thanks also go to the Department of Steel and Timber Structures members for their advices and friendly environment during the study. In particular, I would like to thank Ing. Zdeněk Sokol, Ing. Jan Tomek, Ing. Abhishek Ghimire for help in the laboratory and Ing. Lukáš Blesák for methodological support in the processing of numerical models.

In addition, I would like to thank the staff of the Department of Concrete and Masonry Structures, whose expertise was very helpful.

I would like to thank doc. Jiří Litoš and staff of these workplaces of the Experimental Centre of the Faculty of Civil Engineering CTU in Prague for performing of the experimental tests.

Especially, I would also like to thank my colleague Ing. Alexey Tretyakov for his valuable help in laboratory tests and support during numerical modelling.

Finally, I would like to thank the GAČR and CTU for financial support through the grants GAČR 15-19073S “Models of steel and fibre concrete composite columns exposed to fire”, SGS15/137/OHK1/2T/11, SGS17/127/OHK1/2T/11, SGS16/049/OHK1/1T/11 and SGS19/150/OHK1/3T/11.

https://doi.org/10.14311/dis.fsv.2022.008

Abstrakt

Práce se věnuje experimentálnímu a numerickému modelování a návrhu teplotního a mechanického chování sloupů kruhového dutého průřezu s betonovou výplní vyztuženou ocelovými vlákny vystavených požáru. Jsou shrnuta data z experimentálních studií, je validován numerický model, připravena numerické simulace problematiky pro tvorbu podkladu přílohy evropské normy pro navrhování spřažených ocelobetonových konstrukcí vystavených požáru prEN1994-1-2:202x. Experimentální studie zahrnuje šest vzorků sloupů namáhaných v tlaku při ohřevu na zvýšenou teplotu. Numerický model metodou konečných prvků v softwaru ATENA z objemových prvků byl validován na vlastních experimentech a experimentech z literatury. Cílem numerické simulace je připravit analytický model požární odolnosti centricky a excentricky zatíženého sloupu kruhového dutého průřezu s výplní z drátkobetonu a prostého betonu při vystavení požáru. Analytický návrhový model pro stanovení požární odolnosti spřažených ocelobetonových sloupů s drátkobetonem je připraven jako příloha nebo doplňující technický dokument k připravované evropské normě prEN1994-1-2:202x.

Klíčová slova: ocelobetonový dutý průřez, kruhový dutý průřez, drátkobeton, vláknobeton, mechanické chování, požární odolnost, metoda konečných prvků, analytický model, excentricita.

Abstract

This research is dedicated to the preparation of an analytical model of the mechanical behaviour of circular hollow section columns with steel fibre-reinforced concrete infill in a fire situation based on experimental study and numerical modelling. The work includes data from experimental studies, validation of the numerical model, sensitivity study by numerical simulation and development of an analytical model based on a European standard for the design of reinforced concrete elements in fire EN1994-1-2: 202x. Experimental studies include six full scale column specimens in compression during the heating in steady-state regime. Validation of the three-dimensional numerical finite element method model using ATENA software made based on experimental data. A parametric study aimed to compare fire resistance of centrally and eccentrically loaded circular hollow section columns with steel fibre-reinforced and plain concrete infill in the fire situation. Developed analytical model for determining the design buckling load in the fire situation of the composite steel and fibre-reinforced concrete columns is ready for an Annex or a Supplementary technical document in the corresponding method in prEN1994-1-2:202x.

Keywords: concrete-filled steel tubes, circular hollow section, steel fibre-reinforced concrete, fire resistance, finite element method, parametric studies, analytical model, eccentricity.

LIST OF CONTENT

NOTATION

Letters

A	cross-sectional area of the part
A_m/V	section factor
$N_{fi,cr}$	elastic critical load in the fire situation
$N_{fi,Rd}$	design axial buckling load in the fire situation
$N_{fi,Rd,\delta}$	design axial buckling load in the fire situation in case of eccentric load
N_{Rd}	design axial buckling load at room temperature
$N_{Rd,\delta}$	design axial buckling load at room temperature in case of eccentric load
f_{SFRC}	direct tension strength of SFRC
$W_{d,SFRC}$	critical compressive displacement of SFRC
$W_{d,PC}$	critical compressive displacement of plain concrete
G_f	fracture energy
$(EI)_{fi,eff}$	initial elastic modulus of concrete
$E_{i,\theta}$	modulus of elasticity of the i material at the temperature θ
d_f	diameter of fibre
$f_{c,\theta}$	compressive strength of concrete at elevated temperature
f_c	compressive strength of concrete at room temperature
$f_{y,\theta}$	yield strength of steel at elevated temperature
f_y	yield strength of steel
$k_{i,\theta}$	reduction factor for a material property at elevated temperature
l_θ	buckling length in fire situation
N	applied force
R	standard fire resistance time (min)
t	steel tube thickness
D	diameter of steel tube
e	load eccentricity
K	Initial stiffness of interface
L	length of column
θ	temperature
ε	strain
σ	stress
$\varphi_{i,\theta}^{f}$	flexural stiffness reduction coefficient for steel fibre-reinforced concrete

$\varphi_{i,\theta}$	flexural stiffness reduction coefficient for plain concrete
α_f	reduction coefficient for eccentricity for steel fibre-reinforced concrete
α	reduction coefficient for eccentricity for plain concrete
χ	resistance reduction factor according to the European buckling curves
$\overline{\lambda}$	relative slenderness at room temperature
$\overline{\lambda_\theta}$	relative slenderness in the fire situation
μ	load for centrically loaded columns
ρ_f	percent of the fibro in the concrete

Abbreviations

CFST	Concrete filled steel tube
FRC	Fibre-reinforced concrete
SFRC	Steel fibre-reinforced concrete
CHS	Circular hollow section
FEM	Finite element method
NRCC	National Research Council of Canada
FEA	Finite element analyses
ATENA	Advanced Tool for Engineering Nonlinear Analysis
FRR	fire resistance
NSSFRC	normal strength steel fibre-reinforced concrete
HSSFRC	high strength concrete steel fibre-reinforced concrete
CIDECT	Comité International pour le Développement et l'Etude de la Construction Tubulaire
SDEM	simplified diverse embedment model
PC	Plain concrete
CTICM	Centre Technique Industriel de la Construction Métallique
PFRC	Polymeric Fibre Reinforced Concrete
SCC	Self-consolidating concrete
HFRC	Hybrid fibre reinforced concrete

CHAPTER 1. INTRODUCTION

1.1. OVERVIEW

The modern development of the construction industry requires the use of high-strength, high-performance materials and their composites. Concrete filled steel tube (CFST) members, are widely used in the Czech Republic, EU, China and worldwide. CFST members provide better properties for the members in many aspects and combine the main advantages of concrete, and steel [1]. The advantages of CFST columns are numerous, including attractive appearance, structural efficiency, reduced column footing, fast construction, and high fire resistance without external fire protection [2]. These attractions have enabled CFST members to be used in all types of construction (examples see Figure 1-1).

a) b)

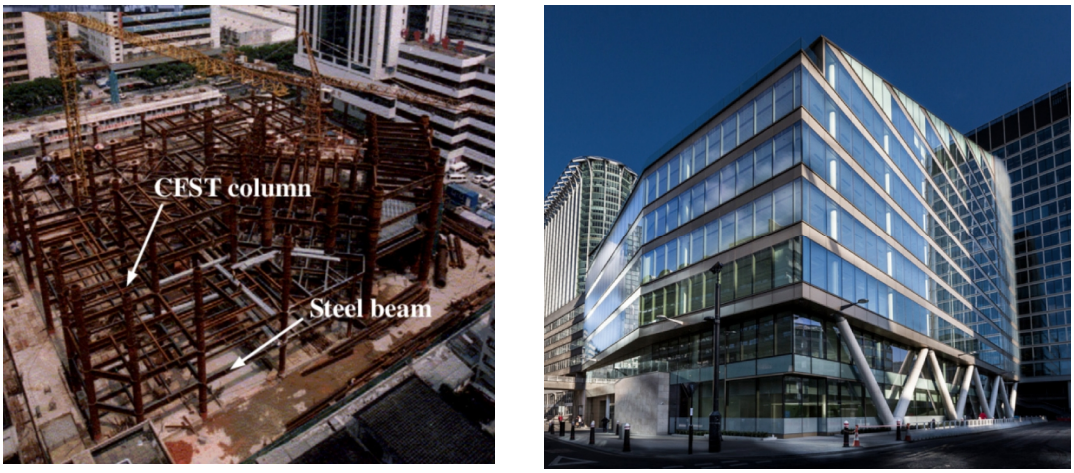

c)

Figure 1-1 a) SEG plaza in Shenzhen, China [3] b) Moorgate Exchange 12-story office building, London, Great Britain [4] c) Yajisha Bridge (360m), China, [5].

Next to concrete-filled steel tubular (CFST) members usage is very likely in building structures. It is crucial to ensure their corresponding fire resistance. Many research investigations have been conducted to study the behaviour of CFST columns in fire situations [6]. It has been proved that the fire performance of CFST columns is better than that of solely steel profiles. Many studies have been directed towards improving the behaviour of CFST columns using different approaches. One of the most important parameters of the design is how long the column will carry the service load during the fire - the column's fire resistance. Different passive methods to increase the fire resistance of CFST columns can be used: outside protection of the steel section, modification of the concrete core, etc. The way to protect the steel section with boards or film is expensive and could change the architectural concept look of the structure. Therefore a more efficient method to increase fire resistance is to add extra steel elements to reinforce the concrete core. Usage of steel-reinforced or fibre-reinforced concrete (example in Figure 1-2) is one of these solutions.

Figure 1-2 Concrete core with steel fibre reinforcement

It is widely known that adding steel fibres to a mixture increases ductility, compressive and tensile strengths of concrete at ambient temperature. Numerous researches were dedicated to studying of the behaviour of steel fibre-reinforced concrete (SFRC) at elevated temperatures and it was found that even a small percentage of fibres in a mixture brings notable changes in the mechanical properties of concrete after exposing it to elevated temperatures [7]. An experimental study on self-consolidating concrete showed that steel fibres improve tensile strength and elastic modulus of concrete at elevated temperatures and, at the same time, do not have much influence on compressive strength or thermal conductivity [8]. These were proven in experimental studies made by Bošnjak et al. [9], Kodur et al. [10] and Pliya et al. [11] for plain FRC and HFRC mixtures with 26 – 85 MPa compressive strength range. The SFRC core at elevated temperatures seems to be more beneficial than plain concrete.

There is a range of numerical models of behaviour of CFST columns in fire. Developed in CVUT [114] numerical model taking into account thermal and mechanical (tension) behaviour of SFRC and was validated on experiments made in CVUT and available in the literature. This model was used in this work for further development.

PrEN1994-1-2:202x method proposed a new analytical model (based on experiments and parametrical study) for the design of CFST steel bars reinforced column at elevated temperature [12]. However, the SFRC infill was not covered. Evaluation of behaviour of composite steel and fibre-concrete columns at elevated temperature requires the development of an analytical method for designers, which is subject to a series of numerical experiments on validated models.

Developed in this work analytical model for determining the fire resistance of the composite steel and fibre-reinforced concrete columns under ISO standard fire conditions can be used as an appendix or supplementary technical basis in the corresponding prEN1994-1-2:202x method.

CHAPTER 2. STATE OF THE ART

This chapter is devoted to the current state of the theoretical investigation and analysis of experimental data obtained by different scientists in the field of structural and fire resistance of steel tubes filled by different types of concrete including concrete filled with steel fiber (SFRC). Owing to importance in better comprehension of the CSFT resistance mechanism, mechanical and thermal properties and constitutive models of its components – SFRC and steel were reviewed and appropriate conclusions for the predesigned investigations in frames of the thesis were drawn.

2.1. GENERAL

The widespread occurrence of CFST structural members, especially in high-rise buildings construction, caused numerous investigations of CFST members' behaviour which have been performed last three decades. Particular place in the total volume of CFST behaviour studies takes place the intensive investigations of CFST fire resistance which are characterized by high levels of complexity of testing equipment, methodology of experimental research and ways of experimental outcomes interpretation. Sometimes the experimental results obtained in a certain test series contradict another one even carried out using the same methodology and equipment.

Despite the presence of mentioned above complexities in the studies of CFST structures, particularly their fire resistance, there is conventional set of problems in fire resistance assessment incorporated by their peculiar objects and characterized by principally similar ways of the solutions. The first group of the problems is referred to the resolution of heat-and-mass transfer problem and its application to the sections of CFST members. As a rule, determination of temperature distribution over the section in a short duration of heating (according to terminology accepted in SP 27.13330.2011) is a previous step to the assessment of the fire resistance. The time-dependent pattern of temperature field can be obtained by using numerical approaches (finite difference method) of solution of nonlinear differential equations of heat transfer with appropriate boundary conditions Lie [13], Tan [14], Wang [15], Chikhladze [16] or by utilizing powerful toolsets of finite element analysis Ding [17]. Mandatory attributes of advanced software based on FE approach, such as ANSYS, ABAQUS, DYNA, ATENA are the modules with the ability to calculate the parameters

of the temperature field over the section. An outstanding role in the area of temperature field modeling belongs to the publications from Lie and co-workers [13] [18] 19], who derived equations for the temperature of the concrete core and steel shell using work from Dusinberre [20] on heat transfer calculations by finite differences.

Problems with constitutive modeling of material – concrete and steel – at normal and elevated temperatures are included in the second group of the considered in the thesis research tasks. There are various proposals for the prediction of concrete behaviour which are available in the literature. A comprehensive review of the state-of-the-art in this area was performed by Li [21] who developed a new model in the frames of this paper, comparing their findings with the derivations from Anderberg [22] and Schneider [23]. Also, Youssef [24] reviewed the developed constitutive laws for concrete and reinforcement still, and proposed models that captured the changes that occur in the mechanical properties of concrete due to confinement effects and high temperatures. They also take into consideration transient creep, using a simplified but sufficiently accurate method. However, as mentioned above, reviews and investigations defining the general trend of concrete behaviour at elevated temperatures did not consider general cases of volumetric stress-strain for concrete and did not have an application to the concrete with steel fibers. Investigations that had been purposefully oriented on SFRC mechanical properties at the high temperatures were performed insufficiently and constitutive law for the SFRC in the general case of volumetric stress state in the full temperature range has been not developed yet.

The third set of studies is oriented toward large-scale model testing under fire conditions and the development of analytical methods of fire resistance prediction. More than 300 large-scale standard fire tests have been carried out globally on CFST columns of various types. The main contributors to the available test database for concrete-filled SHS are the National Research Council of Canada (NRCC) (Kodur and Lie [25] [26], Kodur et al. [27] and the Comité International pour le Dévelopment et l'Etude de la Construction Tubulaire (CIDECT) [28]. However, most testing and modeling to date have focused on normal strength concrete infill, whereas current practice is to use higher strengths [6].

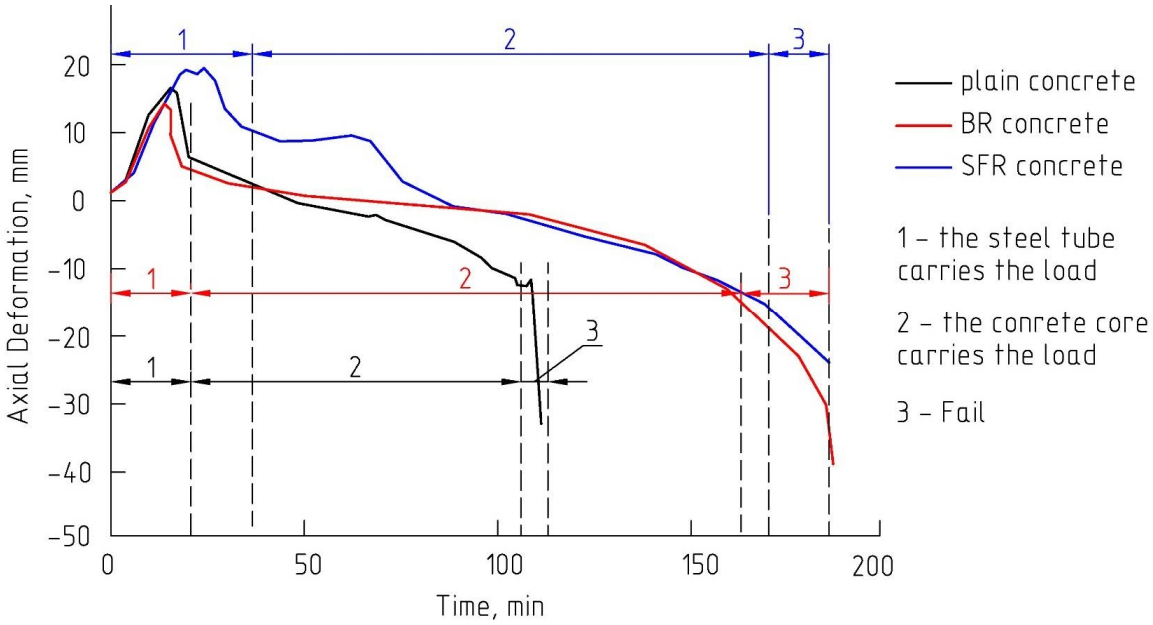

Figure 2-1 Differences in fire behaviour of PC, BRC and SFRC filled composite hollow sections columns

Numerical investigations of the structural members' fire resistance with FE approach - the fourth direction of studies – have gained in importance recently. Certain boom of the works connected with the rapid development of appropriate software is observed in the last decade. Representatives of research schools from Asia – Yu [29], Hui [30], Lu [31], Wang [32] – performed series of CFST resistance simulation including condition of fire. In spite of several difficulties in modelling, results of the simulations in most cases showed satisfactory convergence with test findings.

In the following subsections of the chapter, a detailed revision of the state art on CFST columns subjected to fire is presented. Directions of investigations mentioned above will be considered, and research on SFRC filled steel tubes will be highlighted more explicitly.

2.2. MECHANICAL PROPERTIES OF STEEL AND SFRC AT AMBIENT TEMPERATURE

2.2.1. MECHANICAL PROPERTIES OF STEEL

Steel has perfect strength properties at ambient temperature, nevertheless, like many other materials, steel loses its strength and stiffness with the rise in temperature. The temperature-dependent properties are essential for modelling steel structures' fire response, including thermal, mechanical, and deformation properties. These properties vary with temperature and are also dependent on a number of parameters. To understand and model behaviour of the CFST section in fire, it is

imperative to determine the thermal and mechanical properties of steel at elevated temperature.

A review of the literature indicated that there had been many studies on steel's high-temperature mechanical properties and thermal properties [33]. High temperatures strength properties test could be conducted in mainly two ways: transient and steady-state tests. In transient-state tests, the test specimen is subjected to a constant load and then exposed to uniformly increasing temperature. Temperature and strain are recorded continuously under constant stress. Thermal strain evaluated from a separate test is subtracted from the total measured strain [34].

The transient state tensile test method was used for experimental studies presented by Juri Outinen in his works [35] [36] [34]. Results of tests on structural steels S355, S420, S460, S350GD+Z, S355J2H and austenitic stainless steel EN 1.4031 (AISI 304) were given. It was found that structural steel grades S355, S420 and S460 (App. A, B, H) seemed to follow well the predicted behaviour, and there were not too many differences from the European standard EN1993-1-2 model [37].

Later in the paper by Kodur [33] comparison of the main parameters such as yield strength and elastic modulus were presented. Similar to the comparison of thermal properties, data from different standards, codes and publishers were used. It was found that the use of the EN1993-1-2 [37] high-temperature stress-strain relationship gives a more realistic fire resistance prediction than does the use of ASCE [38] stress-strain relations. This is mainly because the EN1993-1-2 temperature-stress-strain relationship partly takes high-temperature creep into account.

2.2.2. MECHANICAL PROPERTIES OF SFRC AT AMBIENT TEMPERATURE

Today are available many types of fibres and even more types of concrete, so first of all, it is very important to define the range of used steel fibres and concrete. The thesis is pointed on a normal strength SFRC with add of classic hook-ended steel fibres. Therefore state of the art includes only a limited part of researches made in this field.

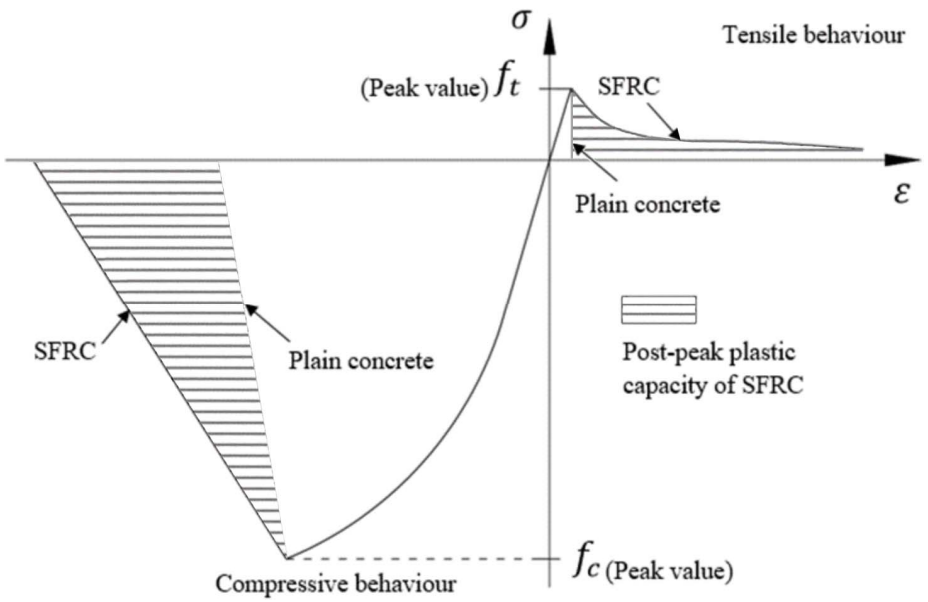

Figure 2-2 Schematic stress strain diagram of SFRC

As mentioned earlier, both tensile and compressive properties of SFRC differ from plain concrete. Adding of steel fibres to the mixture improves peak strength values in compression and tension and provides post-peak plastic capacity for concrete. A schematic stress-strain diagram of SFRC compared to plain concrete is shown in Figure 2-2. From existed experimental studies is apparent that small volume of fibres (<1%) does not improves peak values but significantly effects post-peak behaviour. Consequently, for FEM model development, it is necessary to study the post-peak tensile and compressive behaviour of SFRC. This part of the thesis presents selected experimental studies and analytical models of SFRC at ambient temperature to clarify its plastic behaviour and find analytical methods that could be implemented in the numerical FEM model.

Barros and Figueiras [39] presented the results of their tests performed on specimens and structural elements made of steel fibre-reinforced concrete with a range of 0 to 60 kg/m³ of added fibres. Based on experiments on a cylinder in compression analytical model of compressive behaviour of SFRC concrete was developed. An analytical model was validated on own experiments and experiments of other authors and showed very accurate results. Results of the three-point bending notched beam tests were used to develop the fracture energy concept for the post-peak tensile behaviour of the SFRC.

Xu and Shi [40] proposed correlations between the main mechanical properties of SFRC based on experimental data from existing experimental results in the

literature. Strong correlations between split tensile strength and compressive strength were found.

Tests in compression, tension and four-point bending were made by Abbas et al. [41] to find out the relations between concrete parameters. An extensive experimental study on SFRC concrete specimens with three different geometry of fibres and three values of concrete strength was performed.

Marar et al. [42] made an extensive experimental study intending to define the compressive toughness of normal and high-strength concrete. Concrete with zero and up to 2 % of steel fibres by volume was used. Hooked steel fibres with 60, 75 and 83 length-diameter ratio (30, 60.50 mm and 0.5, 0,8, 0,6 mm respectively) were used. Experiments were done on standard cylinders of 150 x 300 mm size. Significant changes in post-peak compressive behaviour for different fibre volume was observed. Based on the results were proposed equations for compressive toughness prediction.

Ali Amin et al. [43] presented an evaluation of the tensile strength of SFRC as derived from inverse analyses of notched bending tests, where the post-cracking residual tensile strength was defined based on uniaxial tension tests. It was found that the post-cracking behaviour of SFRC can be obtained directly from uniaxial tensile tests or indirectly following an inverse analysis of notched beams in bending.

2.2.3. MECHANICAL PROPERTIES OF SFRC AT ELEVATED TEMPERATURE

It is an experimentally established fact that the addition of steel or polypropylene fibers in concrete improves its ductility and increases both tensile and compressive strength of concrete. Adequate and appropriate understanding of structural degradation of concrete with fibre reinforcement (SFRC) subjected to the simultaneous action of temperature and load is significantly important to create adequate analytical and numerical models of composite columns with steel fibre reinforced concrete operating under fire conditions.

As stated prior, both the tensile and the compressive properties of SFRC vary from plain concrete. of the addition of steel fibres to the mixture improves peak strength values in tension and compression and results in post-peak plastic capacity for concrete. Experimental studies conducted in the past demonstrated that a small volume of fibres (<1%) do not improve peak values. However, the addition of fibres significantly affects post-peak behaviour. Therefore, it is necessary to study the post-peak tensile and compressive behaviour of SFRC for FEM model development. This

part of the thesis puts forth a selection of experimental studies and analytical models of SFRC at ambient temperature to bring clarity to its plastic behaviour and give way to analytical methods that could be implemented in the numerical FEM model.

A set of papers with results of comprehensive research in the field of SFRC behaviour were published over the last two decades. Mahasneh [44] presents a wide range of experimental results on beneficial effect of Polymeric Fiber Reinforced Concrete (PFRC) on compressive strength, tensile strength, and pullout in fire.

Lau and Anson [46] conducted a detailed review of previous investigations on the field of plane concrete (PC) and SFRC behaviour at elevated temperature. Lau and Anson reported about series of tests of SFRC mixtures at temperature ranging between 105°C and 1200°C. The compressive strength, flexural strength, elastic modulus and porosity of concrete reinforced with 1% steel fibre (SFRC) and changes of color to the heated concrete have been investigated. The results showed that steel fibre remains beneficial to concrete that has been exposed to high temperatures up to 1200°C, confirming that at 1%, steel fibre content has no deleterious effect on heated concrete. In fact, the inclusion of steel fibre in the concrete mix leads to an improvement in mechanical properties and a better resistance to heating effects.

Bednar, Wald, Kohoutková and Vodicka [46] showed that SFRC at elevated temperature demonstrates behaviour that is very similar to the resistance of ductile material. Average tensile strength at 20°C to 600°C is similar to the coefficient of strength decrease for cold-formed steel.

Khaliq and Kodur [47], in the series of papers, performed an analysis of a number of tests conducted from 60th to nowadays and presented own experimental results of main SFRC thermal and mechanical properties changing. For thermal properties, specific heat, thermal conductivity, and thermal expansion were measured, whereas for mechanical properties, compressive strength, tensile strength and elastic modulus were measured in the temperature range of 20–800°C. Basically, this research presented the effect of the type of fiber reinforcement (steel fiber, polypropylene fiber, and hybrid - steel + polypropylene fiber) included in the matrix of the self-consolidating concrete (SCC) on their properties under heating up to 800°C. In the paper, we can find curves of the measured thermal conductivity and thermal expansion of SCC and SFRC and their compressive and splitting strength degradation. Data generated from the thermal and mechanical property measurements were utilized to develop thermal and mechanical property

relationships for SCC and SFRC. These properties are expressed in the form of empirical relationships over temperature range of 20–800°C, which could be utilized in fire resistance numerical assessment. In the general conclusions of the pepper, there were mentioned that temperature has a significant influence on thermal conductivity, specific heat and thermal expansion of SCC and SFRC. The thermal conductivity generally decreases with temperature, while the thermal expansion increases with temperature up to 800°C. The addition of steel, polypropylene, and hybrid fibers to SCC does not significantly alter the thermal conductivity throughout 20–800°C temperature range. Despite the increase of ductility and strength of the plain concrete with fiber reinforcement it was established that the addition of steel, polypropylene, and hybrid fibers does not have much effect on high temperature compressive strength of SCC.

Balázs and Lublóy [48] made a series of tests with concrete mixtures containing polymer and steel fibre at temperature from 20°C to 800°C to investigate post-heating compressive strength of SFRC. The test results show that the advantageous effects of polypropylene and steel fibers in concrete subjected to high temperatures are mainly observed for thin fibers and not for thick fibers. Strength reduction and surface cracking are detailed for the various tested fiber-reinforced concretes.

It is necessary to mention the investigation of Kim et al. [49], who studied the factors influencing the mechanical tensile properties of steel-fibre-reinforced concrete exposed to high temperatures. Test specimens reinforced with fibres of two types (twisted or hooked) and three series of fibre contents (volume fractions of 0.25%, 0.5%, or 1%) were tested after exposure to four different maximum temperatures (room temperature, 300°C, 500°C, and 700°C). Test results show that the residual compressive strength, tensile strength and rupture energy of the specimens decreased with their increased heating. After the SFRC was exposed to the high temperatures, the relative loss in tensile strength was higher than that in compressive strength, but the relative loss of rupture energy was comparatively lower. After exposure to high temperature, the behaviour of the samples was more sensitive to the volume fraction and aspect ratio of the fibre than to its type. As a result, the authors proposed a model of prediction of the residual tensile strength of heated SFRC based on the test results. Also, the recent state of influence of elevated temperature on SFRC was clearly presented.

Investigations of SFRC multiaxial behaviour, especially under elevated temperatures, have not yet been conducted. As it was indicated by Rush et al. [50], the lack of experimental data makes it difficult to the creation of adequate numerical models in the assessment of fire resistance and complicates the comprehension of SFRC failure mechanism on the whole. Also, there is no constitutive model of SFRC for the general case of volumetric stresses, including heating cases. The last circumstance disables the development of the generalized model for analyzing behaviour of CFST operated in fire and contemporary researches are forced to concentrate their efforts on particular cases of the studies.

Rush et al. [50] identified that a shortage of experimental data presents a problem for the creation of adequate numerical models in the assessment of fire resistance. A lack of reliable data makes it harder to gain an understanding of the SFRC failure mechanism. Additionally, no constitutive model of SFRC exists for the general case of volumetric stressesor heated cases. The latter point hinders the development of the generalized model for analyzing behaviour of CFST operated in fire, and modern-day investigations are forced to focus on specific cases of the studies.

Experiments in compression and splitting tension on standard 150x150mm cubes at elevated temperatures were carried out by Novak and Kohoutkova [36]. The experiments were done for plain concrete SFRC and hybrid fibre reinforced concrete with polypropylene fibres. 40 kg/m³ of hooked (RC-80/60-BN) steel fibres were added to fibre-reinforced mixtures. Compressive experiments from all aggregates yielded similar results. However, a large difference was observed between experimental results and EN1992-1-2 recommendations for tensile strength reduction factors.

The most recent experimental study on SFRC specimens at elevated temperature was done by Bošnjak et al. [9]. The study includes experiments in compression (cubes), split tension (cylinders), bending (notched beams), and compression for elastic modulus definition (square prisms). A difference between fibre-reinforced and plain concrete in split tensile strength and fracture energy was observed. At least two orders of magnitude higher fracture energy were described in a whole range of temperature. Concurrent, it was concluded that the presence of fibres does not improve elasticity modulus. Tretyakov [114] developed SFRC material model in ATENA Červenka software [51] based on available literature and own full-scale CFST columns in bending at ambient and elevated temperature.

2.3. FIRE BEHAVIOUR

There exists a broad gamut of research about fire behaviour in various circumstances and conditions. However, within the framework of the thesis objective, description of fire behaviour is limited only for nominal standard fire curve, which is common in the testing of building structures.

A number of fire curves are utilized to predict temperature development. However, primarily in the case for building elements, fire testing in fire nominal standard fire curve [52] is using. The standard temperature-time curve, otherwise referred to as the cellulosic fire curve, is the thermal representation of the burning rate of the materials often used for building and are kept in interiors. The timing of the ignition, smouldering and cooling phases is not taken into consideration. Temperature development of ISO curve follows the the logarithmic function:

$$\theta = 20 + 345 \cdot \log(8 \cdot t + 1), \quad (1)$$

where θ is the temperature and t time of fire. The function graph is shown in Figure 2-3.

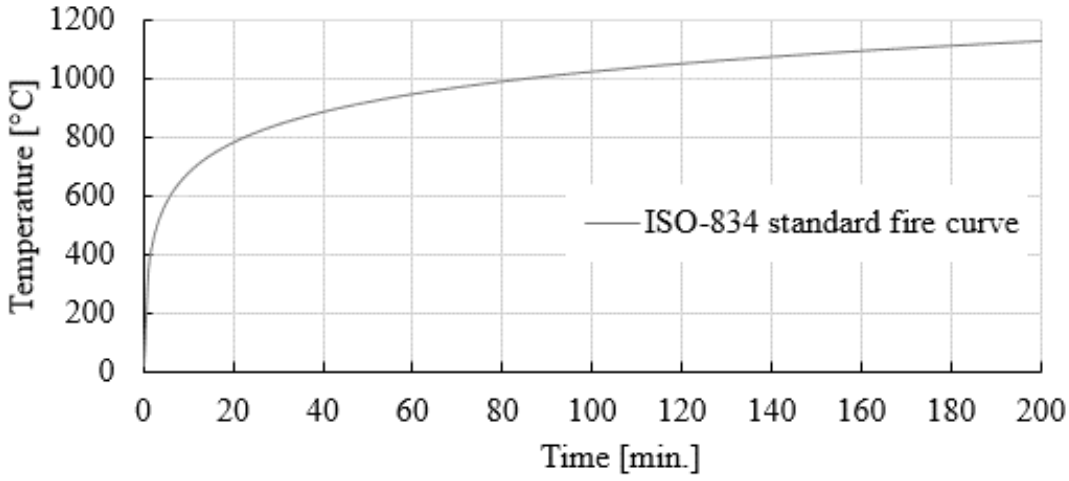

Figure 2-3 Nominal standard fire curve [52]

2.4. THERMAL PROPERTIES

2.4.1. THERMAL PROPERTIES OF STEEL

Specific heat and thermal conductivity are the primary thermal properties that influence the temperature increase in steel. Those parameters can be found in various sources such as codes, written standards, or published test data.

Kodur [33], in a paper, that reviews and compares data from Eurocode 3 [37], , Touloukian [40], Powell and Tye [53], ASCE [54] standard and publications by Rempe and Knudson [55], Yawata Iron and Steel Co. [56].

The aforementioned studies demonstrated that there is no meaningful difference between thermal conductivity parameters. Furthermore, the author noticed the absence of significant variation in ASCE and EC3 constitutive models for high-temperature thermal properties below 700°C. It must be noted, however, that significant variations exist for temperatures above 700°C.

2.4.2. THERMAL PROPERTIES OF SFRC

Thermal properties of concrete core affect heat transfer in sections and have the capacity to significantly affect the fire resistance of columns. Through examining concrete microstructure at high temperature, low thermal conductivity results in internal cracking and spalling of concrete exposed to fire [57]. While specific heat and thermal capacity values for plain concrete are included in the corresponding European standard EN1992-1-2 [58], no available official guidance for SFRC exists.

Lie and Kodur [59] examined a set of specimens from FRC and plain concrete to define the thermal properties of SFRC, and it was concluded that the thermal properties of SFRC are like those of plain concrete.

Kodur and Khaliq [60] aimed to define thermal properties by performing an experimental study on heated specimens from different high strength concrete types. It was found that the addition of steel and polypropylene fibres does not have a significant influence on thermal conductivity. Higher specific heat was detected in concrete with steel fibres. Relationships of thermal properties were set forth from the experimental data.

With the evolution of computational power, models of FRC began to see use. These models were mostly used for predicting mechanical behaviour. Liang and Wu [61] developed a mesoscale model of fibre-reinforced concrete to examine its thermal conductivity. Model shows exact results compared to experimental data, and thus models with different types and volumes of fibres were investigated. One of the findings was that the addition of steel fibres has a noticeable effect on the thermal conductivity of the composite. Further conclusions included that the diameter of fibres has a greater effect on thermal conductivity than their length. An analytical equation was developed from the results. The resulting model does not consider moisture and thermo-mechanical behaviour.

2.5. TRANSFER OF HEAT IN CFST SECTIONS

By reason of the high temperature over the fire, the degradation of the composite section materials took place. Accordingly, the development of the temperature in the section is one of the most crucial factors that influenced the final fire resistance time. A relation between the CFST field temperature within time and the fire itself must be established to forecast material properties for structural analysis. Therefore, there was plenty of research regarding this transfer of heat.

Being known the behaviour of fire during time, a relationship between the CFST field temperature within time and the fire itself has to be established in order to predict material properties for structural analysis. With this aim, there was plenty of investigation regarding this transfer of heat.

There are multiple ways to acquire the temperature field in the column's cross section. In the field of theoretical-analytical methods, authors like Lie [13], Tan [14] and Wang [15] have made notable contributions. The latter authors proposed a solution for this problem in CFST using Green's functions in a strictly analytical approach.

It is also worth noting that finite element analysis numerical models were proposed by researchers like Ding and Wang [62], Hong and Varma [63]. Thus, many software tools were designed by authors like Iding [64], Sterner, Wickstrom [65] and Franssen [66].

The work done by Lie and colleagues managed to obtain equations for predicting the temperature of both the concrete core and the steel tube, basing their work on heat transfer calculations by finite differences by Dusinberre [65]. The following studies can be consulted for more information: Lie [13], Lie & Chabot [18], Lie & Irwin [67].

When discussing material properties at elevated temperatures of steel and concrete, the work done by from Li & Purkiss [21], who reviewed state of the art and made a new proposal on concrete material constitutive models is worth considering. To achieve this, they compared their work with previous models from Anderberg and Thelandersson [22] and Schneider [23].

Particularly, the work of Lie [13] in the field of CFT columns it is of great interest. This author developed high temperature constitutive equations for steel and concrete which were eventually proved to be accurate for CFT columns. Furthermore, Han [69] obtained experimental constitutive equations for concrete at elevated temperature,

considering the additional lateral confinement effect provided by the steel tube. Youssef and Moftah [24] also studied confined concrete and proposed two analytical models based on previous models.

The intricacy of the hygroscopic behaviour of porous materials at elevated temperatures, such as in the case of concrete, requires the creation of coupled thermo-hygro-mechanical models. The model made by Bianco [70] at Pádova University is an example of this type of models. To solve the problem of heat-and-mass transfer in porous medium like concrete, the original approach was proposed by Chikhladze et al. [16]. According to the developed mathematical model, concrete is considered a three-phase medium composed of a solid skeleton, liquid, and gas phases in pores. Developed system of differential equations of heat-mass exchange takes into account vaporization of the moisture and movement of the evaporation zone's edge. The proposed model enables to obtain solutions for the stress state of SHS filled by plane concrete in dependence of temperature distribution over the composite cross-section at an arbitrary time of heating.

2.6. EXPERIMENTAL INVESTIGATIONS OF CFST COLUMNS UNDER FIRE CONDITIONS

The fire resistance of CFT columns subjected to concentric axial loads has been widely investigated through experimental testing. In the framework of the research projects from the National Research Council of Canada (NRCC) [71] [72] [73], the Comité International pour le Développement et l'Etude de la Construction Tubulaire (CIDECT) [74] [75] or by the Romero et al. [76], the effect of eccentricity was studied on the rather small number of specimens.

Some of the main fire testing programs carried out worldwide have taken the load eccentricity into account (Lie and Chabot [18], Grandjean et al. [74], Kordina and Klingsch [75]), but were limited by a small number of column specimens.

At the Centre Technique Industriel de la Construction Métallique (CTICM), France, a specific fire testing program focusing on eccentrically loaded CFT columns was carried out. In the structure of CIDECT research project 15R [77] to validate the work on developing a simplified calculation method for eccentrically loaded columns was carried out within the CIDECT project 15Q [78]. Four columns were tested under large eccentricities (e/D=0.75 and 1.5), half having square shapes and half having circular shapes. All columns were filled with bar-reinforced normal strength concrete.

It still stands that the results of this fire testing program are limited in scope and need to be expanded upon.

Other tests were also conducted in Tianjin (China) by the research group headed by Han [79] on CFT columns considering eccentric loads. In this program, 13 columns of circular sections were tested, four of them subjected to eccentric load. The parameters investigated were the cross-section diameter, the steel tube wall thickness, the fire protection coat thickness and the load eccentricity ratio (e/D=0–0.3).

Lu et al. [80] carried out a series of fire tests at Monash University (Australia) on high strength, self-consolidating concrete-filled steel tubular stub columns, with consideration for the eccentricity of the load. Six square section columns were tested, two of them under eccentric load.

The most current study on eccentrically loaded columns was done by Molier et al. [81] and dealt with the circular section columns with relative slenderness of all the specimens above 0.5. Additionally, the experimental program investigates the effect of using high strength concrete (HSC) and different types of reinforcement, such as steel fibres or reinforcing bars, in combination with eccentricity. The authors concluded that for slender columns, reinforcing bars yielded a greater benefit for HSC than for NSC. While Schaumann et al. [82] reported that the fire resistance of HSC filled hollow section columns can be considerably improved by using steel fibres as reinforcement, the authors did not record any increase in the fire resistance for the range of the slender columns that were examined. Also, in the presented paper, the simple calculation model for composite columns from EN1994-1-2 [83] was assessed through the results of this series of fire tests.

In contrast with previous results obtained for axially loaded columns, where the method had been found unsafe for slender columns [72], under eccentric loads, This method is considered to be safer. The drawback being that it produces high errors for those columns which do not use reinforcing bars. For bar-reinforced columns, the method proposes correct predictions. The authors conclude that the current simple calculation model in EN1994-1-2 should be developed further.

Kim et al. [84] performed tests on anchor type CFT columns in a vertical furnace with various infills. Three column sets were considered: one with bar reinforcement, one with steel fibre reinforcement, and one with fire-resistant paint. A set of columns with SFRC consisted from six columns. Tests with two different test loads and three

(0%, 0.25% and 0.375% per volume) fibre contents were performed. Hook-end steel fibres of 60mm in length and 0.75 diameters were used. A maximum of 46 MPa strength of concrete in compression was reached after 28 days for 0.375% reinforced mixture. It was found that for a load ratio 0.35 infill concrete reinforced with 0.375% improved fire resistance by 35%. For load ratio, 0.5 29% improvement for the same reinforcement value was observed. Meanwhile, infill reinforced with 0.25% steel fibres did not have much effect compared to plain concrete. It was determined that with the increase of the fibre amount, the contraction of the columns was slower, and fire resistance performance was improved. This effect was explained by the cracking delay due to the presence of steel fibres.

Kinoshita et al. [85] performed an experimental study on circular columns filled with plain and fibre-reinforced concrete under simultaneous axial load and double curvature bending in which theexperiments were performed in a vertical furnace. Circular columns with 609.6 mm diameter and 12.7 mm thickness from STK 490 grade steel (f_y=315 MPa) were used. Fibre-reinforced concrete contained 1% of fibres per volume (80kg/m³). Steel fibre of 30 mm in length and 0.62 mm in diameter were added to the mixture. Concrete compressive strength of 84.3 MPa for plain and 83.1 MPa for SFRC was measured before experiments. Up to 42%, higher fire resistance (70 min. for plain concrete and 121 min. for SFRC) was observed for the column with SFRC infill.

2.7. NUMERICAL MODELS

Advanced numerical modelling plays an integral role in modern research. The ability to carry out numerical simulation of complicated tasks was made possible through the use of innovative software tools, which were based on finite element method analysis. While much of today’s software focus primarily on on heat transfer problems, such as FIRES-T3, TASEF and SAFIR, othersfocus on general finite element calculations which offer a wide gamut of different tools and are very reliable in thermo-mechanical problems. In this category, renowned software such as ANSYS or ABAQUS serves as examples. Since both types of structural elements and FEM are have been around for a longer time, a wide range of studies already exists. Major available numerical investigations are reviewed in this part of the work.

The finite element method is commonplace in the field of advanced numerical modelling of CFST in fire. It could be utilized using one-dimensional, two-dimensional,

and three-dimensional elements for calculation. While using one-dimensional models is more efficient due to the short computing time, three-dimensional models offer many advantages.

Wang [86] presented the one-dimensional global model, which allows for the evaluation of the effects of structural continuity on the fire resistance of composite columns of concrete-filled steel tubes. Bailey [87] proposed another global study on a one-dimensional finite element model to increase the effective length of columns in fire used in European standards.

Later studies were based on two and three-dimensional models. Zha [88] presented a study about the behaviour of concrete-filled CHS columns subjected to fire on all sides with the corresponding fire resistances computing using FEA. The analyses of these studies consider the influence of temperature on the materials and the time-temperature relation obtained from the standard fire tests. The temperature distribution during the fire was determined by the two-dimensional numerical program FIRES-T. This program was later put into the finite program to carry out the time-dependent stress analysis. The time-dependent thermal stress analysis is performed using DYNA3D, a three-dimensional nonlinear finite element transient analysis program.

Ding and Wang [62] used the commercial finite element analysis package ANSYS to model the behaviour of isolated CFT columns in fire, and an advanced three-dimensional model for square and circular section columns was completed. The model considers the effect of slip between the steel section and concrete core, using surface-to-surface contact, including air gap thermal resistance. Properties of the materials at elevated temperature were assumed according to EC 4 part 1-2 [83]. Moisture content was also accounted for.

Another three-dimensional model was developed by Hong and Varma [89]. ABAQUS FEA software was used to predict the standard fire behaviour of square concrete-filled columns. An analytical approach consisting of three sequentially coupled analysis steps, namely, fire analysis, heat transfer analysis, and stress analysis, was used to predict the behaviour of the CFT columns subjected to standard fire loading. A detailed sensitivity analysis was conducted to select the values of the relevant input parameters for the numerical models. The results from the sensitivity analyses indicated the following conclusions: the steel tube should be modelled using the Poh [90] σ –ε–T model, the concrete infill should be modelled using the Lie and

Irwin [68] σ –ε–T model, linear thermal expansion models can be used for the steel and concrete materials, and full composite action with no local buckling may be used to model the CFT column specimens.

An FEA model was developed by Professor Han at Tsinghua University (Beijing, China) [91] to predict the load versus deformation relationships of concrete-filled steel tube (CFST) stub columns subjected to a combination of temperature and axial compression. The model was employed in the simulation of a set of CFST stub column experiments under various thermal and mechanical loading conditions, including tests at high temperature, tests on the residual strength of specimens subjected to uniform heating, and tests on samples exposed to the ISO-834 standard fire without initial loads. The FEA model was developed in the commercial program ABAQUS,and it has been used to perform a parametric analysis to investigate the influence of parameters such as the fire duration time, steel ratio and axial load ratio on the load versus deformation relationships of CFST stub columns considering the mutual influence of temperature and loading histories. The load ratio and the fire duration time were found to have a significant effect on the permanent axial strain developed in the column during the heating process.

Recently, Espinos et al. [92] developed a finite element three-dimensional model with the aim of studying the behaviour of axially loaded concrete-filled tubular (CFT) columns with circular cross-sections exposed to fire. The model was performed in ABAQUS software. It consisted of three components: the concrete core, the steel tube and the loading plate. Drucker-Prager material model was used for concrete material. Due to symmetry on both the geometry and the boundary conditions, only a quarter of the column was modelled for those specimens with pinned–pinned or fixed–fixed end conditions. The mesh density was controlled to have a maximum element size of 2 cm, which proved to be satisfactory in predicting the thermal and mechanical behaviour of the CFT columns under fire with sufficient accuracy. The initial geometric imperfection of the column specimens was assumed as L/1000 and simulated in the model as the first buckling mode shape of the hinged column multiplied by an amplification factor. The fire behaviour of a series of column specimens previously tested by other researchers was predicted with the use of the model. An extensive sensitivity analysis was carried out using the validated numerical model, covering the main aspects of the problem. With the results of this sensitivity

study, a number of modelling recommendations for CFT columns in the fire were proposed.

Investigate the fire performance of eccentrically loaded concrete partially encased column using the advanced calculation method was proposed by Fellouh [93]

Together with the earlier described experimental study, Kinoshita et al. [94] developed a numerical model using the ABAQUS FEM model. SFRC material model was calibrated based on previous experimental studies. Higher compressive toughness and tensile strength were inputted to reach the corresponding behaviour. The model shows rather good consistency with experimental studies. A three-dimensional FEM fire response model of the steel fibre reinforced concrete filled tubular column under ISO standard fire conditions using ATENA Červenka software was performed by Tretyakov, Tkalenko and Wald [114]. SFRC material model in the ATENA software to determine mechanical and thermal behaviour was developed. These properties were implemented in the global behaviour model. Developed numerical model taking into account thermal and mechanical (tension) behaviour of SFRC and was validated on own experiments made and available in the literature. The ATENA Červenka software was chosen due to the included fracture-plastic temperature-dependent concrete model. The limitation in the thermal model was found in terms of modelling the air gap between steel and concrete. The problem was solved by adjusting the fire load independently for steel and concrete. This assumption causes a higher temperature of the steel tube and provides accurate temperature distribution in the concrete core for chosen validation cases. Fracture – plastic model of concrete material developed by Červenka was used in mechanical FEM model. Post-peak plastic strain of SFRC in compression and tension were implemented using compression toughness index proposed by Marar et al. [95] and SDEM method by Lee et al. [96]. Both methods were verified against experimental studies on advanced models performed in ATENA. Verification was made for concretes with different compressive strengths and percentages of steel fibres and showed relatively accurate results. The combination of chosen methods allows predicting post-peak behaviour of FRC depending on compressive strength and fibre-reinforcement index. This model was adopted in the presented work for additional validation in steady-state experiments and parametric study.

2.8. Analytical approaches for assessment of CFST members' resistance in fire conditions.

While the standard fire resistance test is time consuming and expensive, and the dimension of the test specimen is limited by the size of the furnace, the development of codes and FE models or operating of the commercial software require expert knowledge and time in handling necessary computer programs from ordinary designer. As a sound alternative to the test and FEM based methods, simplified calculation approaches are also developed to assess the fire resistance of CFST columns.

The first work which can be found in the literature on the analytical resolution of the transient heat conduction in concrete filled steel hollow sections exposed to fire is that from Lie [13]. In the presented, works he not only derived a mathematical solution for the heat transfer problem, but also proposed a theoretical structural model which permits to calculate the deformations and the fire resistance of the columns. Based on the finite differences method by Dusinberre [20], Lie derived expressions which allow to calculate the temperature of the concrete core and steel tube by subdividing the cross-sectional area of the column in a number of layers for CHS columns (Lie [13], Lie and Chabot [18], Lie [97]) or elements in the case of RHS columns (Lie and Irwin [19]). Once the cross-sectional temperature field is known for every step time, the strength of the column can be calculated by a method based on a load-deflection or stability analysis. The model from Lie was validated against experimental results, and employed specific formulations for the constitutive laws of steel and concrete at elevated temperatures.

A theoretical structural model was also proposed by Han [69], capable of predicting the fire resistance of CFT columns and beam-columns with circular or square sections. The model took into account the physical and geometrical nonlinearities. Han employed a specific formulation of the stress-strain relations of concrete at elevated temperatures, making allowance for the confinement effect. This theoretical model was used to calculate the fire resistance of CFT columns used in actual buildings, such as the SEG Plaza in Shenzhen (China).

Wang and Tan [15] presented a theoretical approach for the heat transfer analysis of concrete filled steel circular hollow sections subjected to fire based on an analytical Green's function solution. This approach can be used to predict the

temperature field inside the composite domain and the heat flux at the fire and steel concrete interfaces.

Developed an analytical nonlinear model which uses the constitutive high temperature equations presented in Li and Purkiss [21] for normal strength concrete and the steel constitutive model from Lie [97]. Temperatures were calculated by solving the corresponding heat transfer equations, and the strains and stresses were obtained by assuming that the columns were perfectly straight and the axial load applied in such a way that makes the column fail in compression without any bending. These authors evaluated and compared the fire performance of circular and square sections, showing that for columns with the same steel and concrete cross-sectional areas, the circular column presented a slightly higher fire resistance.

The significant theoretical researches in the area of analytical modelling of CFST fire behaviour belong to the school headed by professor Chikhladze [16]. For the analytical estimation of the stress-strain state of the CFST column with SHS section the contact between the concrete core and steel tube was considered as dependent on level of the normal and shear stresses. The strained–stress state of the column is investigated by taking into account the dependence of the Young modulus and the Poisson's ratio on the level of loading and of the temperature at the point. As a result, the closed system of the differential equation for describing of deformable state of CFST column operating under load and temperature action was obtained. Also, mathematical model and calculation procedures for the definition of temperature and humidity fields were presented. It is important to note that this approach is able to account degradation process in concrete during the heating.

Espinos [98] proposed simplified design method for evaluating the fire resistance of unprotected CFST columns under ISO standard fire conditions. The essence of the method of obtaining empirical properties for the reduction coefficients for flexural stiffness and eccentricity. The method was developed through an extensive parametric study which included 20.500 numerical analysis cases approximately. This study was carried out through the numerical models developed by UPV and CTICM, which were validated against the results of a previous experimental campaign carried out by the authors within the European Project FRISCC. Proposed simplified design method considers that differential axial displacements between the outer steel tube and the concrete core are allowed –i.e. free slip at the top end of the column – and recommends a minimum percentage of

reinforcement of a 2.5% for CHS and SHS columns with relative slenderness over 0.5. The method provides safe predictions for columns with relative slenderness at ambient temperature up to 2.0. The proposed solutions are reflected in EUROCODE 4 method [12].

Nowadays, when there are only a few researchers focused their efforts on mechanical and thermal modelling of CFST filled by SFRC at elevated temperature (Lie, Kodur), plenty of them had a wide range of numerical and analytical models of concrete filled tubular (CFST) columns with plain concrete or another reinforcement type. Thus, lack of experimental data and theoretical investigation of the SFRC filled CHS columns is a widely acknowledged gap in the field of CFST fire resistance.

The analytical model proposed in this paper is a proposal to supplement the EUROCODE 4 method [12].

2.9. Models of CFST fire resistance provided by Design Guidelines

The necessity in the use and development of simple methods for calculating the fire resistance of CFST columns is growing due to the increased usage of this structural typology. Calculation tools are sought by designers in order to obtain an estimation of the fire resistance of the structural member is relatively simple way or conversely to be able to determine the minimum dimensions which fulfill the required fire resistance.

A plenty of design guides on the calculation of the fire resistance of CFT columns have been developed. The most common are the Corus Tubes guide (Hicks [99]) and the CIDECT guide. In the latter of these guides, practitioners can find a number of design charts valid for the more commonly used cross-sectional dimensions, where the load-bearing capacity of the column for a certain fire exposure time is given as a function of its buckling length, cross-sectional dimensions and percentage of reinforcement.

Zhao, Han and Lu [2] presented the exhaustive information about calculation models of CFT columns, where authors summarize and fully compare design approaches of CFT members at ambient and elevated temperature by different standards (Eurocode 4 [83], BS5400 Part 5 [100] and Chinese Standart DBJ13-51 [101]). One year later, Rush et al. [6] also have reviewed the current methods that exist for calculating the fire resistance of CFT columns. Of all the studies contained therein, the following must be mentioned.

Kodur [102] with colleagues proposed a design equation for obtaining the fire resistance of CFT columns based on the results of the experimental program supported by the National Research Council of Canada. The published design equation is valid for CFT columns of circular and square shapes, filled with normal or high-strength concrete and using different types of reinforcement: longitudinal bars or steel fibers. Kodur and Lie (1996) conducted a series of experiments on circular steel contrite composite columns filled with steel fibro reinforced concrete. Formula to determine fire resistance (R) in minute given on equation (2).

$$R = f\frac{(f_c' + 20)}{(\mathrm{KL} - 1000)}D^2\sqrt{\frac{D}{N}}, \tag{2}$$

where

f is reduction factor: 0.075-0.085 for SFRC,

KL is effective length, mm

$f_c'$is 28 day, cylinder concrete strength, MPa,

D is outside diameter,

N is applied force.

In Europe, the most extended methods for calculating the fire resistance of CFT columns are those included in EN 1994-1-2 [83]. Three levels of design are allowed: a) tabulated data, b) simple calculation models and c) advanced calculation models. Option a) is available in Clause 4.2.3.4 in the form of a selection table which provides the minimum cross-sectional dimensions and reinforcement that a CFT column must have in order to achieve a rated standard fire resistance under a certain load level. This approach is the most simplistic and results highly conservative as pointed out by Rush et al. [50]. Option b), simple calculation models, are the most widespread, and amongst them a full method is presented for calculating the fire resistance of composite columns in Clause 4.3.5.1 based on the elastic buckling theory. A specific method for columns composed of unprotected concrete filled hollow sections is also given in Annex H of the same code. Finally, advanced calculation models (option c) allow the use of finite element models capable to simulate the realistic fire behaviour of the element based on the modelling of the actual thermo-mechanical problem. This last approach can provide a more accurate approximation of the behaviour, but is generally out of reach of practitioners and often due to limited time or resources it is only applied to very specific a design situations.

EUROCODE 4 method [12] proposed a simplified design method for evaluating the fire resistance of unprotected CFST columns under ISO standard fire conditions, based on the general method in EN 1994-1-2 [83] for composite columns, extended over the current applicability limits. The method makes it possible to obtain design buckling load in the fire situation:

$$N_{fi,Rd} = \chi \cdot N_{fi,pl,Rd} \quad (3)$$

According to the requirements of Eurocode 4 Part 1.2 [83] Wang [103] proposed an approximated approach for obtaining the reduced squash load and rigidity of CFST columns with CHS section at elevated temperatures. The method was developed through the analysis of the results of an extensive parametric study where numerical modelling procedures were used. The simple method proposed by Wang was valid for both unprotected and protected columns. Han et al. [79] presented an empirical design equation based on the results from an experimental program carried out in China, where the influence of the main design variables that affect the fire behaviour of CFT columns was investigated. Expressions for circular and square geometries were adjusted, which provided the strength index of the columns at elevated temperatures, as referred to as their maximum axial capacity at room temperature. Also, a simple equation for obtaining the residual strength of CFT columns after fire exposure was developed by Han and co-workers (Han and Huo [104]). Several design codes are also in use nowadays, which are a result of the numerical and experimental investigations carried out by the main groups working in this field of research.

The expressions proposed by Han et al. [79] have been incorporated in the Chinese Code DBJ13-51 [101], which establishes an equation to calculate the thickness of the external fire protection required to achieve a certain fire resistance, as well as a method for calculating the strength index of unprotected columns in the fire situation.

Kodur and co-workers proposed an approach [26] [102] [105], which is in use in North America after having been incorporated into the National Building Code of Canada ASCE/SFPE 29-99 [106] and ACI 216 [107].

Korea’s view on the problem and empirical formula was suggested by Park et al. [108] for square CFT columns subjected to axial loading, using regression analysis based on a previously established relationship between the fire resistance and the parameters width of the column, concrete strength and applied axial load ratio.

Xiong [1] presented a design guide for concrete-filled tubular members with high-strength materials. This design guide is based on Eurocode 4 (EN 1994-1-1, 2004 [109]) and summaries test data from the literature on concrete-filled steel tubes with normal and high-strength materials to develop the design methods at ambient and elevated temperature.

The latest paper in the field of simplified models for the codes was presented by Wang [110] from the School of Civil Engineering of Wuhan University (China). The authors proposed a simple approach to evaluate the fire resistance of circular CFST columns in localized fires. A simple model was provided to calculate the column temperatures in a localized fire. The concept of equivalent fire severity or time equivalent was used to correlate the localized fires with the standard fire. The simple model used in the Chinese code was used to calculate the load capacity of the circular CFST columns subjected to the equivalent standard fire exposure. The proposed approach, by correlating real fires with the standard fire, only includes heat transfer analysis and avoids the complex structural analysis, which provides an easy and efficient way for performance-based fire safety design.

Later Espinós, with colloquies [98] developed a numerical analysis of the fire resistance of circular and elliptical slender concrete-filled tubular columns. Her work includes three numerical models, which were validated on fire tests' results of experimental research since 80's. Also, this work presented development of a simple calculation model of CFT columns and proposed an advanced model for predicting the fire response of concrete-filled tubular columns. The method provides safe predictions for columns with relative slenderness at ambient temperature up to 2.0. The proposed solutions are reflected in EUROCODE 4 method [12].

CHAPTER 3. OBJECTIVE

3.1. General

The thesis's main objective is to develop an analytical model for determining the fire resistance of the composite steel and fibre-reinforced centrically and eccentrically loaded SFCR columns under ISO standard fire conditions. This model should determine the design buckling load in the fire situation of the composite steel and fibre-reinforced concrete columns, and can be used as an appendix or supplementary technical basis in the corresponding method prepared for prEN1994-1-2:2024.

From the review of the available literature and research, several could be concluded:

3.2. THE STATE OF THE ART

- FRC infill for CFST columns in a fire situation and elevated temperature has many advantages that make it a practical alternative to plain concrete and bar reinforced concrete infill. Nevertheless, a European design guide for CFST columns with SFRC infill in the fire situation has not been developed yet.

- The limited number of experiments in a vertical furnace on CFST columns with SFRC infill were performed. Some authors do not observe differences between SFRC and plain concrete [76] [81]. Others have found SFRC infill very beneficial [25] [102].

- Numerical model of CFST columns with SFRC infill at elevated temperature was developed by Tretyakov [114] in ATENA Červenka software. Material model of SFRC was performed, including reduction factors for SFRC mechanical properties due to elevated temperature.

- A range of analytical models was developed in the field of CFST columns in fire. However, there are only a few researchers who focused their efforts on mechanical and thermal modelling of CFST filled by SFRC at elevated temperature [60] [97] with plain concrete or another reinforcement type. Thus, the

lack of experimental data and theoretical investigation of the SFRC-filled CHS columns is a widely acknowledged gap in the field of CFST fire resistance.

- prEN1994-1-2:2024 method [12] proposed a new analytical model (based on experiments and parametrical study) for the design of CFST steel bars reinforced column at elevated temperature. However, the SFRC infill was not covered.

3.3. SCOPE OF THE RESEARCH

Based on the made conclusions, the following scope of the work was defined:

- Available numerical models validated on experimental data from the experiments on CFST columns with SFRC in the fire. However, there are no experiments for steady-state heated centrically loaded full-scale CFST columns with SFRC in the literature. It is necessary to conduct additional experiments.

- Provide validation of global FEM model on conducted steady-state experiments to ensure proper functionality for further studies.

- Conduct a parametrical study determining the fire resistance of the composite steel and fibre-reinforced centrically and eccentrically loaded columns with plain and steel fibre reinforced concrete infilling under ISO standard fire conditions.

- Develop a simplified model to determine the design buckling load in the fire situation of the composite steel and fibre-reinforced concrete column, which can be used as an appendix or supplementary technical basis in the corresponding method prepared for prEN1994-1-2:2024.

- Based on the conducted research, provide recommendations for further development and experimental studies in the field.

CHAPTER 4. EXPERIMENTAL STUDIES

4.1. OVERVIEW

This chapter deals with the description of the experimental program conducted for this thesis. To verify the numerical model, specimens were prepared in the hydraulic stand in the Experimental Centre of the Faculty of Civil Engineering CTU in Prague. Full-scale column specimens were used for experimental studies. Six pinned-pinned columns were tested in compression at an elevated temperature at the steady-state regime. Columns were heated first to planned temperature and then loaded till the failure.

4.2. MATERIALS

The average cubic compressive strength of SFRC on the test day was 75 MPa. Concrete with 40 kg/m³ of Dramix RC-80/60-BN steel fibres was used to infill of steel tubes. The exact concrete mixtures are shown in Table 4-1.

Table 4-1 Concrete mixture

Ingredient	kg/m³
Cement 42,5	490
Water	154
Aggregates 0/4	890
Aggregates 4/8	100
Aggregates 8/16	745
Plasticizer Sika Visco Crete 1035	4,9
Steel fibers Dramix RC-80/60-BN	40

Concrete composite is composed of easily available and widely used components which include Portland cement 42,5 R characterized by high early strength in accordance with CSN EN 197-1, water and siliceous aggregate. The workability of fresh concrete mass was maintained by using the plasticizer Sika Visco Crete 1035, which also reduces the content of used mixing water.

The chosen fibre reinforced concretes also contain two types of fibres. Single hook end steel fibres Dramix RC-80/60-BN with tensile strength 1225 MPa serve as reinforcement in the concrete composite. Whereas polypropylene fibres were added to concrete with an aim to reduce the risk of explosive concrete spalling, which occurs at a higher temperature at elevated temperature tests.

Four standard cubic specimens at elevated temperatures of 200 °C, 400 °C and 600 °C were tested in compression in the laboratory of CVUT. Cubes were insulated

by Fiberfrax (Grade 1250, Density 96kg/m^3) and heated using ceramic pads heaters (60V, 2,7kW) shown on Figure 4-5. Experimental tests of concrete compounds were carried out to determine their behaviour. Obtained results are presented in Figure 4-1.

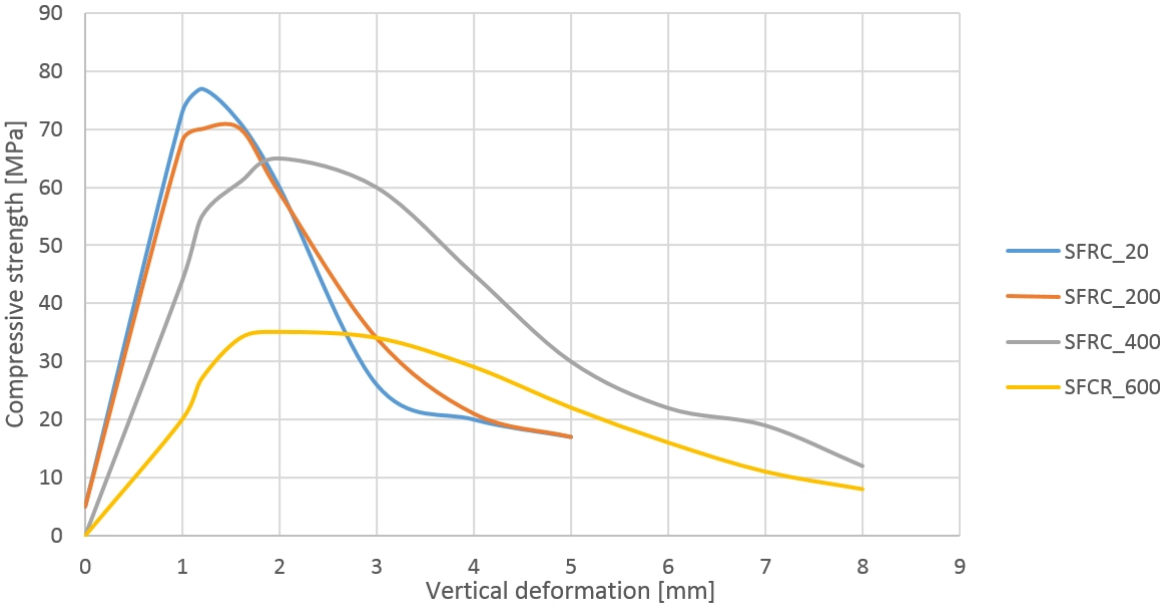

Figure 4-1 Compressive strength-displacement diagram of SFRC

Steel hollow structural sections (HSS) meeting the requirements of EuroCode 4 was used S355 which has minimum yield strength of 350 MPa.

4.3. STEADY-STATE REGIME TESTS

For steady-state regime experiments, six 3850 mm long columns were produced. A circular cross-section with 244,5 mm outside diameter and t = 6 mm wall thickness was used for all specimens (Figure 4-2).

The hollow steel sections were fabricated by cutting the supplied sections to 3800 mm in length. Steel end plates were then welded to both sections. The total column length was 3850 mm, including end plates. A hole (diameter 210 mm) was cut in each plate to provide an opening through which the concrete was poured.

The hollow steel sections and end plates were first joined by a groove weld. In the end, a fillet weld was added around the outside diameter of the hollow steel section.

Fore small holes were drilled in the wall of the steel sections (see Figure 1). Two pairs, 13 mm in diameter, located 450 mm from each end of the columns, were provided as vent holes for the water steam produced during the experiment.

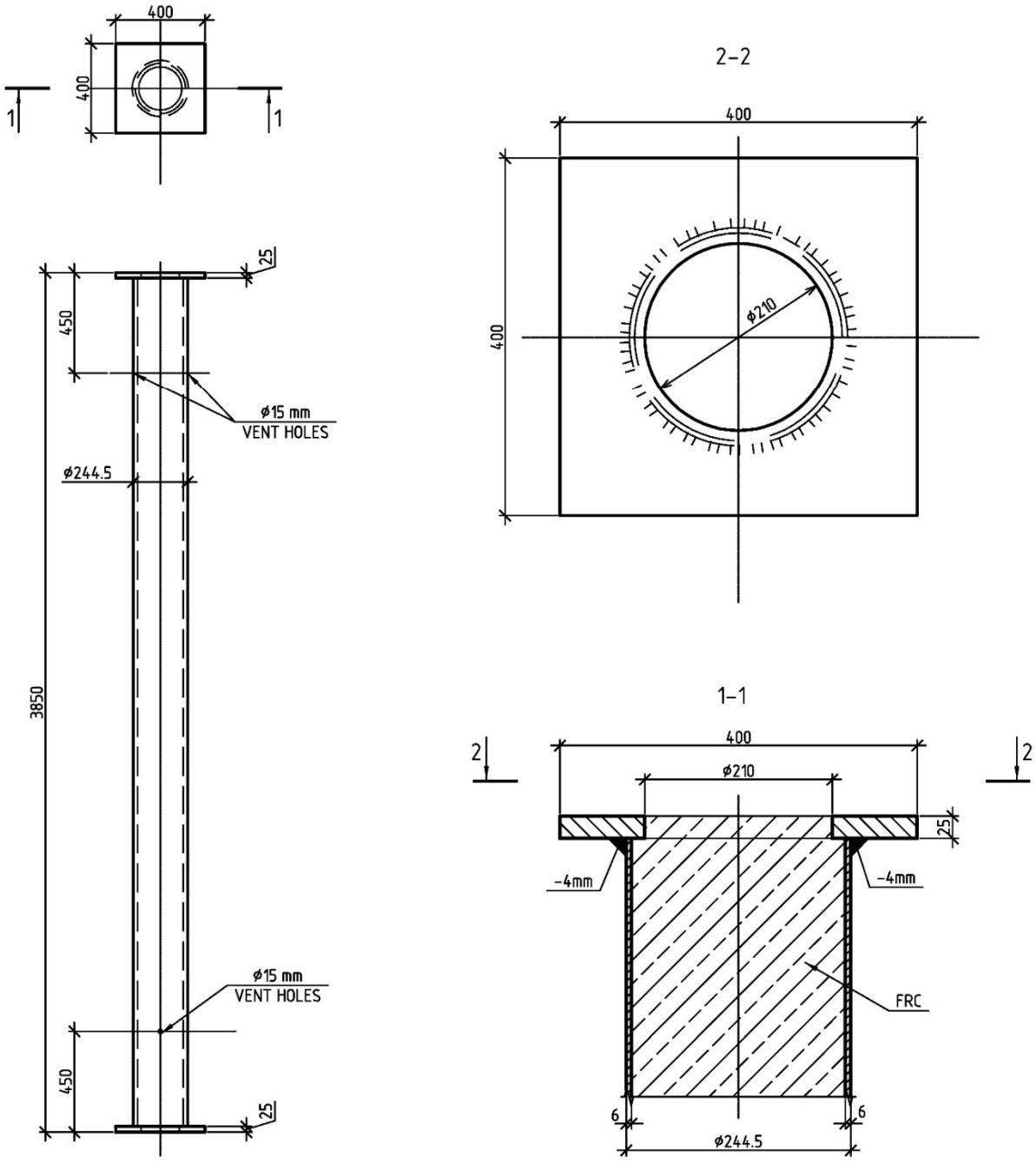

Figure 4-2 Geometry of tested columns

The concrete with steel and polymer fiber was mixed in a concrete plant in Prague, Czech Republic. The columns were put in an upright position and filled with concrete. A concrete placement bucket and a funnel were used to deposit the concrete in the steel column. An internal vibrator was used to consolidate the concrete inside the column. The top surface of the column was finished with a small trowel. The columns were left upright for 28 days and then stored horizontally at open-

air temperature from 04/2015 till 11/2015 (until the test date). Preliminary 6,5 months elapsed between the time a column was poured and the time it was tested.

Measurements of geometrical imperfections are made by calibrated tape measure with a scale division of 1 mm. Measurement error - 0.5 mm.

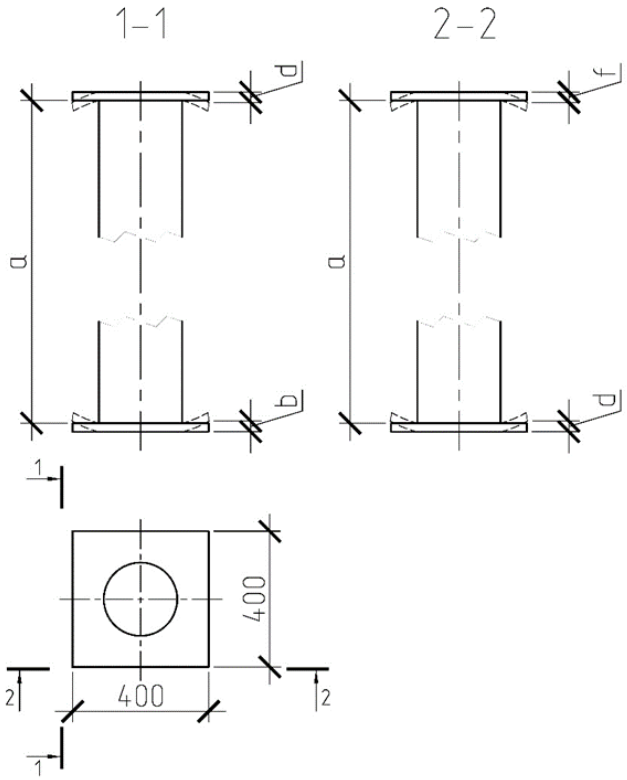

Figure 4-3 – Scheme of measured imperfections

The measurement results are entered in *Figure 4-3* and Table 4-2.

Table 4-2 *Imperfections*

Size	Measured dimensions for each column, mm					
	1	2	3	4	5	6
a	3796	3795	3796	3796	3797	3796
b	1	3	0	3	0	2
c	1	1	1	2	2	0
d	0	2	0	1	1	
f	1	1	0	1	1	1

Steady-state testing columns were installed into the test bench and equipped with thermocouples. Specimens were installed with hinge supports.

Figure 4-4 - Column's ends

The middle part of the specimen was heated by 24 ceramic pads. Minnings HTC 70 kW heating machine was used to power ceramic pads heaters (60V, 2,7kW) as shown on Figure 4 5. Fiberfrax (Grade 1250, Density 96kg/m3) blankets and aluminium foil were used to insulate specimens. The temperature during experiments was measured in the middle of a specimen and for four groups of pads (one thermocouple for six pads). On specimen 8, thermocouples on the steel surface, concrete core centre and quarter were installed in a different sections. The test setup scheme is shown in Figure 4-7 (numbers 1 to 8 indicate the location of the thermocouples). Photos of the specimen before insulation (a) and prepared for the experiment (b, c) are shown in Figure 4-6.

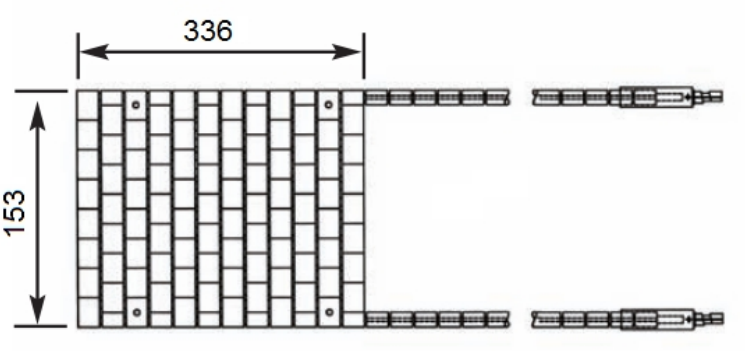

Figure 4-5 – Ceramic pad

a) b) c)

Figure 4-6 – Photo of specimen a) with installed ceramics pads before insulation b) after insulation c) with extra foil installed

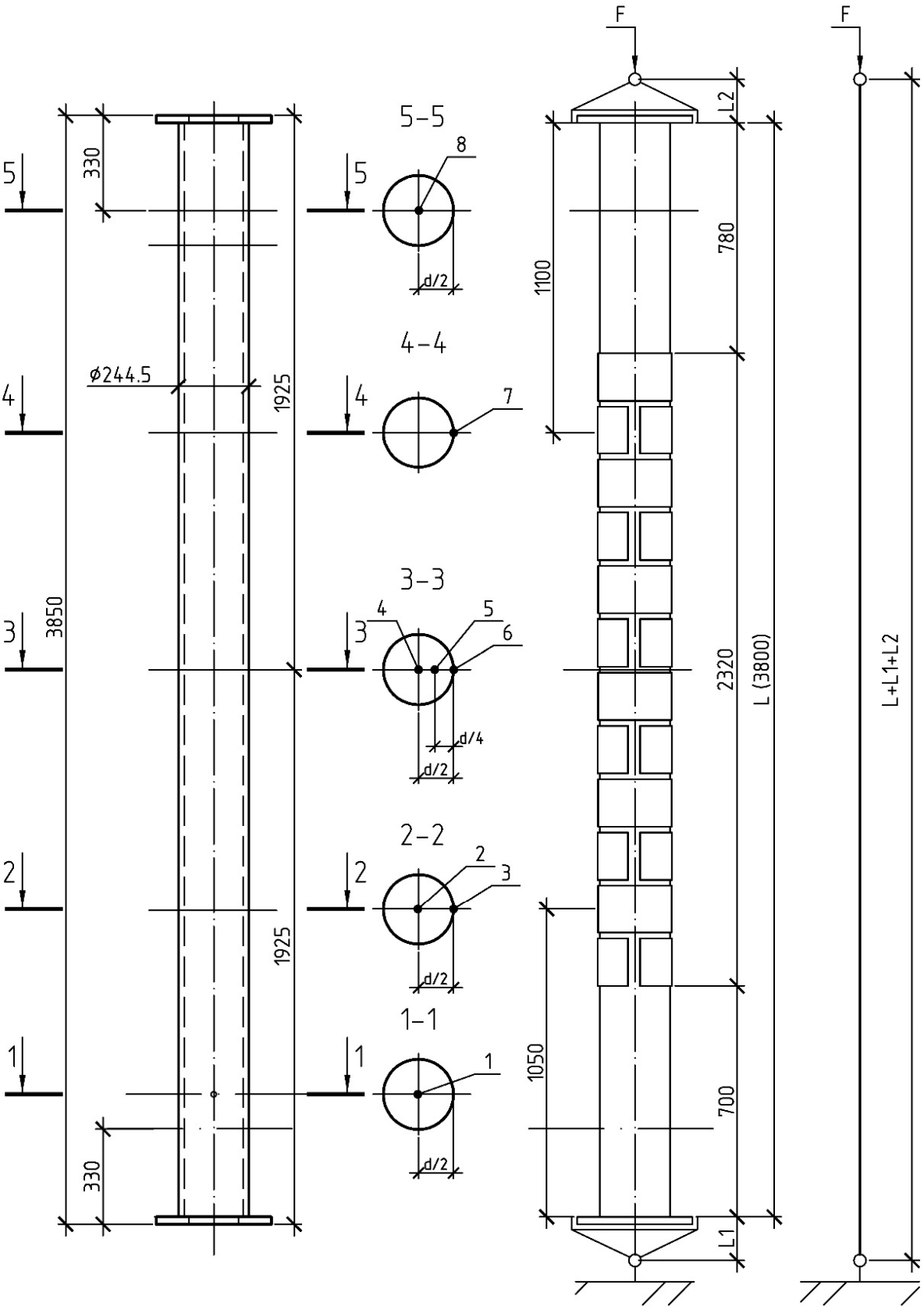

Figure 4-7 – Test setup of SFRC composite column

Before the mechanical load application specimen was heated by ceramic pads with maximum installed temperature of 600 °C and 500°C.

For load application, a jack with a maximum of 2000 kN force was used. Loading was applied with 5 mm/min speed. Deflectometers measured displacements. The scheme of location of the deflectometers is illustrated in Figure 4-7.

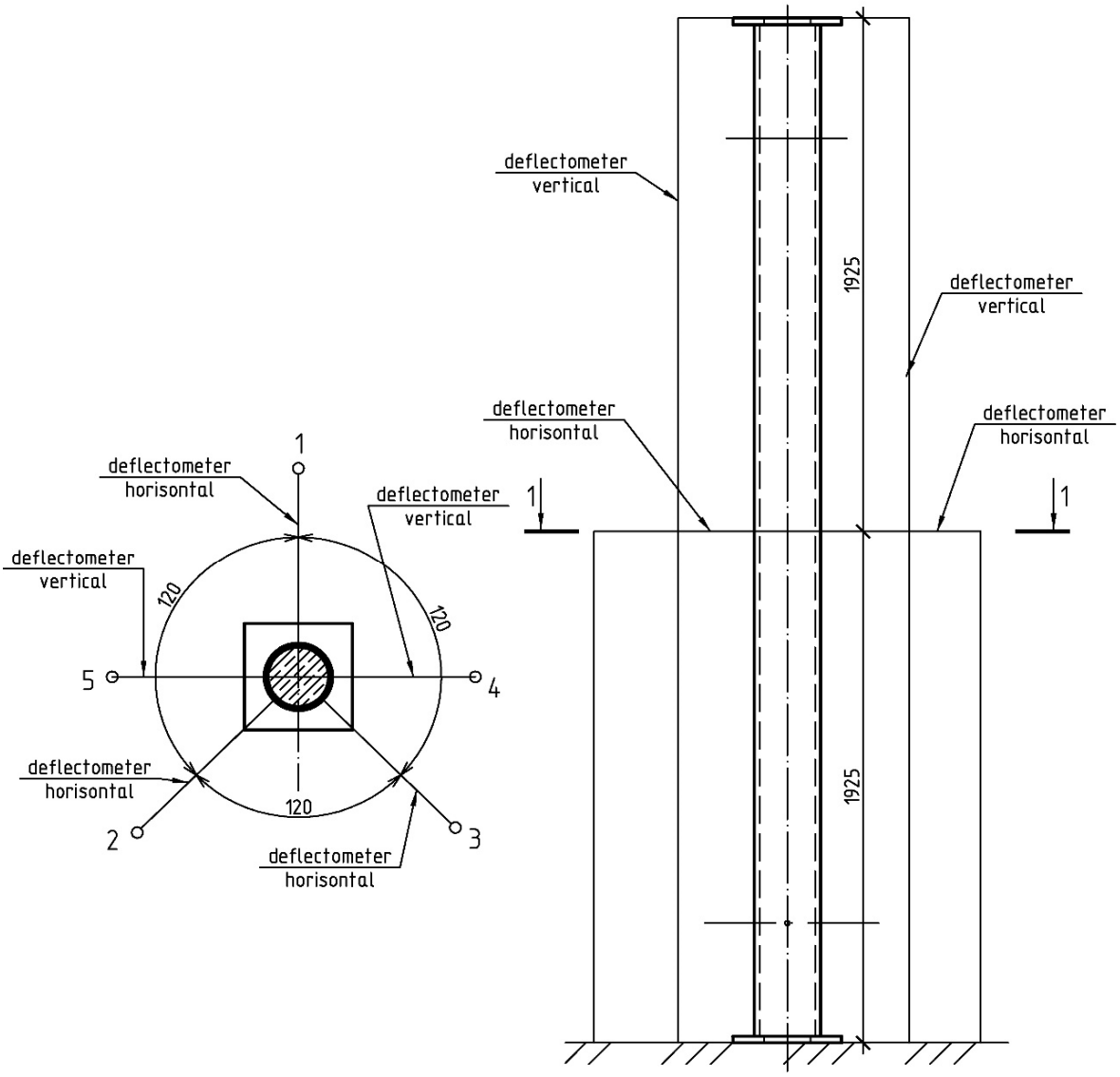

Figure 4-8 - Position of deflectometers

The heating of pads was performed as in a Figure 4-9.

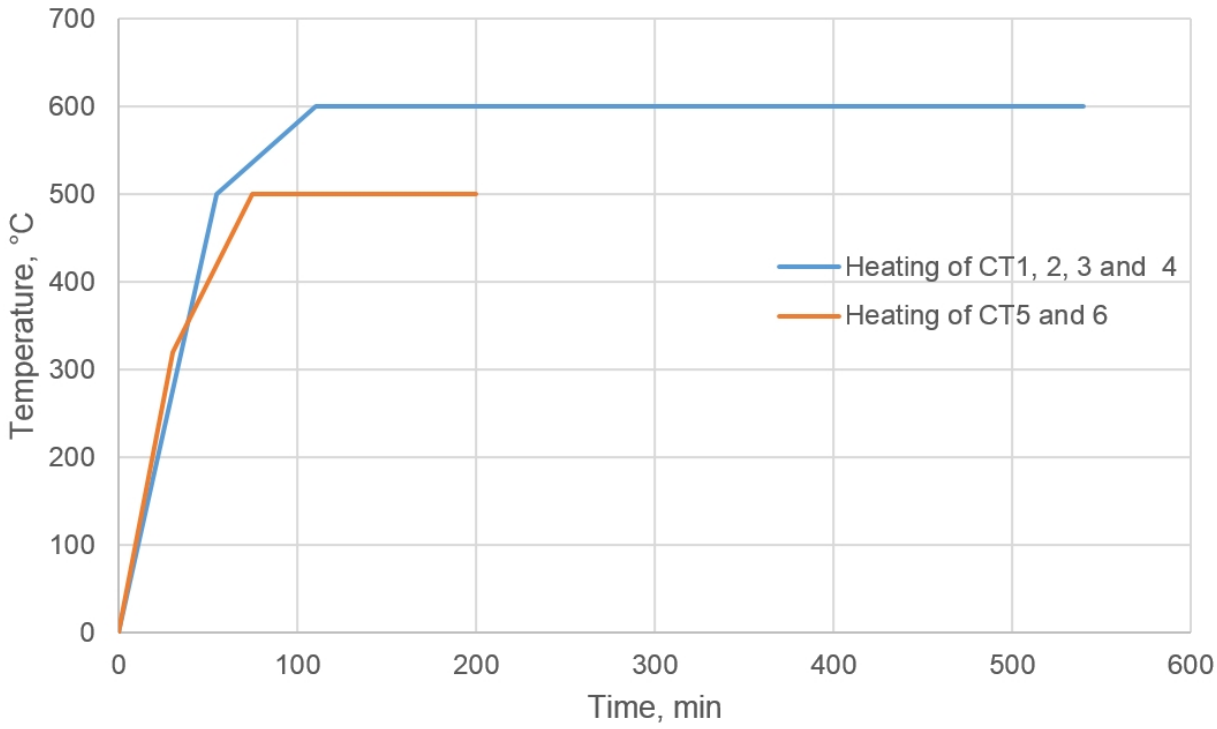

Figure 4-9 - Ceramic pads heating procedure

The time of heating, reached temperatures in the middle of specimen and applied load is shown in Table 4-3. Measured temperatures before loading is shown in Figure 4-14. Measured force-displacement diagrams are shown in Figure 4-11.

Table 4-3 Elevated temperature specimen list

Test	Test date	Time of heating, min	Type of heating	Temperature of pads, °C	Temperature of steel, °C	Temperature of concrete, C	Failing force, kN
CT1	12.11	1200	Local	1000	~900	-	300
CT2	30.11	540	Uniform	600	600	600	786
CT3	7.12	300	Uniform	600	608	502	763
CT4	10.12	270	Uniform	600	610	378	1082
CT5	14.12	170	Uniform	500	495	255	1860
CT6	17.12	200	Uniform	500	505	279	>2000

Specimen CT1 was overheated up to 1000 °C due to a technical failure and incorrect display of the temperature. Several ceramic panels were damaged and chanced. In a Figure 4-10 a) local buckling and overheated area is shown. Typical global backing frailer shown in Figure 4-10 b).

a)  b) 

Figure 4-10 - Fail of the tested specimens a) local buckling of the CT1 b) global buckling CT4.

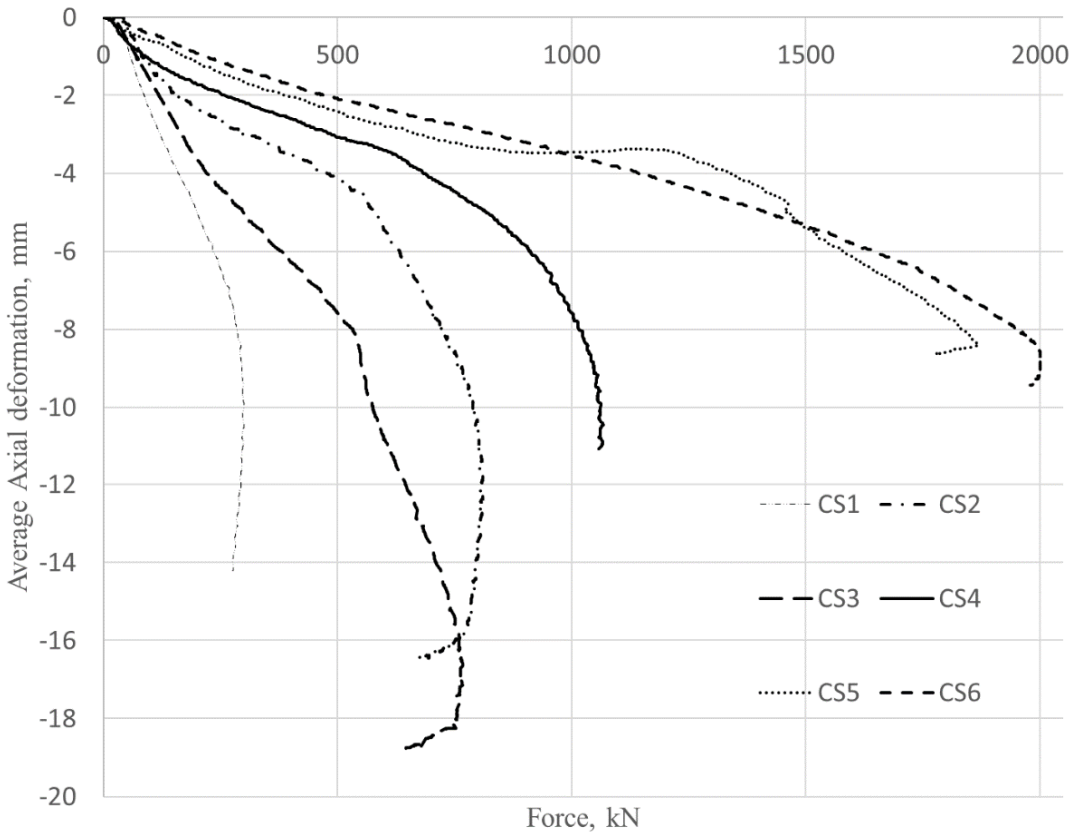

Figure 4-11 - Force – displacement diagrams

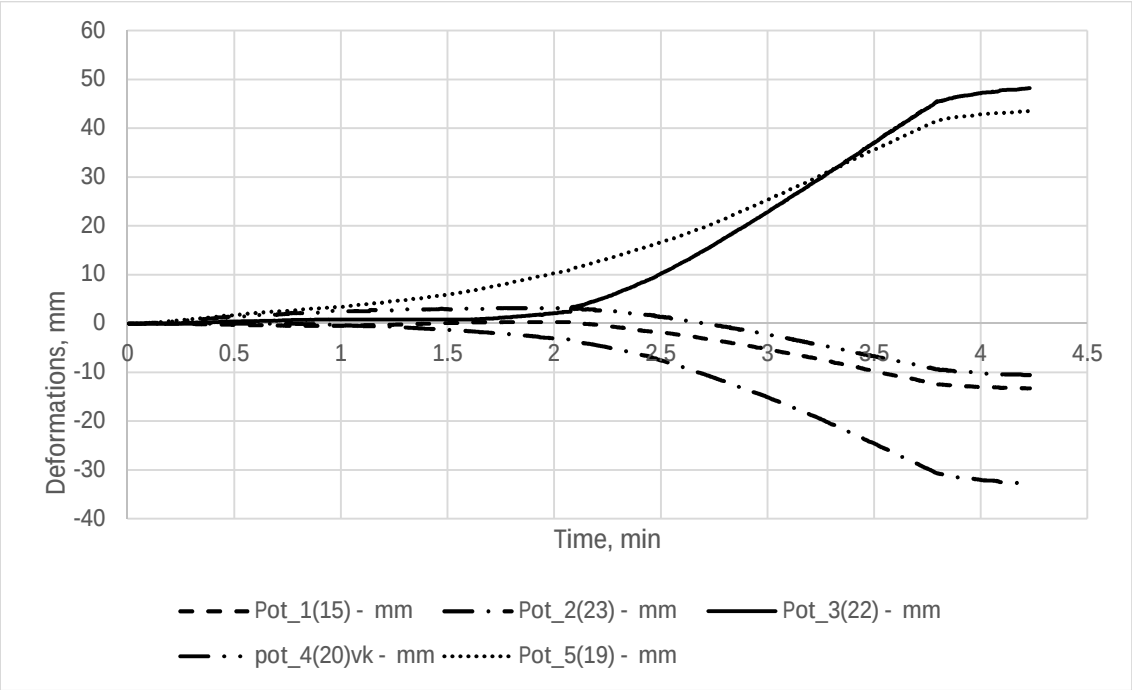

Figure 4-12 - Measured values of deflictometrs CT2

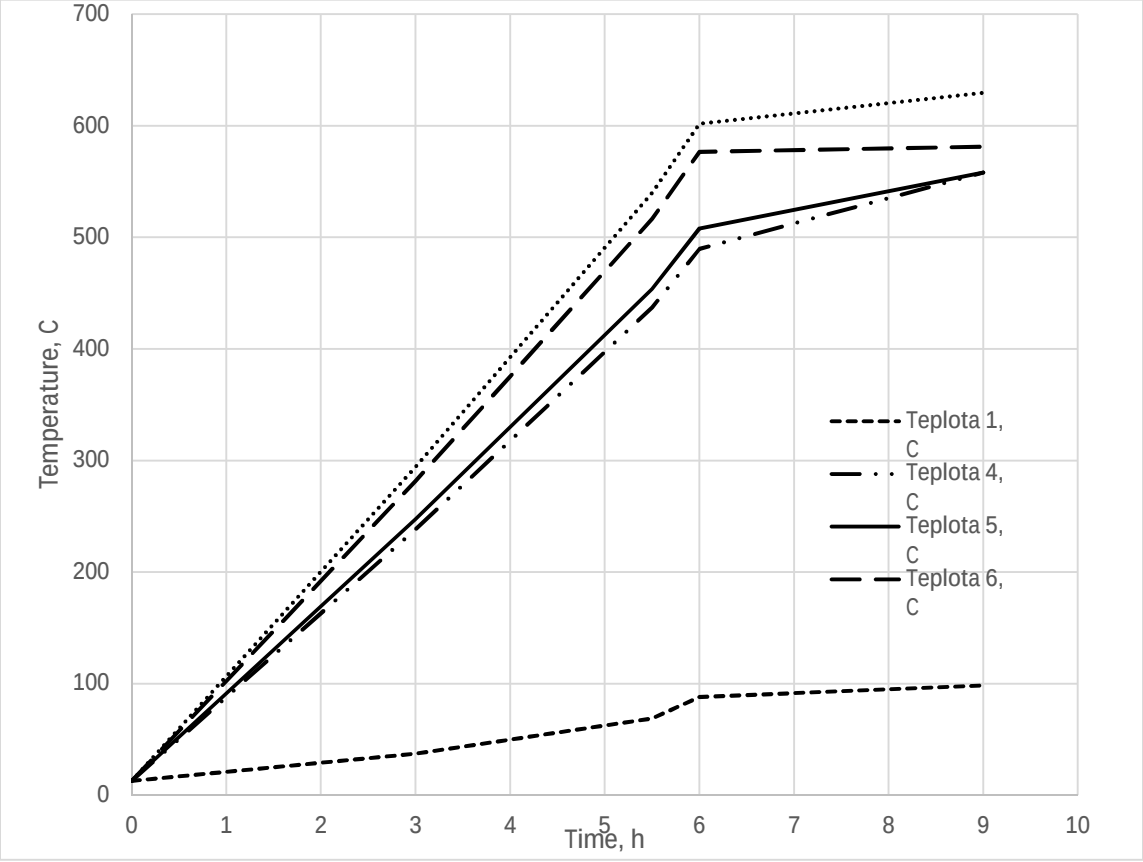

Figure 4-13 - Measured temperature for CT2 specimen

The measured temperature for CT2 specimen is shown in Figure 4-13. During the experiments, it was difficult to achieve a uniform and coordinated operation of all ceramic panels, which affected the final heating of the samples. The load on the CT6

column reached 2000 kN (the maximum of the hydraulic cylinder), so it is not quite correct to consider it as collapsed.

The measured temperature for thermocouple Figure 4-13s 4 and 6 for the speciments CT1, CT2, CT3, CT4, CT5 AND CT6 shown in a Figure 4-14.

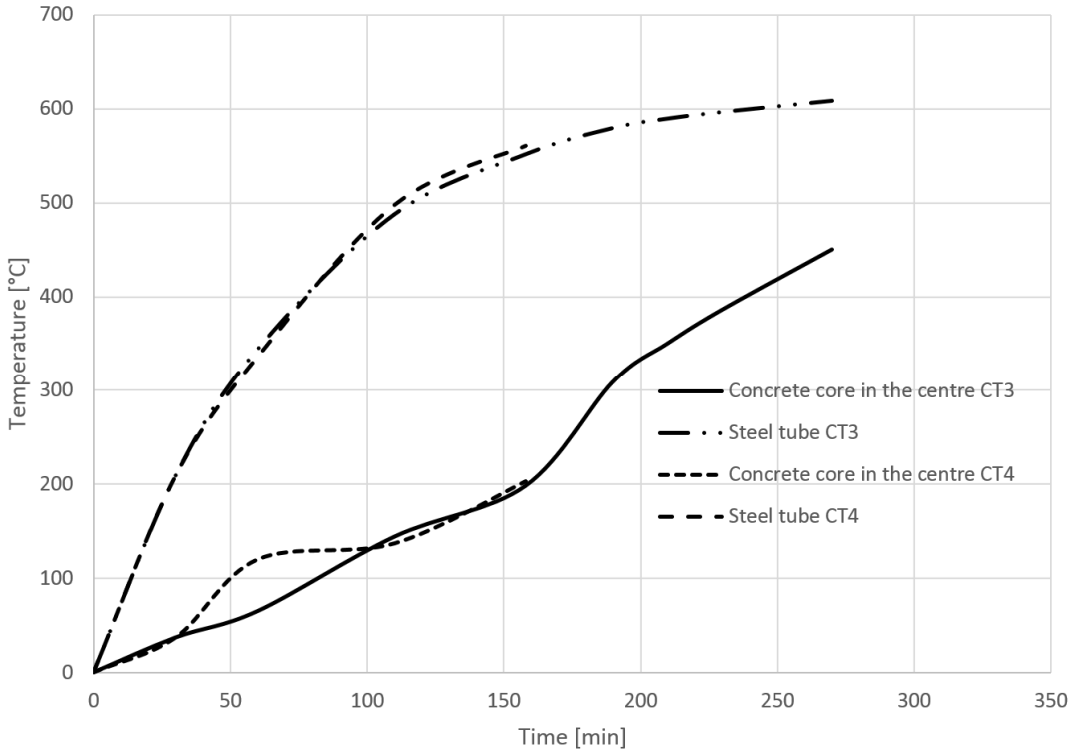

a)

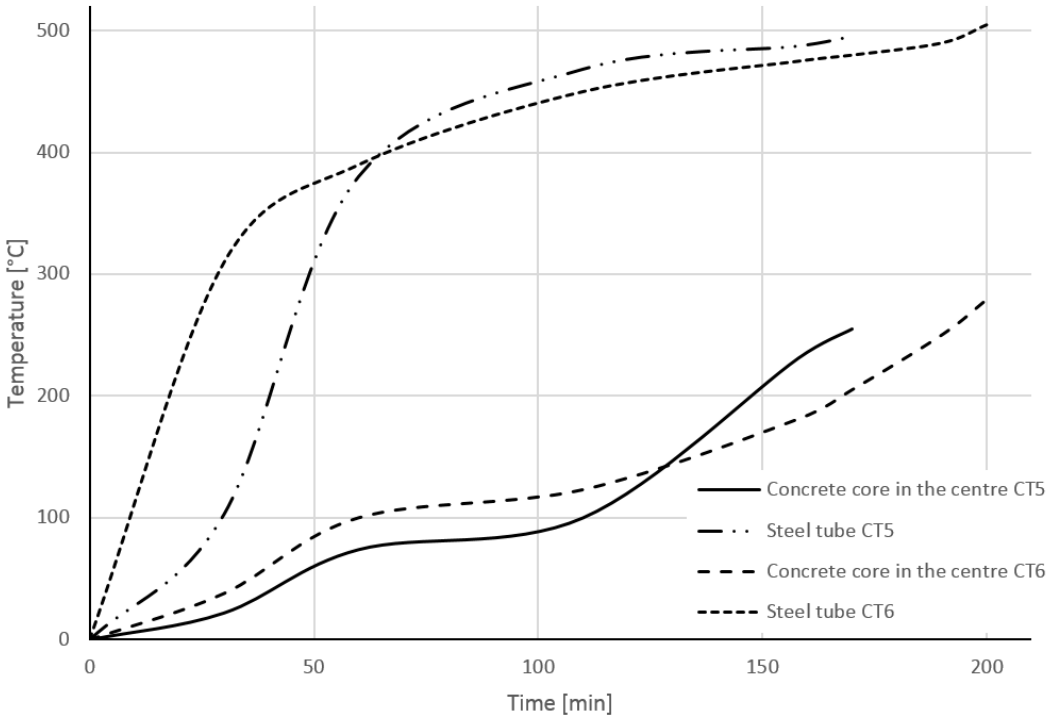

b)

Figure 4-14 - Measured temperature for specimens a) CT3 and CT 4 b) CT5 and CT6

CHAPTER 5. NUMERICAL MODEL AND VALIDATION

5.1. GENERAL

A FEM fire response model of the steel fibre reinforced concrete filled tubular column (three-dimensional) using ATENA Červenka software was performed by Tretyakov, Tkalenko and Wald [114]. SFRC material model in the ATENA software to determinate mechanical and thermal behaviour was developed. These properties were implemented to global behaviour model. Developed numerical model considering account thermal and mechanical (tension) behaviour of SFRC and was validated. The ATENA software was chosen due to the included fracture-plastic temperature-dependent concrete model. The limitation in the thermal model was found in terms of modelling the air gap between steel and concrete. The problem was solved by adjusting the fire load independently for steel and concrete. This assumption causes a higher temperature of the steel tube and provides accurate temperature distribution in the concrete core for chosen validation cases. Fracture – plastic model of concrete material developed by Červenka was used in the mechanical FEM model. Post-peak plastic strain of SFRC in compression and tension were implemented using compression toughness index proposed by Marar et al. [95] and SDEM method by Lee et al. [96]. Both methods were verified against experimental studies on advanced models performed in ATENA. Verification was made for concretes with different compressive strengths and percentages of steel fibres and showed relatively accurate results. The combination of chosen methods allows for predicting post-peak behaviour of FRC depending on compressive strength and fibre-reinforcement index.

The advanced FEM model for steady-state regime was developed in ATENA software with a GID pre-processor based on described approach. This model was validated on own experiments from CHAPTER 4.

The steady-state global model of the column consists of the mechanical and thermal models. The thermal model calculates heat transfer and the mechanical model calculates the response of the column from vertical force and thermal loading. Analysis of the mechanical response was designed in the ATENA Static module. ATENA Transport module was used for the calculation of heat transfer.

A three-dimensional FEM fire response model of the steel fibre reinforced concrete filled tubular column in ATENA was used for parametrical study, as well.

5.2. DESRIPTION OF THE NUMERICAL MODEL

Thermal and mechanical models were made in 3-dimensional space. For higher efficiency of calculation and nature of the load, only half column was modelled. Model in GID pre-processor interface consists of points, lines, surfaces and volumes. Volumes sizes and placement were assumed in agreement with the need for measuring points and heating area. A six-sided volume and hexahedral mesh were chosen to expedite the modelling process. Thermal and mechanical models are compounds with the same volumes but from different mesh sizes and contact properties.

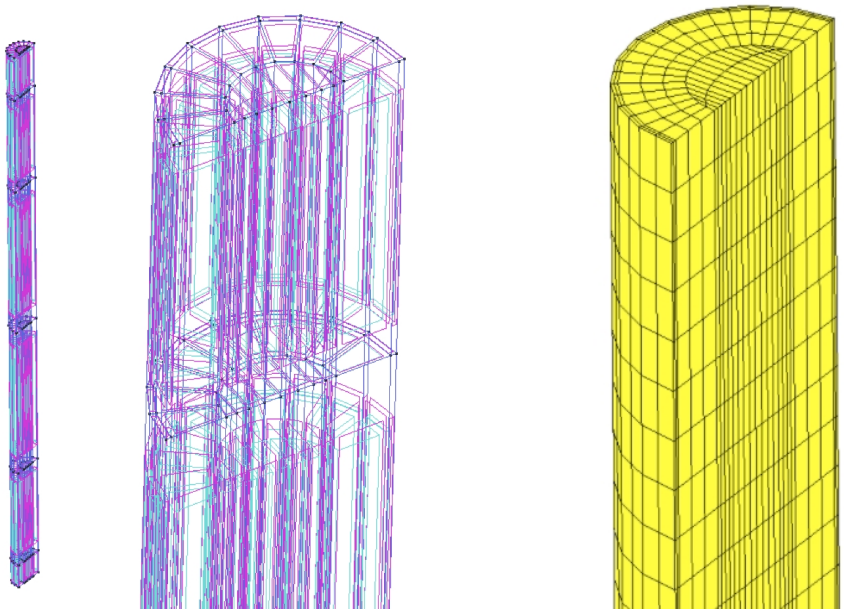

a) b)

Figure 5-1 Geometry of model: a)Surfaces and volumes; b) Mesh

The thermal model consists of steel pipe and concrete core. The elastic plates for assigning boundary conditions and contact 3D surfaces between materials were also accepted in the mechanical model. Geometry is shown in Figure 5-1.

The thermal properties of materials are reduced by two parameters – heat capacity and thermal conductivity. Following recommendations from the latest research in the branch of CFST columns [98] [111] both parameters were assumed under corresponding European standards.

For the concrete core, thermal properties were assumed according to EN 1992-1-2 [82]. Following EN1994-1-2 new method proposal recommendations,

concrete thermal conductivity for lower limit and heat capacity for 4 % concrete humidity was assumed [12].

For steel structures calculation, Von Mises yield criterion in ATENA software was used. The definition of the steel material model includes parameters such as Young Modulus, Poisson's ratio, yield strength, and the possibility of degradation due to elevated temperature. Bi-linear stress-strain relationship as per EN1993-1-1 [112] with reduction factors according to EN 1993-1-2.

The fracture-plastic model of concrete material developed by Červenka [51] was used in the mechanical model (material prototype CC3DNonLinCementitious2 WithTempDepProperties). Definition of the concrete material model includes parameters as compressive strength crack reduction factor, Young's modulus, Poisson's ratio, tension strength, fracture energy, aggregate size, plastic strain, the onset of crushing, critical compression displacement and a possibility to set degradation due to elevated temperature. SFRC material model compatible with ATENA and GID interface was developed by Tretyakov [114].

The thermal expansion of the steel material under the corresponding EN 1993-1-2 [37] standard was assumed. The thermal expansion coefficient of the SFRC material was assumed to be a constant value of α_c = 3.5x10^{-6}°C^{-1}. The influence of the thermal expansion is described in more detail below in the sensitivity study.

Because of the separate deformation of the steel tube and concrete core during the heating, the contact interfaces between the materials were assigned. The interface between the top and vertical interfaces was assumed to have a tangential strength of 1 MPa (cohesion), zero normal strength (tension), and a friction coefficient of 0.3. The bottom interface was assumed to be fixed owing to the calculation efficiency. The stiffness of the interfaces based on the ATENA Troubleshooting manual [113] was set. Value of initial stiffness is given by equation *(5)*

$$K = E / elem\_size \cdot 10 \quad (4)$$

The residual stiffness value was set as K /1000 under manual recommendation.

The interface between top and vertical interfaces were assumed with 1 MPa tangential strength (cohesion), zero normal strength (tension), and 0.3 friction coefficient. The bottom interface was taken as fixed due to calculation efficiency.

Tangential stiffness of the side surface was assumed as 1/100 of the top surface to prevent possible residual tensile stress appearance during steel expansion.

Specimens have pinned-pinned boundary conditions. All geometrical parameters (including heating area) were taken from the experimental study as in Figure 4-7. Analyses of the mechanical model in three intervals with different boundary conditions were performed. In the first interval, imperfections such as L/1000 horizontal middle deformation in the first bending mode based on the work of Espinos [111] recommendation were accepted.

For the first interval, the pinned constraint and vertical forces on the side of the elastic plate for bending on the ends of the column were assigned.

Steel and concrete materials for the first interval were set as elastic with a negligible elasticity module. Thus, only the deformed shape with no residual stresses continues to the second interval calculation. Monitors for deflection and temperature measurements were set as per the experimental setup. For the second interval, boundary conditions on the ends of the columns, in agreement with the experiment were accepted. In the third interval, identical boundary conditions were left, and the fire load from the thermal model was imported.

In the fourth interval, a load of 2 kN was added to half of the column in one step until the sample failed.

The thermal model was calculated at a two-calculation interval with thermal loading. For validation, only a part of the column inserted into the furnace was loaded. The fire loading implements the following experimental values from ceramic pads (Figure 4 9). In the first interval, the temperature was set to 599°C and 499°C, respectively. In the second heating interval, after reaching this temperature, until the end of heating, the temperature rose by another °C. This method of loading in the steady-state regime is associated with the peculiarities of the ATENA software.

Boundary conditions for the thermal model are shown in Figure 5-2.

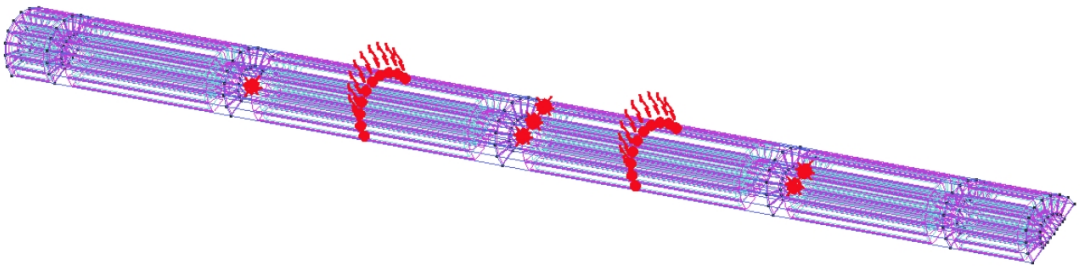

Figure 5-2 Boundary conditions - view on thermal model

5.3. CALCULATION PROCEDURE

While all the parameters of the FEM model and made assumptions were discussed, the procedure of the calculation and exact input parameters will be shown in this chapter. As mentioned above, the model was performed in GID preprocessor software and is further calculated with ATENA software. Firstly thermal calculation in ATENA Transport should be performed, and in the second step global mechanical model in the ATENA Static module is calculated using thermal model results. The calculation of the thermal model is adjusted for the two calculating intervals. The analysis of the mechanical model proceeds within four calculating intervals. Where for each interval, different boundary conditions and materials are used. A graphical illustration of the calculation procedure is shown in *Figure 5-3*.

The whole input parameters for GID preprocessor software for the ATENA Transport module are shown in Table 5-1.

Table 5-1 Input parameters for GID pre-processor for ATENA Transport module

Part	**Parameter**	**Description**
GEOMETRY	Volume type	Six sided volumes
	Mesh type	Hexahedral
	Mesh size	Max. size 40 mm
	Materials	SFRC, Steel
THERMAL PROPERTIES OF FRC	Concrete material prototype	CCTransportMaterial
	Activate Temperature	ON
	K TEMP TEMP NORMAL (Thermal conductivity)	= 1.36 $\frac{W}{C \cdot m}$
	C TEMP TEMP NORMAL (Heat capacity)	= $2.07 \cdot 10^6 \frac{J}{m^3 \cdot C}$
	Activate Temperature Advanced	ON
	Activate Temperature Variable Values	ON
	K TEMP TEMP FNC	ON
	Activate K TEMP TEMP FNC TEMP	ON, function under EN 1992-1-2, for lower limit
	C TEMP TEMP FNC	ON
	Activate C TEMP TEMP FNC	ON, function under EN1994-1-2, for 4% moisture content

Part	Parameter	Description
THERMAL PROPERTIES OF STEEL	Concrete material prototype	CCTransportMaterial
	Activate Temperature	ON
	K TEMP TEMP NORMAL (Thermal conductivity)	= 53.334 $\frac{W}{C \cdot m}$
	C TEMP TEMP NORMAL (Heat capacity)	= $3.45 \cdot 10^6 \frac{J}{m^3 \cdot C}$
	Activate Temperature Advanced	ON
	Activate Temperature Variable Values	ON
	K TEMP TEMP FNC	ON
	Activate K TEMP TEMP FNC TEMP	ON, function under EN 1993-1-2
	C TEMP TEMP FNC	ON
	Activate C TEMP TEMP FNC	ON, function under EN1993-1-2,
BOUNDARIES I. INTERVAL	1. Fire boundary for surface	ETK fire curve, on steel outer surface
	2. Fire boundary for surface	ETK fire curve, on concrete outer surface
	Monitors for point	3x in ½ of length, in ½, ¼ of concrete core and on steel outer surface

The whole input parameters for GID preprocessor software for ATENA Static module are shown in Table 5-2.

Table 5-2 Input parameters for GID pre-processor for ATENA Static module

Part	Parameter	Description
GEOMETRY	Volume type	Six sided volumes
	Mesh type	Hexahedral
	Mesh size	Max. size 40 mm
	Materials	I. Interval: elastic concrete, elastic steel, bond bottom interface, bond side interface, bond top interface, elastic plates for boundary conditions II.-III. Intervals: fracture-plastic concrete, Von Mises steel, realistic top interface, realistic side interface, bond bottom interface elastic plates for boundary conditions

Part	Parameter	Description
ELASTIC PLATES	Material prototype	SOLID Elastic
	Young's Modulus	= 20000000000 GPa
	Poisson's ration	= 0.3
	Thermal expansion – alpha	= 0 $℃^{-1}$
ELASTIC CONCRETE	Material prototype	SOLID Elastic
	Young's Modulus	= 10 kPa
	Poisson's ration	= 0.2
	Thermal expansion – alpha	= 0 $℃^{-1}$
ELASTIC STEEL	Material prototype	SOLID Elastic
	Young's Modulus	= 10 kPa
	Poisson's ration	= 0.3
	Thermal expansion – alpha	= 0 $℃^{-1}$
BOND INT.TOP	Material prototype	CC3DInterface
	Normal stiffness	= $2.0 \cdot 10^{10} \frac{MN}{m^3}$
	Tangential stiffness	= $2.0 \cdot 10^{10} \frac{MN}{m^3}$
	Cohesion	=500 MPa
	Friction coefficient	=1
	Tension strength	=50 MPa
	Min Norm Stiff-K NN MIN	= $2.0 \cdot 10^{7} \frac{MN}{m^3}$
	Min Tang Stiff-K TT MIN	= $2.0 \cdot 10^{7} \frac{MN}{m^3}$
BOND INT.SIDE	Material prototype	CC3DInterface
	Normal stiffness	= $2.0 \cdot 10^{10} \frac{MN}{m^3}$
	Tangential stiffness	= $2.0 \cdot 10^{10} \frac{MN}{m^3}$
	Cohesion	=500 MPa
	Friction coefficient	=1
	Tension strength	=50 MPa
	Min Norm Stiff-K NN MIN	= $2.0 \cdot 10^{7} \frac{MN}{m^3}$
	Min Tang Stiff-K TT MIN	= $2.0 \cdot 10^{7} \frac{MN}{m^3}$
BOND INT. BOTTOM	Material prototype	CC3DInterface
	Normal stiffness	= $2.0 \cdot 10^{10} \frac{MN}{m^3}$
	Tangential stiffness	= $2.0 \cdot 10^{10} \frac{MN}{m^3}$
	Cohesion	=500 MPa
	Friction coefficient	=1
	Tension strength	=50 MPa
	Min Norm Stiff-K NN MIN	= $2.0 \cdot 10^{7} \frac{MN}{m^3}$

Part	Parameter	Description
	Min Tang Stiff-K TT MIN	= $2.0 \cdot 10^7 \frac{MN}{m^3}$
VON MISES STEEL	Material prototype	CC3DBiLinearVonMises WithTempDepProperties
	Young's Modulus	= 210 GPa
	Poisson's ration	= 0.3
	Stress-strain relationship type	Bilinear
	Yield Strength	Corresponding to the case MPa
	Hardening modulus	0 MPa
	Temp. Dep. Mat. Function for E	EN1993-1-2 Table 3.1
	Temp. Dep. Mat. Function for Yield St.	EN1993-1-2 Table 3.1
	Temp. Dep. Mat. Function for EPS T	EN1993-1-2 3.4.1.1
FRACTURE-PLASTIC CONCRETE/FRC	Material type	SOLID Concrete – Concrete EC2
	Material prototype	CC3DNonLinCementitious2 WithTempDepProperties
	Young's Modulus	Corresponding to the case and EN1992-1-1
	Poisson's ration	= 0.2
	Tension strength	Corresponding to the case PC - EN1992-1-1 – mean value SFRC – SDEM + Xu and Shi [22]
	Compression strength	Corresponding to the case EN1992-1-1 – mean value
	Fracture energy	Corresponding to the case PC - EN1992-1-1 – mean value SFRC – SDEM + Xu and Shi [22]
	Fixed crack	= 1
	Activate Aggregate Interlock	ON
	Agg Size	= 0.02 m
	Plastic Strain – EPS CP	Corresponding to the case and EN1992-1-1
	Onset of Crushing – FC0	Corresponding to the case Generation formula –FT(PC)*2.1
	Critical compressive displacement	Corresponding to the case NSC = -1.35 mm, HSC = -0.5 mm (validated for 40 mm mesh) SFRC: $W_{d,SFRC} = W_{d,PC} \cdot T_{if}$ per Marar et al [24]
	Fc Reduction	PC: = 0.8, SFRC: = 1

Part	Parameter	Description
	Eccentricity - EXC	= 0.52 (Default value)
	Direction of plastic Flow-BETA	= 0 (Default value)
	Rho - Density	= 2300 kg/m³
	Temp. Dep. Mat. for E	Per EN1992-1-2
	Temp. Dep. Mat. for FT	Per EN1992-1-2
	Temp. Dep. Mat. for FC	Per EN1992-1-2
	Temp. Dep. Mat. for FC0	Per EN1992-1-2
	Temp. Dep. Mat. for WD	Per EN1992-1-2
	Temp. Dep. Mat. for EPS CP	Per EN1992-1-2
	Temp. Dep. Mat. for GF	PC: default Siliceous FRC: as for FT per EN1992-1-2
	Temp. Dep. Mat. for EPS T	Corresponding to constant α_c = 3,5x10^{-6}°C^{-1}
REAL INT.TOP	Material prototype	CC3DInterface
	Normal stiffness	= $4.0 \cdot 10^5 \frac{MN}{m^3}$
	Tangential stiffness	= $4.0 \cdot 10^5 \frac{MN}{m^3}$
	Cohesion	=1 MPa
	Friction coefficient	=0.3
	Tension strength	=0 MPa
	Min Norm Stiff-K NN MIN	= $4.0 \cdot 10^2 \frac{MN}{m^3}$
	Min Tang Stiff-K TT MIN	= $4.0 \cdot 10^2 \frac{MN}{m^3}$
REAL INT.SIDE	Material prototype	CC3DInterface
	Normal stiffness	= $2.0 \cdot 10^5 \frac{MN}{m^3}$
	Tangential stiffness	= $2.0 \cdot 10^3 \frac{MN}{m^3}$
	Cohesion	=0.1 MPa
	Friction coefficient	=0.3
	Tension strength	=0 MPa
	Min Norm Stiff-K NN MIN	= $2.0 \cdot 10^2 \frac{MN}{m^3}$

Part	Parameter	Description
	Min Tang Stiff-K TT MIN	= $2.0\frac{MN}{m^3}$
BOUNDARIES I. INTERVAL - IMPREFECTION	Surface constraint	Surfaces flat mirror side in axis Y
	Point constraint	Top and bottom middle point of circle Constraint in all directions
	Force for point	Top and bottom outer points on flat side. Forces in opposite directions in Z axis to bent sample
	Monitors for point vertical displacement	2xMiddle top points on top interface on the concrete and elastic plate
	Monitors for point hor. displacement	1xOn the outer point in the middle of height, direction X
	Monitors for point temperature	3x in ½ of length, in ½, ¼ of the concrete core and on the steel outer surface
	Interval multiplier	Corresponding to the case to reach H/1000 imperfection
	Number of steps	= 5
BOUNDARIES II. INTERVAL – MATERIALS	Surface constraint	Surfaces flat mirror side in axis Y
	Point constraint	Corresponding to the case: P-P
	Interval multiplier	Corresponding to the case to define load
	Number of steps	= 5
	ON material activity for interval	material change from elastic to “realistic”
BOUNDARIES III. INTERVAL – THERMAL LOAD	Surface constraint	Surfaces flat mirror side in axis Y
	Point constraint	Corresponding to the case: P-P
	Interval multiplier	1
	Number of steps	Corresponding to the case
	Read transport data	ON

Part	Parameter	Description
BOUNDARIES IV. INTERVAL – MECHANICAL LOAD	Surface constraint	Surfaces flat mirror side in axis Y
	Point constraint	Corresponding to the case: P-P, F-P, F-F
	Interval multiplier	2
	Number of steps	Corresponding to the case
	Force for point	Top point of column, corresponding to case (axial)
	Read transport data	ON

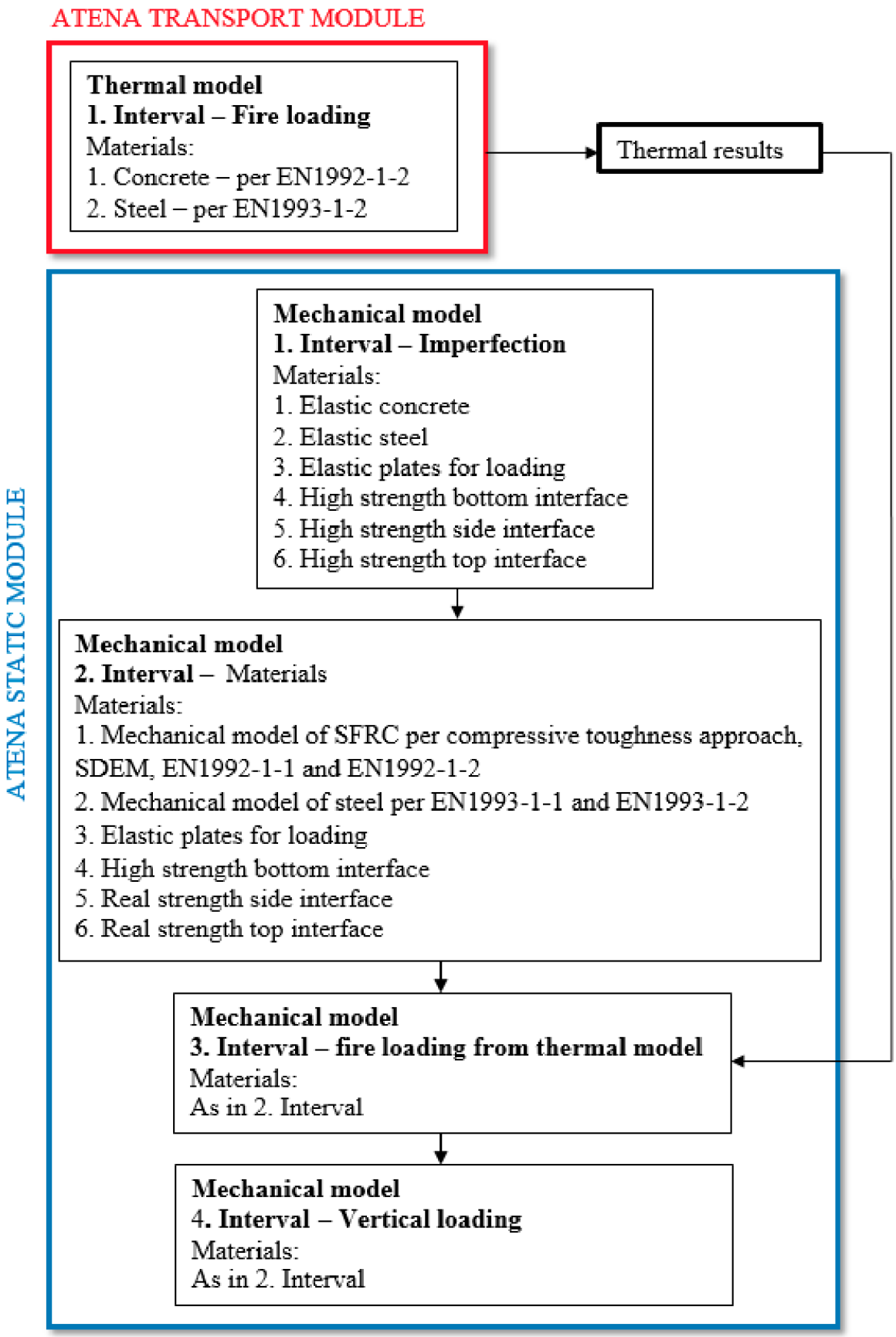

Figure 5-3 Calculation procedure

5.4. THERMAL MODEL VALIDATION

Heating by ceramic pads was necessary to obtain a certain temperature on the steel tube and inside the concrete core. During the experiments, it was difficult to achieve a uniform and coordinated operation of all ceramic panels, which affected the final heating of the samples. However, applied thermal load in ATENA shows acceptable convergence of results as shown in the Figure 5-5 and Figure 5-4.

a)

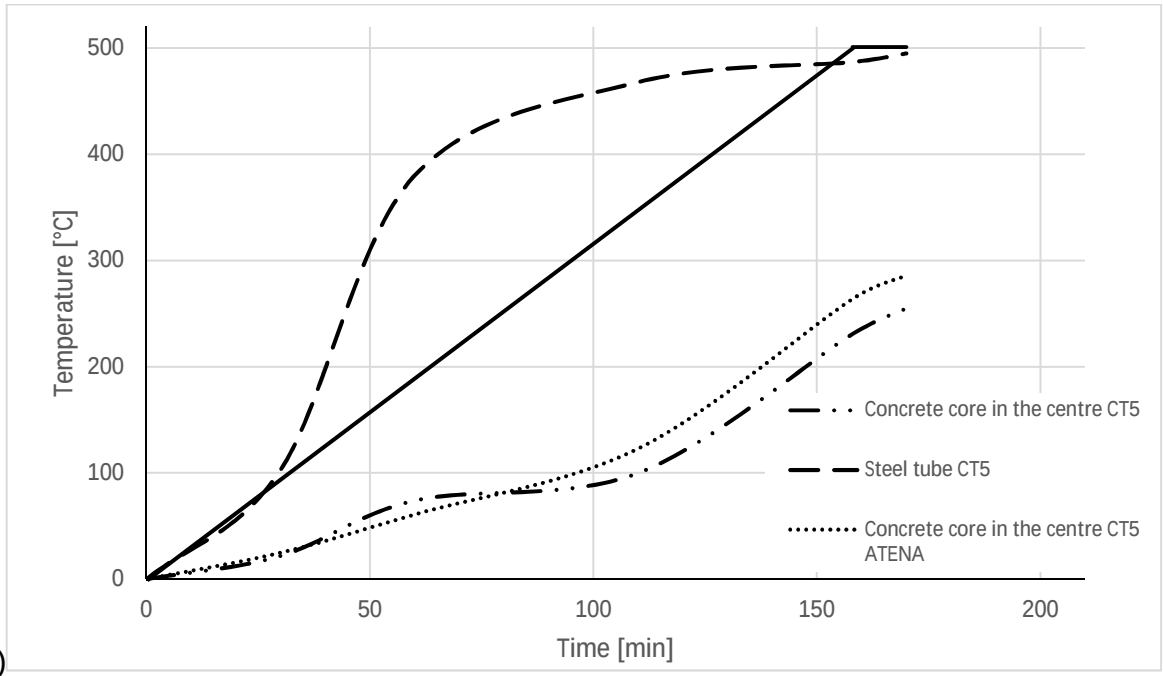

b)

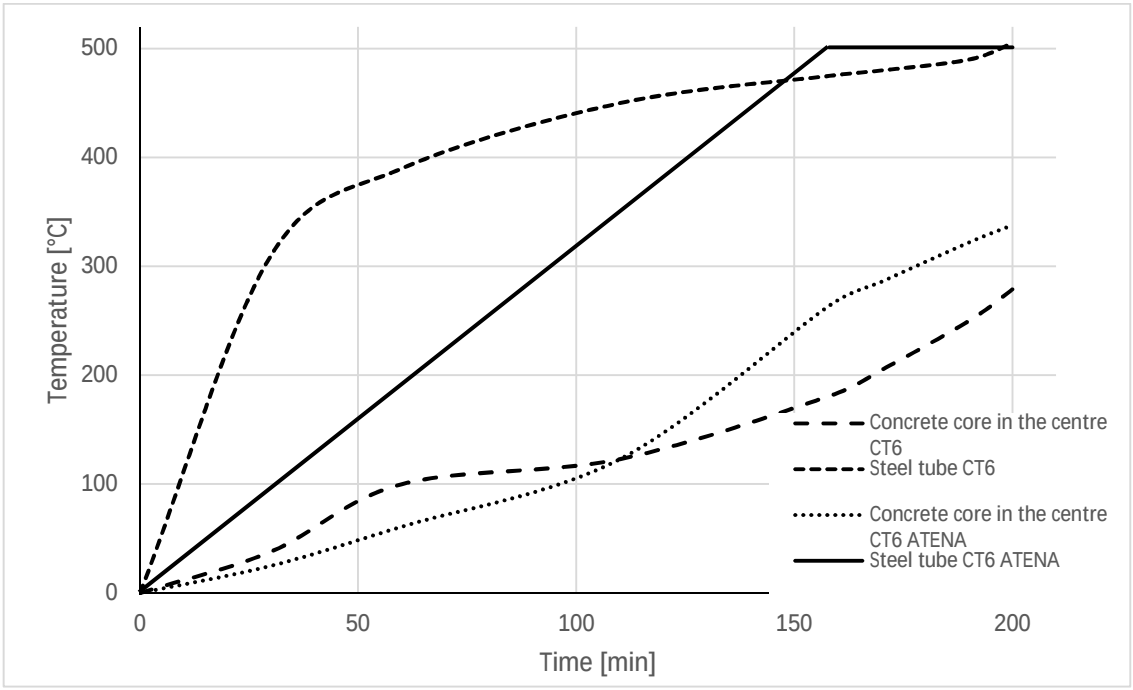

Figure 5-4 Temperature distribution comparison between experiment and FEM calculation for a) CT5 b) CT6

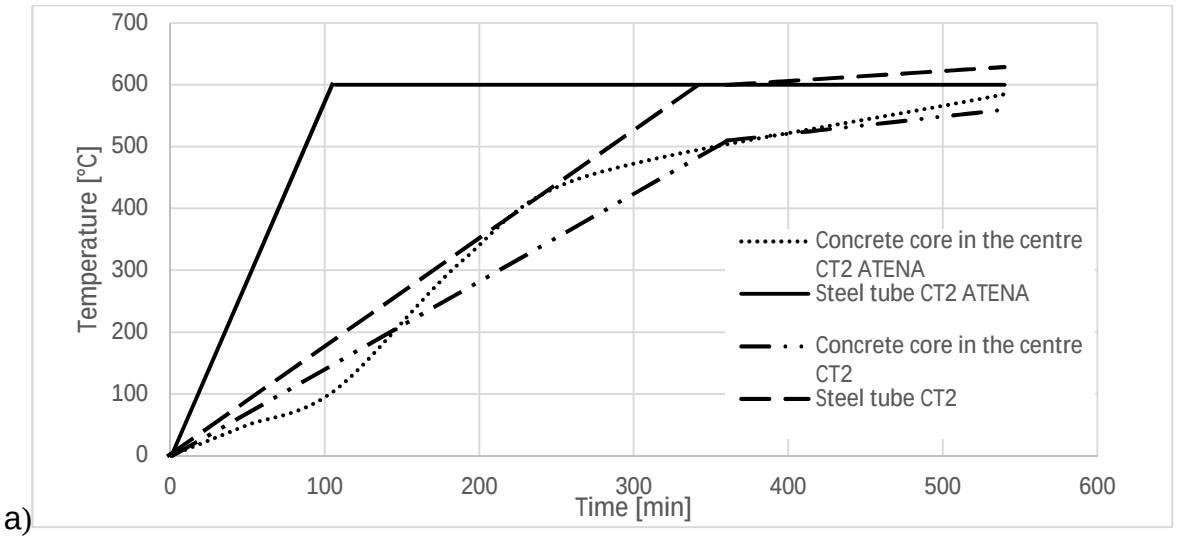

a)

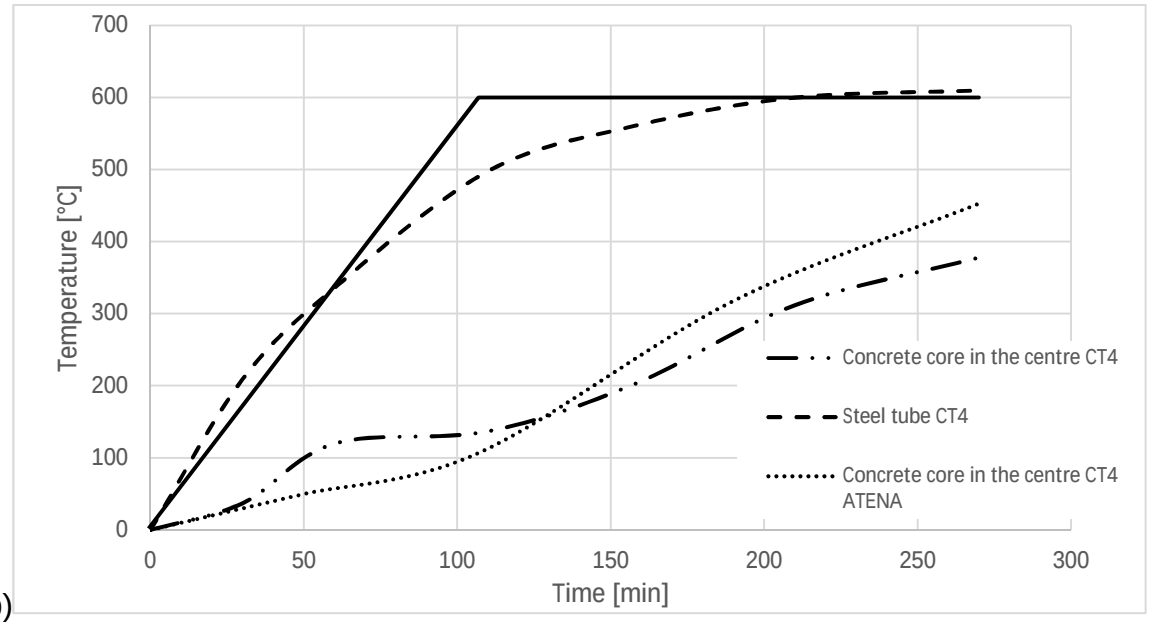

b)

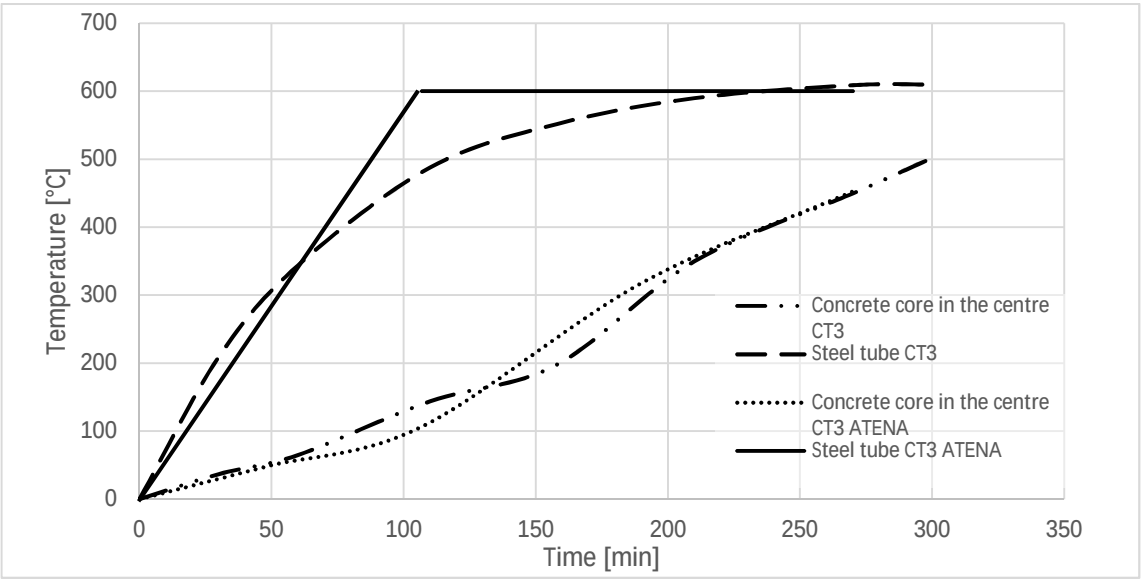

c)

Figure 5-5 Temperature distribution comparison between experiment and FEM calculation a) CT2 b) CT3 c) CT4

With CT3 and CT6, up to 21 % higher temperature in centre of the concrete core in FEM was attained. The different concrete moistures can explain this deviation. Also, problems can be due to not proper control during the heating process or insolation problem. Assumed that the heating of the column was performed improperly. Other columns concrete temperature difference does not exceed 12 %. The difference in the temperature of the steel tubes does not exceed 5 %.

While the thermal model shows good agreement for thin-walled pipes, the different temperature distribution in the section could happen with the change in the pipe wall thickness. The further numerical and parametrical study does not include pipe thickness change (6 mm). Because of the accurate temperature distribution in concrete in the selected cases, the thermal model was considered acceptable for the project.

5.5. VERIFICATION ON EXPERIMENTS IN STEADY STATE

For the SFRC following material properties ware taken in account: f_c =75 MPa, W_d =-1,33 mm, f_t = 2,6 MPa and G_f = 8100 N/m. These values correspond to those proposed by Tretykov [114]. Calculation results are presented in Table 5-3. The typical failure modes observed are shown in Figure 5-6.

Table 5-3 Comparison of FEM and experimental results

Col. No	Time of heating, [min]	Temperature of pads, C	N, kN		$\frac{N_{FEM}}{N_{TEST}}$
			Test	FEM	
CT2	520	600 C	786	692	0,88
CT3	300	600 C	763	740	0,97
CT4	270	600 C	1082	844	0,78
CT5	170	500C	1860	1640	0,88
CT6	200	500 C	> 2000	1252	0,63

All results are on the safe side. For the specimens CT2, CT3, CT4 and CT5 average difference is 13%<15%.

For CT6 difference of more than 37%. As shown in Figure 5-4, during the numerical test temperature of the concrete core was much more than experiment value. It is assumed that the heating of the column was performed improperly.

a)  b) 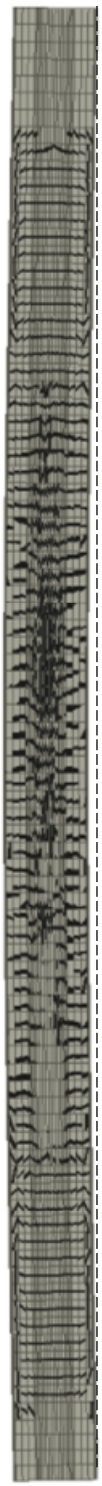

Figure 5-6 Comparison between a) actual fail of the CT2 and b) predicted deformed model

The behaviour of columns during the experiment in steady-state regime shows global buckling failure mode. Average axial deformation curves of specimens in steady-state compression test and predicted using FEM shown in Figure 5-7.

a)

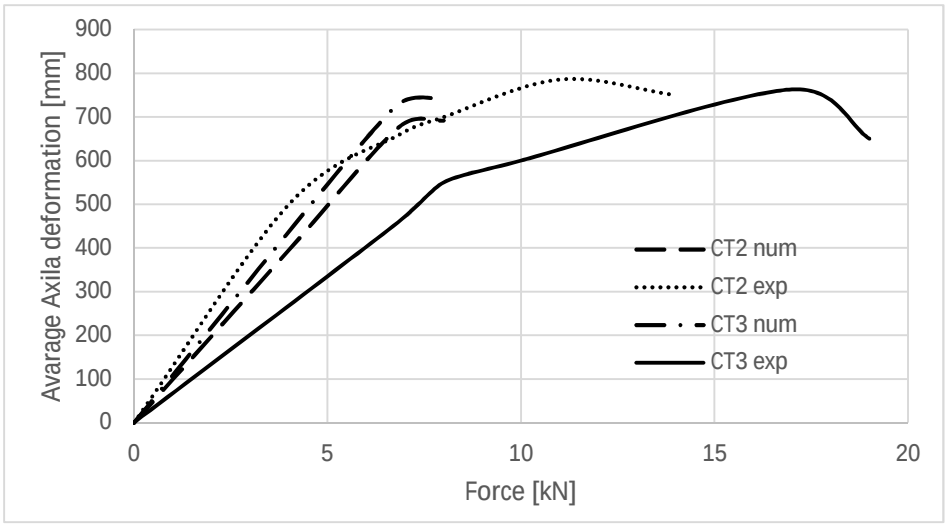

b)

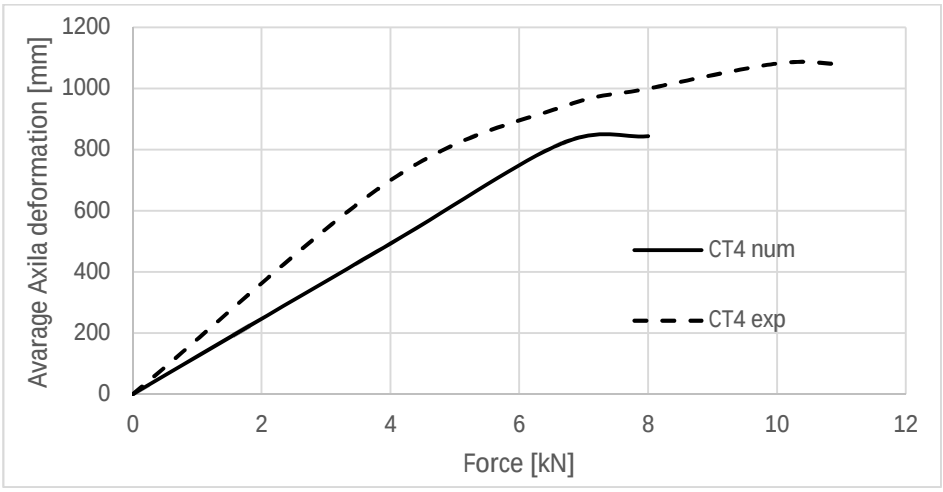

c)

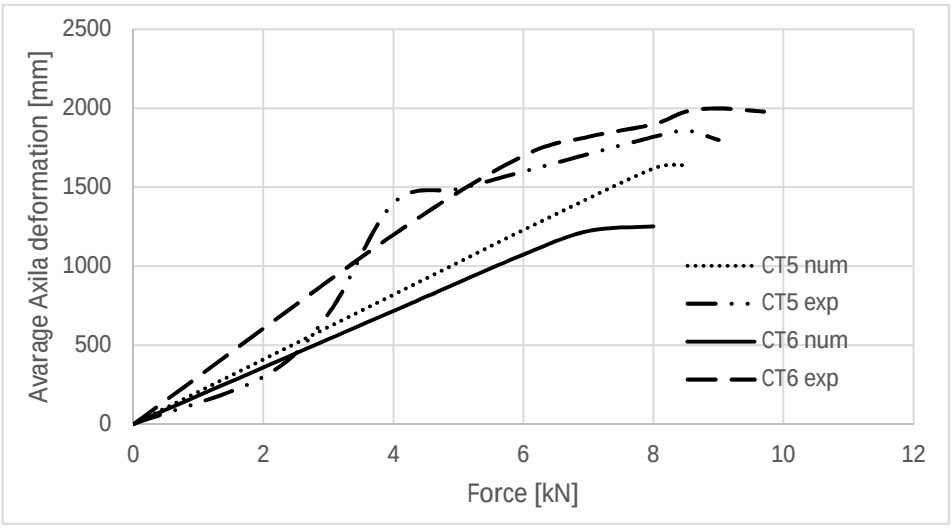

Figure 5-7 Average axial deformation curves of specimens and predicted a) CT2 and CT3 b) CT4 c) CT5 and CT6.

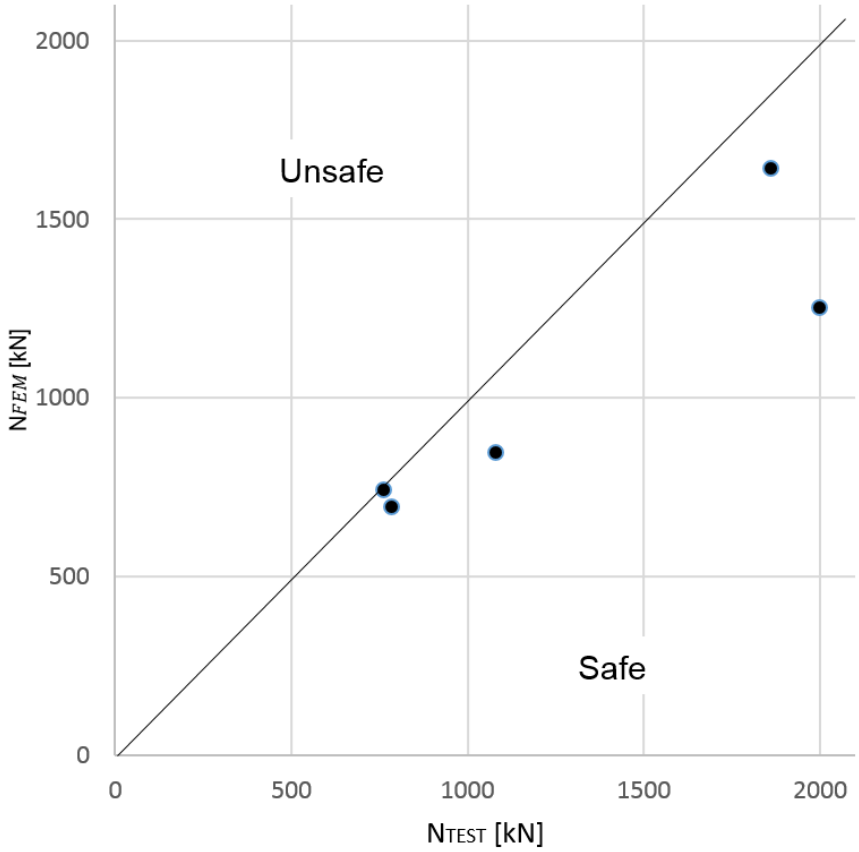

Figure 5-8 Predicted buckling load and experimental load for SFRC

A graphical representation of the results is presented in Figure 5-8. From the graphical representation, it can be observed model gives -13% safety in steady-state regime.

The proposed model has been validated in the steady-state experiments and can be used in further studies. The results obtained are in the safe area.

CHAPTER 6. PARAMETRIC STUDY

6.1. GENERAL

The numerical model developed in ATENA software was used for conducting a parametric study under ISO standard fire conditions. Numerical experiments were provided based on prepared combinations. A parametric study aimed to compare fire resistance of centrally and eccentrically loaded circular hollow section columns with steel fibre-reinforced and plain concrete infill in a fire situation.

6.2. COMBINATIONS OF ANALYSIS CASES FOR THE PARAMETRIC STUDIES.

The parameters studied were the outer diameter D of the columns, the wall thickness of the steel tube *t*, the relative slenderness of the columns at room temperature $\bar{\lambda}$, fiber content ρ_f the load level μ and the relative eccentricity e/D.

A study was carried out in order to define the cases for analyse in the parametric study. The cross-section dimensions and ranges of variation of the parameters were decided. Table 6-1 shows the range of variation of the parameters, resulting in a total of 9 circular columns, which means a total amount of 82 numerical simulations combining the different parameters. It should be pointed out that specimens were designed without bar reinforcement. Input parameters adopted were as follows: P-P (pinned-pinned) boundary conditions, 4 % moisture content, 355 MPa steel tube yield strength, 30 MPa cylindrical concrete compressive strength.

Table 6-1 - Combinations of analysis cases for the parametric studies

D, mm	159	324	406,4
t, mm		6	
$\bar{\lambda}$	0,3	0,5	1
ρ_f,%		0,5	0
Concrete		C 30 /37	
e / *D*	0	0,25	0,5
$N_{fi,Rd,num}$ is percentage of N_{Rd} or $N_{Rd,\delta}$, %	20	40	60

The thermal model has calculated at a single calculation interval with fire thermal loading. For validation, only a part of the column inserted into the furnace was loaded. The fire loading under the ISO834 and EN 1363-1 nominal standard fire curve with a 0,7 emissivity value of 25 W/Cm^2 was set independently for steel and

concrete in one model. Boundary conditions for the thermal model are shown in *Figure 6-1*.

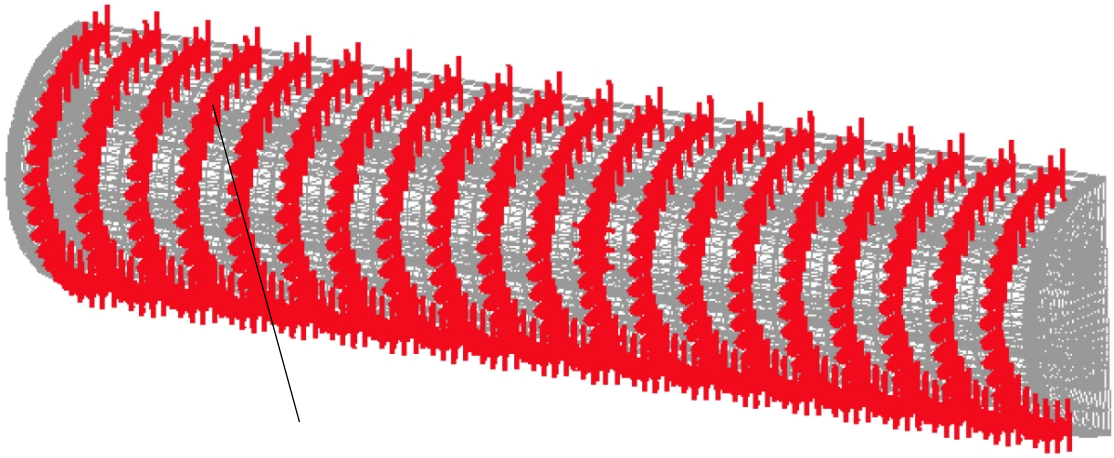

Figure 6-1 Boundary conditions - view on thermal model

Analyses of the mechanical model in three intervals with different boundary conditions were performed. In the first interval, imperfections such as L/1000 horizontal middle deformation in the first bending mode were accepted. For the first interval, the pinned constraint and vertical forces on the side of the elastic plate for bending on the ends of the column were assigned. Steel and concrete materials for the first interval were set as elastic with negligible elasticity moduli; thus, only the deformed shape with no residual stresses continues to the second interval calculation. Monitors for deflection and temperature measurements were set as per the experimental setup. For the second interval boundary conditions on the ends of the columns, in agreement with the experiment, the vertical force was accepted. In the third interval, identical boundary conditions were left, and the fire load from the thermal model was imported.

A graphical illustration of the calculation procedure is shown in *Figure 6-2*.

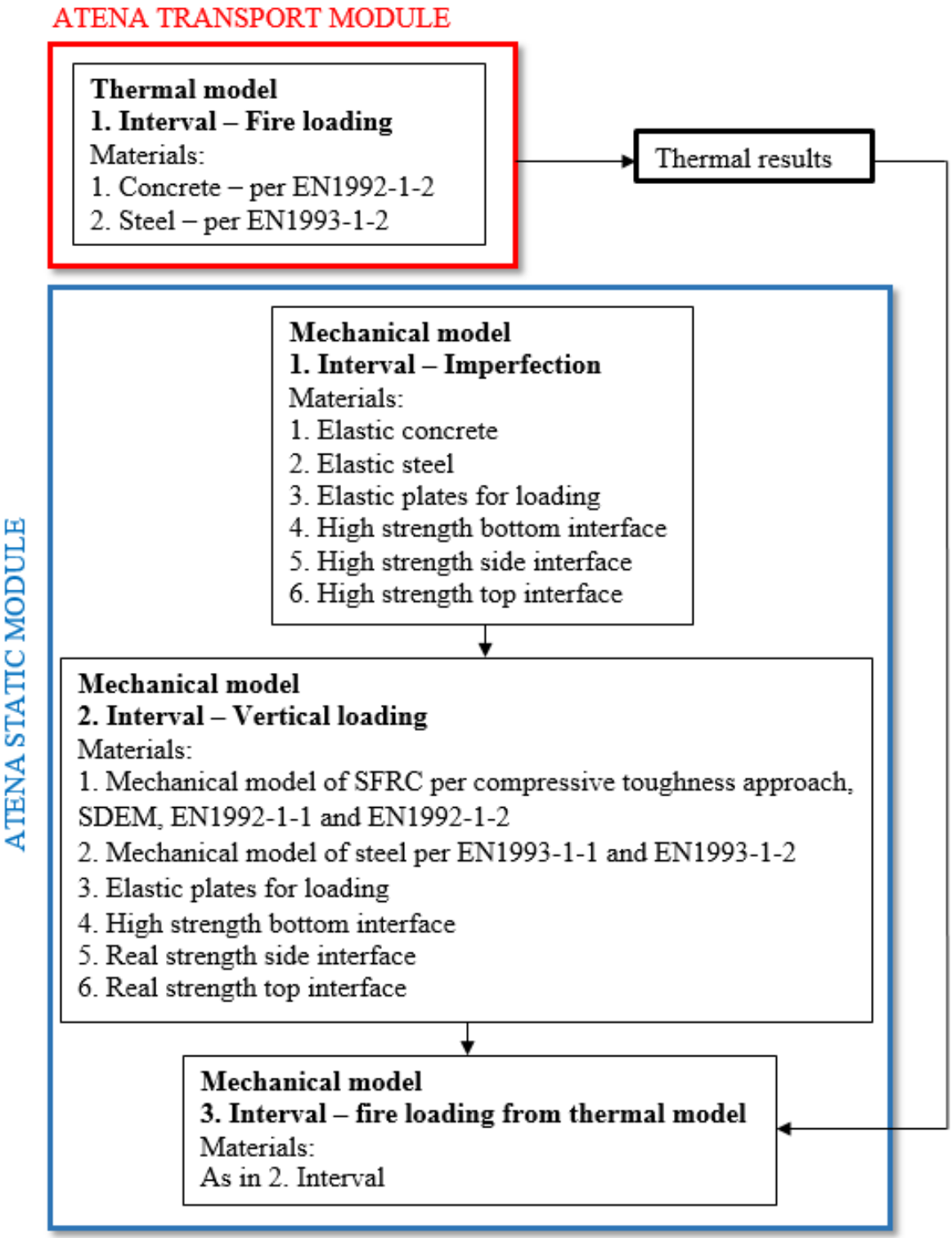

Figure 6-2 Calculation procedure

In addition to Table 5-1 and Table 5-2, the input parameters for transient-state numerical experiments loading steps for GID pre-processor software for ATENA Static module are shown in Table 6-2.

Table 6-2 Input parameters for transient-state numerical experiments GID pre-processor for ATENA Static module

Part	Parameter	Description
BOUNDARIES I. INTERVAL - IMPREFECTION	Surface constraint	Surfaces flat mirror side in axis Y
	Point constraint	Top and bottom middle point of circle Constraint in all directions
	Force for point	Top and bottom outer points on flat side. Forces in opposite directions in Z axis to bent sample
	Monitors for point vertical displacement	2xMiddle top points on top interface on the concrete and elastic plate
	Monitors for point hor. displacement	1xOn the outer point in the middle of height, direction X
	Monitors for point temperature	3x in ½ of length, in ½, ¼ of the concrete core and on the steel outer surface
	Interval multiplier	Corresponding to the case to reach H/1000 imperfection
	Number of steps	5
BOUNDARIES II. INTERVAL – MECHANICAL LOAD	Surface constraint	Surfaces flat mirror side in axis Y
	Point constraint	Corresponding to the case: P-P
	Force for point	Top point of column, corresponding to case (axial/eccentric)
	Interval multiplier	Corresponding to the case to define load
	Number of steps	= 5
	ON material activity for interval	Before the load is applying material change from elastic to “realistic”

BOUNDARIES III. INTERVAL – THERMAL LOAD	Surface constraint	Surfaces flat mirror side in axis Y
	Point constraint	Corresponding to the case: P-P
	Interval multiplier	1
	Number of steps	Corresponding to the case
	Read transport data	ON

6.3. RESULTS

The parametrical study made in ATENA software. Samples with 15 min < R < 240 min were excluded from the analysis. Total number of the numerical experiments limited by 84 calculations due to insufficient computing power. Parametrical study results for centrically loaded columns (30 pcs.) are presented in Table 6-3.

Table 6-3 - Parametrical study result for centrically loaded columns.

D, mm	L, mm	$R_{pc,num}$, min	$R_{sfrc,num}$, min	$N_{fi,Rd,num}$, kN
159	750	45	57	299,43
159	750	39	47	598,87
159	750	22	26	898,30
159	1900	24	34	538,23
159	1900	17	21	807,34
159	3800	16	16	579,78
324	1500	39	97	1586,67
324	3750	65	105	753,56
324	3750	22	28	1507,12
324	3750	18	21	2260,68
324	7500	16	17	1625,92

D, mm	L, mm	$R_{pc,num}$, min	$R_{sfrc,num}$, min	$N_{fi,Rd,num}$, kN
406,4	4600	41	150	1072,59
406,4	4600	23	36	2145,19
406,4	4600	22	35	3217,78
406,4	9300	16	17	2307,33

Parametrical study results for eccentrically loaded columns (54 pcs.) presented in Table 6-4.

Table 6-4 - Parametrical study result for eccentrically loaded columns.

D, mm	*L*, mm	*e/D*	$R_{pc,num}$, min	$R_{sfrc,num}$, min	$N_{fi,Rd,\delta,num}$, kN
159	750	0,25	95	119	149,96
159	750	0,25	67	78	299,91
159	750	0,25	50	60	449,87
159	750	0,50	92	105	110,42
159	750	0,50	62	86	220,85
159	1900	0,25	24	32	278,10
159	1900	0,50	26	32	201,76
159	3800	0,25	18	22	212,67
159	3800	0,50	24	26	152,68
324	1500	0,25	35	55	950,82
324	1500	0,25	30	53	1426,23
324	1500	0,50	32	46	585,12
324	1500	0,50	26	34	877,68
324	3750	0,25	68	71	424,21
324	3750	0,25	27	36	848,42
324	3750	0,25	24	26	1272,64
324	7500	0,50	45	47	197,48
324	7500	0,50	29	30	526,61
406,4	4600	0,25	26	36	583,99
406,4	4600	0,25	19	22	1167,98

D, mm	L, mm	e/D	$R_{pc,num}$, min	$R_{sfrc,num}$, min	$N_{fi,Rd,\delta,num}$, kN
406,4	4600	0,25	17	18	1751,97
406,4	4600	0,50	22	24	737,67
406,4	4600	0,50	18	20	1106,51
406,4	9300	0,25	24	28	799,14
406,4	9300	0,25	19	22	1198,71
406,4	9300	0,50	24	25	532,76
406,4	9300	0,50	20	21	799,14

A parametric study shows that in all experiments shows that $R_{sfrc,num}$, min > $R_{pc,num}$, min (Figure 6-3).

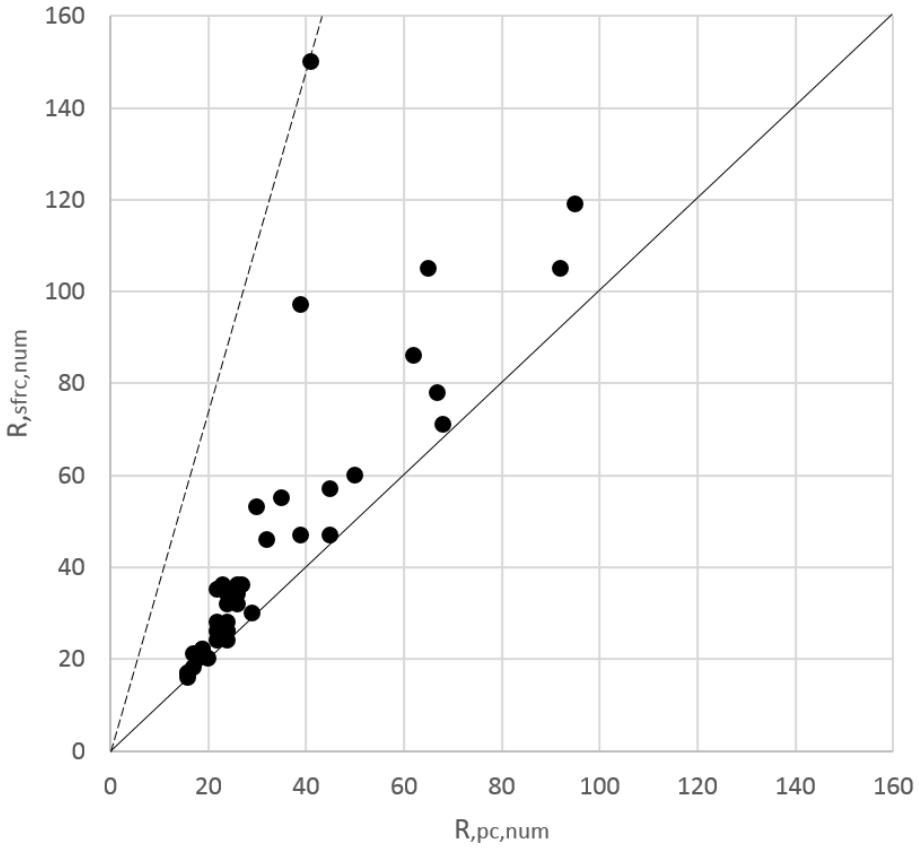

Figure 6-3 Comparison fire resistance results of PC and SFRC

In parametric study, we obtain R in min for the same load, but different concrete infilling of the CHS. Analytical model based on fact that of each centrically loaded

numerical experiments $N_{fi,Rd}$ for PC equal to $N_{fi,Rd}$ for SFRC, as well as for eccentrically loaded $N_{fi,Rd,\delta}$ for PC equal to $N_{fi,Rd,\delta}$ for SFRC.

$N_{fi,Rd,PC} = N_{fi,Rd,SFRC}$ to define flexural stiffness reduction coefficient. (5)

$N_{fi,Rd,\delta,PC} = N_{fi,Rd,\delta,SFRC}$to define reduction coefficient for eccentricity. (6)

Thus, it is necessary to solve the inverse problem.

CHAPTER 7. ANALYTICAL MODEL

7.1. GENERAL

This chapter focuses on the development of the analytical model and simplified method in addition to EC1994-1-2 [83] approach for the usage of SFRC CHS columns. As was shown in previous studies [114], SFRC concrete has benefits in bending compared to plain concrete. It is shown that EC1994-1-2 gives to conservative value of fire resistance (or fire design buckling load) because the stiffness of the SFCR core is not considered.

The method is based on the fact that fiber-reinforced concrete affects the effective flexural stiffness and, as a result, the design buckling load of the composite member. Analytical model to calculate flexural stiffness reduction coefficient $\varphi_{c,\theta}^{f}$and reduction coefficient for eccentricity α_f were proposed.

It is important that this solution is developed for the columns without bar reinforcement. Only SFR was used. Proposed simplified model in general in applicability limits of prepared for prEN1994-1-2:2024.

7.2. *PREN1994-1-2:2024* METHOD

Design axial buckling load in the fire situation:

$$N_{fi,Rd} = \chi \cdot N_{fi,pl,Rd} \quad (7)$$

Resistance reduction factor according to the European buckling curves χ (buckling curve “a”, reduction coefficient 0,21):

$$\chi = \frac{1}{\Phi + \sqrt{\Phi^2 - \bar{\lambda}_\theta{}^2}} \quad (8)$$

$$\Phi = 0{,}5 \cdot \left[1 + 0{,}21 \cdot \left(\bar{\lambda}_\theta - 0{,}2\right) + \bar{\lambda}_\theta{}^2\right] \quad (9)$$

relative slenderness in the fire situation:

$$\bar{\lambda}_\theta = \sqrt{\frac{N_{fi,pl,Rd}}{N_{fi,cr}}} \quad (10)$$

plastic fire design resistance of the cross-section to axial compression:

$$N_{fi,pl,Rd} \quad (11)$$

elastic critical load in the fire situation:

$$N_{fi,cr} = \pi^2 (EI)_{fi,eff} / l_\theta^2 \quad (12)$$

in our case l_θ (buckling length in the fire situation) equal to buckling length in room temperature as long as all column in fire.

Effective flexural stiffness in the fire situation

$$(EI)_{fi,eff} = \varphi_{a,\theta} E_a(\theta_{a,eq}) I_a + \varphi_{c,\theta} E_c(\theta_{c,eq}) I_c + \varphi_{s,\theta} E_s(\theta_{s,eq}) I_s \quad (13)$$

$\varphi_{a,\theta} E_a(\theta_{a,eq}) I_a$ – *following prEN1994-1-2:2024* [12].

$\varphi_{s,\theta} E_s(\theta_{s,eq}) I_s = 0$*, because bar reinforcement is absent.*

$\varphi_{c,\theta} E_c(\theta_{c,eq}) I_c$ *to be modified.*

For PC infilling for CHS coefficient is fixed to $\varphi_{c,\theta} = 0{,}8$. when the initial tangent stiffness (calculated as 3/2 times the secant modulus) is used. If the secant modulus of concrete is used, this coefficient $\varphi_{c,\theta} = 0{,}8$ equals 1,2. This assumption proposes by the authors [12]. This approached used for PC, however SFR improves ductility, compressive and tensile strengths of concrete, which are proposed to be taken into account by increasing flexural stiffness.

$$\varphi_{c,\theta} E_c(\theta_{c,eq}) I_c \rightarrow \varphi_{c,\theta} \cdot (3/2) \cdot k_c \cdot \left(\frac{f_c}{\varepsilon_{cu,\theta}}\right) \cdot I_c \quad (14)$$

Simplified cross-sectional temperature fields and reduction factors (including k_c) for a material property at elevated temperature following prEN1994-1-2:2024 [12].

For centrically loaded cased is necessary to modify flexural stiffness reduction coefficient $\varphi_{c,\theta}$ for plane concrete to $\varphi_{c,\theta}^f$ for SFCR (can be >1).

For eccentrically loaded columns design buckling load as following:

$$N_{fi,Rd,\delta} = \alpha \cdot \left(\frac{N_{Rd,\delta}}{N_{Rd}}\right)_{room} \cdot N_{fi,Rd} \quad (15)$$

N_{Rd} and $N_{Rd,\delta}$ following the design rules in EN 1994-1-1 [109].

Reduction coefficient for eccentricity

$$\alpha = \alpha_{Am/V} \cdot \alpha_{D/t} \cdot \alpha_R \cdot \alpha_s \quad (16)$$

$\alpha_{Am/V}$ and $\cdot\, \alpha_{D/t}$ *following prEN1994-1-2:2024* [12].

$\alpha_R = 6{,}9598 \cdot R^{-0{,}221} \qquad l_\theta / D \leq 15$

$\alpha_R = 0{,}92 \qquad l_\theta / D > 15$

$\alpha_s = 0{,}8$ - plane concrete.

For eccentrically loaded columns, it is necessary to add a reduction coefficient for SFRC - α_f, because steel fibres used as a reinforcement in CHS and Eurocode do not give a solution in this case.

$$\alpha = \alpha_{Am/V} \cdot \alpha_{D/t} \cdot \alpha_R \cdot \alpha_s \cdot \alpha_f \quad (17)$$

$$\alpha_f \; can \; be > 1$$

if *R*≥ 60min, $\alpha = 0{,}92 \cdot \alpha_s \cdot \alpha_f$.

7.3. FLEXURAL STIFFNESS REDUCTION COEFFICIENT

Solution of the inverse problem.

$$N_{fi,Rd,PC} = N_{fi,Rd,SFRC} \quad (18)$$

$$\chi_{pc} \cdot N_{fi,pl,Rd,pc} = \chi_{SFRC} \cdot N_{fi,pl,Rd,SFRC}, \qquad \chi_{pc}, \chi_{SFRC} \leq 1 \quad (19)$$

We can find express from buckling curves χ as a function of $\bar{\lambda}_\theta$.

Using the linear approximation method, we simplify

$$\chi = -0{,}5014\bar{\lambda}_\theta + 1{,}1465, \qquad 0{,}2 \leq \bar{\lambda}_\theta \leq 1{,}6 \quad (20)$$

Consequently,

$$\left(-0{,}5014\bar{\lambda}_{\theta,pc} + 1{,}1465\right)N_{fi,pl,Rd,pc} = \left(-0{,}5014\bar{\lambda}_{\theta,SFRC} + 1{,}1465\right)N_{fi,pl,Rd,SFRC}, \quad (21)$$

$$\bar{\lambda}_{\theta,pc} = \sqrt{\frac{N_{fi,pl,Rd,pc}}{N_{fi,cr,pc}}}, \qquad \bar{\lambda}_{\theta,SFRC} = \sqrt{\frac{N_{fi,pl,Rd,SFRC}}{N_{fi,cr,SFRC}}} \quad (22)$$

$$\left(-0{,}5014\sqrt{\frac{N_{fi,pl,Rd,pc}}{N_{fi,cr,pc}}}+1{,}1465\right)N_{fi,pl,Rd,pc}=$$
$$=\left(-0{,}5014\sqrt{\frac{N_{fi,pl,Rd,SFRC}}{N_{fi,cr,SFRC}}}+1{,}1465\right)N_{fi,pl,Rd,SFRC} \tag{23}$$

$$0{,}5014\sqrt{\frac{N_{fi,pl,Rd,SFRC}}{N_{fi,cr,SFRC}}}N_{fi,pl,Rd,SFRC}-0{,}5014\sqrt{\frac{N_{fi,pl,Rd,pc}}{N_{fi,cr,pc}}}N_{fi,pl,Rd,pc}=$$
$$=1{,}1465(N_{fi,pl,Rd,SFRC}-N_{fi,pl,Rd,pc}) \tag{24}$$

$$0{,}5014\sqrt{\frac{N_{fi,pl,Rd,SFRC}}{N_{fi,cr,SFRC}}}N_{fi,pl,Rd,SFRC}=$$
$$=1{,}1465(N_{fi,pl,Rd,SFRC}-N_{fi,pl,Rd,pc})$$
$$+0{,}5014\sqrt{\frac{N_{fi,pl,Rd,pc}}{N_{fi,cr,pc}}}N_{fi,pl,Rd,pc} \tag{25}$$

$$\sqrt{\frac{N_{fi,pl,Rd,SFRC}}{N_{fi,cr,SFRC}}}=\frac{1{,}1465(N_{fi,pl,Rd,SFRC}-N_{fi,pl,Rd,pc})+0{,}5014\sqrt{\frac{N_{fi,pl,Rd,pc}}{N_{fi,cr,pc}}}N_{fi,pl,Rd,pc}}{0{,}5014N_{fi,pl,Rd,SFRC}} \tag{26}$$

It is obvious that

$$N_{fi,cr,SFRC}=\frac{(0{,}5014N_{fi,pl,Rd,SFRC})^2N_{fi,pl,Rd,SFRC}}{\left(1{,}1465(N_{fi,pl,Rd,SFRC}-N_{fi,pl,Rd,pc})+0{,}5014\sqrt{\frac{N_{fi,pl,Rd,pc}}{N_{fi,cr,pc}}}N_{fi,pl,Rd,pc}\right)^2} \tag{27}$$

$N_{fi,cr,pc}, N_{fi,pl,Rd,pc}, N_{fi,pl,Rd,SFRC}$ – calculated following new Eurocode 4 approach (*p=0%).*

$$\frac{N_{fi,cr,pc}}{N_{fi,cr,SFRC}}=\frac{(EI)_{fi,eff,pc}}{(EI)_{fi,eff,SFRC}} \tag{28}$$

$$\frac{N_{fi,cr,pc}}{N_{fi,cr,SFRC}} = \frac{\left(\varphi_{a,\theta}E_a(\theta_{a,eq})I_a\right)_{pc} + (\varphi_{c,\theta}E_c(\theta_{c,eq})I_c)_{pc}}{\left(\varphi_{a,\theta}E_a(\theta_{a,eq})I_a\right)_{sfrc} + \varphi^f_{c,\theta}\cdot(3/2)\cdot(\frac{f_c}{\varepsilon_{cu,\theta}})(k_c\cdot I_c)_{sfrc}} \quad (29)$$

Consequently

$$\varphi^f_{c,\theta} = \frac{\frac{\left(\varphi_{a,\theta}E_a(\theta_{a,eq})I_a\right)_{pc} + (\varphi_{c,\theta}E_c(\theta_{c,eq})I_c)_{pc}}{\frac{N_{fi,cr,pc}}{N_{fi,cr,SFRC}}} - \left(\varphi_{a,\theta}E_a(\theta_{a,eq})I_a\right)_{sfrc}}{(3/2)\cdot(\frac{f_c}{\varepsilon_{cu,\theta}})(k_c\cdot I_c)_c} \quad (30)$$

To obtain simplified the equation for $\Delta\,\varphi^f_{c,\theta,simp}$,$\Delta\varphi^f_{c,\theta,num}$ were calculated using the data from parametrical study (Table 7-1).

$$\varphi^f_{c,\theta} = \varphi_{c,\theta} + \Delta\,\varphi^f_{c,\theta,simp} = 0{,}8 + \Delta\,\varphi^f_{c,\theta,simp} \quad (31)$$

Table 7-1 – Parametrical study results for flexural stiffness reduction coefficient

D, mm	*L, mm*	A_m/V	l_θ/D	R_{pc}, *min*	R_{sfrc}, *min*	$\Delta\varphi^f_{c,\theta,num}$	$\Delta\varphi^f_{c,\theta,simp}$
159	750	25	4,72	45	57	0,32	0,34
159	750	25	4,72	39	47	0,27	0,34
159	750	25	4,72	22	26	0,33	0,34
159	1900	25	11,95	24	34	0,14	0,12
159	1900	25	11,95	17	21	0,18	0,12
159	3800	25	23,90	16	16	0,04	0,11
324	1500	12	4,63	39	97	0,44	0,34
324	3750	12	11,57	65	105	0,08	0,13
324	3750	12	11,57	22	28	0,10	0,13
324	3750	12	11,57	18	21	0,16	0,13
324	7500	12	23,15	16	17	0,11	0,10
406,4	4600	10	11,32	41	150	0,11	0,13
406,4	4600	10	11,32	23	36	0,11	0,13
406,4	4600	10	11,32	22	35	0,12	0,13
406,4	9300	10	22,88	16	17	0,10	0,09

At the same time, a nonlinear relationship between l_θ/D and $\Delta\varphi^f_{c,\theta}$ is observed.

$$\Delta\varphi_{c,\theta}^{f} = f(l_\theta / D) \tag{32}$$

Folowing prEN1994-1-2:2024 [12] a power function was chosen to approximate. Regression equation:

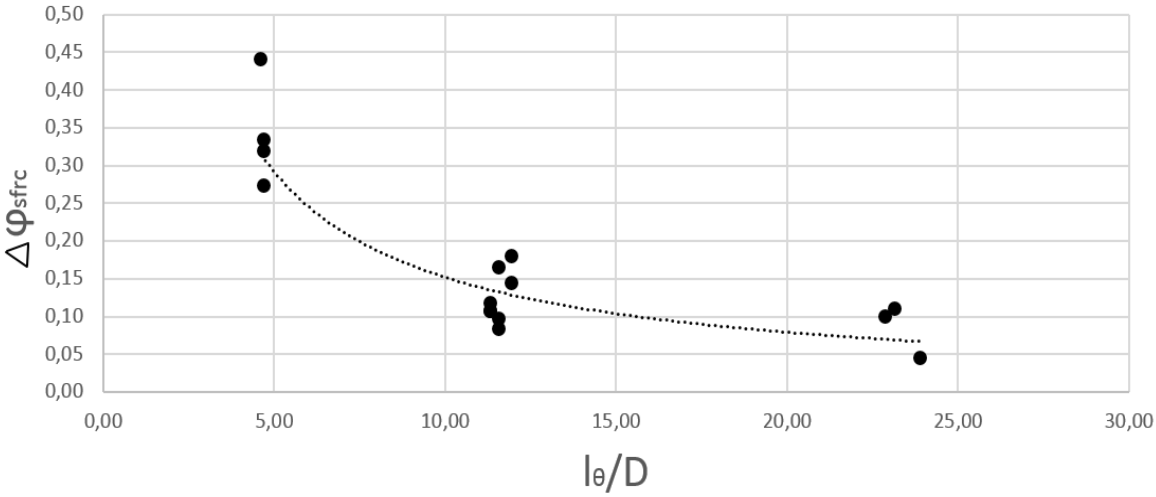

Figure 7-1 Results for flexural stiffness reduction coefficient calculation for SFRC.

$\Delta\varphi_{c,\theta,simp}^{f} = 1{,}3237(l_\theta / D)^{-0{,}94}$, for content of fibre 0,5 % (33)

with standard deviation $\Delta\varphi_{c,\theta,num}^{s}$ and $\varphi_{c,\theta,simp}^{f}$ = 0,1.

A new approach for eccentrically loaded CFST columns is developed next in order to complete the proposal of the simplified design method.

7.4. REDUCTION COEFFICIENT FOR ECCENTRICITY

Solution of the inverse problem.

$$N_{fi,Rd,\delta,PC} = N_{fi,Rd,\delta,SFRC} \tag{34}$$

$$\alpha_{PC} \cdot \left(\frac{N_{Rd,\delta,PC}}{N_{Rd,PC}}\right)_{room} \cdot N_{fi,Rd,PC} = \alpha_{SFRC} \cdot \left(\frac{N_{Rd,\delta,SFRC}}{N_{Rd,SFRC}}\right)_{room} \cdot N_{fi,Rd,SFRC} \tag{35}$$

When determining the design axial buckling load at room temperature, we use methods from the existing code. Therefore, it is true that:

$$\frac{N_{Rd,\delta,PC}}{N_{Rd,PC}} = \frac{N_{Rd,\delta,SFRC}}{N_{Rd,,,SFRC}} \tag{36}$$

Consequently

$$\alpha_{PC} \cdot N_{fi,Rd,PC} = \alpha_{SFRC} \cdot N_{fi,Rd,SFRC} \quad (37)$$

$$\alpha_{Am/V} \cdot \alpha_{D/t} \cdot \alpha_{R,PC} \cdot \alpha_{s,pc} \cdot N_{fi,Rd,PC} = \\ = \alpha_{Am/V} \cdot \alpha_{D/t} \cdot \alpha_{R,SFRC} \cdot \alpha_{s,sfrc} \cdot \alpha_f \cdot N_{fi,Rd,SFRC} \quad (38)$$

if *p = 0% and* p_f *= 0,5 %*→ $\alpha_{s,sfrc} = 1$, if R ≥ 60min, $\alpha = 0{,}92 \cdot \alpha_f$.

Consequently

$$\alpha_{R,PC} \cdot 0{,}8 \cdot N_{fi,Rd,PC} = \alpha_{R,SFRC} \cdot \alpha_f \cdot N_{fi,Rd,SFRC}$$

$$\alpha_R = 6{,}9598 \cdot R^{-0{,}221} \quad l_\theta / D \leq 15$$
$$\alpha_R = 0{,}92 \quad l_\theta / D > 15 \quad (39)$$

$$\alpha_f = 0{,}8 \frac{N_{fi,Rd,PC}}{N_{fi,Rd,SFRC}} \left(\frac{R_{pc}}{R_{sfrc}}\right)^{-0{,}221} \quad l_\theta / D \leq 15$$
$$\alpha_f = 0{,}8 \frac{N_{fi,Rd,PC}}{N_{fi,Rd,SFRC}} \quad l_\theta / D > 15 \text{ or R} \geq 60\text{min}, \quad (40)$$

$N_{fi,Rd,PC}$ calculated following new Eurocode 4 approach (*p=0%).*

$N_{fi,Rd,SFRC}$ calculated following chapter 8.3 taking in account $\varphi_{c,\theta,simp}^{sfrc}$.

To obtain a simplified the equation for $\alpha_{f,simp}$,$\alpha_{f,num}$ were calculated using the data from the parametrical study (Table 7-2).

Table 7-2 - Results of reduction coefficient for eccentricity

D, mm	*L, mm*	A_m/V	l_θ/D	*R_{pc}, min*	*R_{sfrc}, min*	$\alpha_{f,num}$	$\alpha_{f,simp}$
159	750	25	4,72	95	119	1.252	1.11
159	750	25	4,72	67	78	1.054	1.11
159	750	25	4,72	50	60	1.073	1.11
159	750	25	4,72	92	105	1.037	1.11
159	750	25	4,72	62	86	1.481	1.11
159	1900	25	11,95	24	32	1.395	1.04
159	1900	25	11,95	26	32	1.197	1.04
159	3800	25	23,90	18	22	1.188	0.92
159	3800	25	23,90	24	26	0.968	0.92
324	1500	12	4,63	35	55	1.114	1.11
324	1500	12	4,63	30	53	1.223	1.11
324	1500	12	4,63	32	46	1.053	1.11

D, mm	*L, mm*	A_m/V	l_θ/D	*R_{pc}, min*	*R_{sfrc}, min*	$\alpha_{f,num}$	$\alpha_{f,simp}$
324	1500	12	4,63	26	34	1.037	1.11
324	3750	12	11,57	68	71	0.854	1.04
324	3750	12	11,57	27	36	1.072	1.04
324	3750	12	11,57	24	26	0.872	1.04
324	7500	12	23,15	45	47	0.836	0.92
324	7500	12	23,15	29	30	0.853	0.92
406,4	4600	10	11,32	26	36	1.068	1.04
406,4	4600	10	11,32	19	22	0.916	1.04
406,4	4600	10	11,32	17	18	0.839	1.04
406,4	4600	10	11,32	22	24	0.862	1.04
406,4	4600	10	11,32	18	20	0.878	1.04
406,4	9300	10	22,88	24	28	0.985	0.93
406,4	9300	10	22,88	19	22	0.984	0.93
406,4	9300	10	22,88	24	25	0.841	0.93
406,4	9300	10	22,88	20	21	0.857	0.93

The sought function almost does not correlate with A_m/V and R.

At the same time, a nonlinear relationship between l_θ/D and α_f is observed.

$$\alpha_{f,simp} = f(l_\theta/D) \tag{41}$$

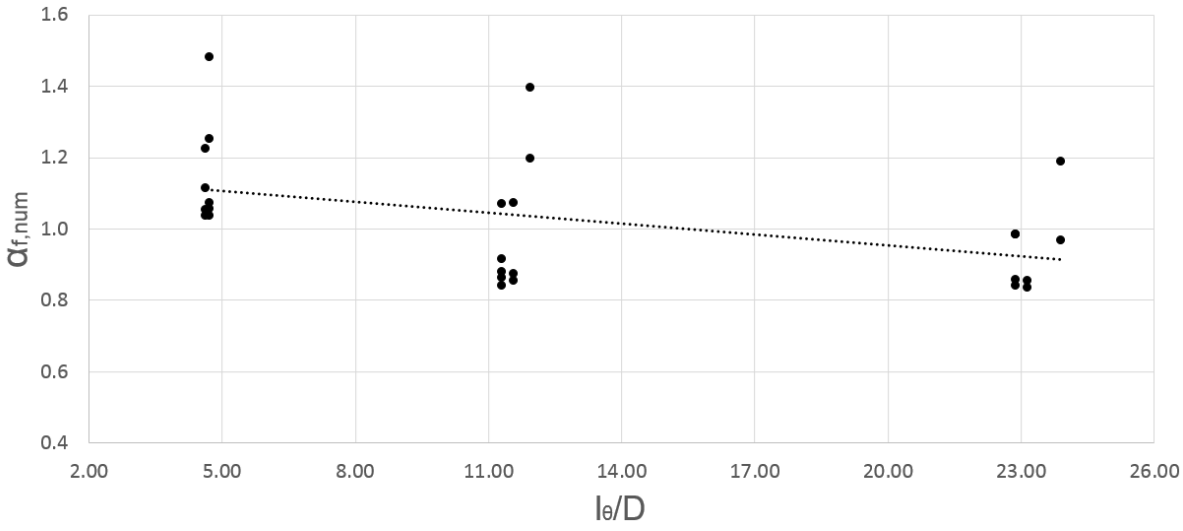

Figure 7-2 Results for reduction coefficient for eccentricity calculation for SFRC.

A linear function was chosen to approximate. Regression equation:

$$\alpha_{f,simp} = -0{,}0102 \cdot (l_\theta / D) \quad + 1{,}1592,$$

for content of fibre 0,5%,

if *p=0% and* p_f*=0,5%*→ $\alpha_{s,sfrc} = 1$, if R≥ 60min, $\alpha = 0{,}92 \cdot \alpha_f$ (42)

Standard deviation $\alpha_{f,simp}$ and α_f is 0,13.

Using the obtained analytic dependences, we will verify the obtained simplified method.

7.5. VERIFICATION

The criteria used in this study for verifying the accuracy of the developed simplified design method was that approved by CEN/TC250/SC4 Horizontal Group Fire [7-3].

Three criteria should be met for a calculation method to be considered accurate:

1. The calculation result shall not be on the unsafe side by more than 15% of the reference result.

2. Maximum of 20 % of individual calculation results shall be on the unsafe side.

3. Thirdly, the mean value of all percentage differences between calculation results and reference results shall be on the safe side.

7.5.1. VERIFICATION OF CENTRICALLY LOADED SFRC CHS COLUMNS.

Based on proposed method, $N_{fi,Rd,sfrc}^{pre}$ was predicted (Table 7-2).

Table 7-3 - Verification of centrically loaded SFRC CHS columns

D, mm	L, mm	R_{sfrc}, min	$N_{fi,Rd,sfrc}^{num}$, kN	$N_{fi,Rd,sfrc}^{pre}$, kN
159	750	57	299,43	243,38
159	750	47	598,87	314,79
159	750	26	898,30	655,19
159	1900	34	538,23	210,18
159	1900	21	807,34	458,84
159	3800	16	579,78	503,08
324	1500	97	1586,67	1168.05
324	3750	105	753,56	397.43
324	3750	28	1507,12	1714.10
324	3750	21	2260,68	2264.83
324	7500	17	1625,92	1606.46
406,4	4600	150	1072,59	594.31
406,4	4600	36	2145,19	2504.78
406,4	4600	35	3217,78	2562.79
406,4	9300	17	2307,33	2572.66

The results shown in Fig. 7-2 were obtained by applying these proposed reduction coefficients for SFRC to all concentrically loaded cases from the parametric studies.

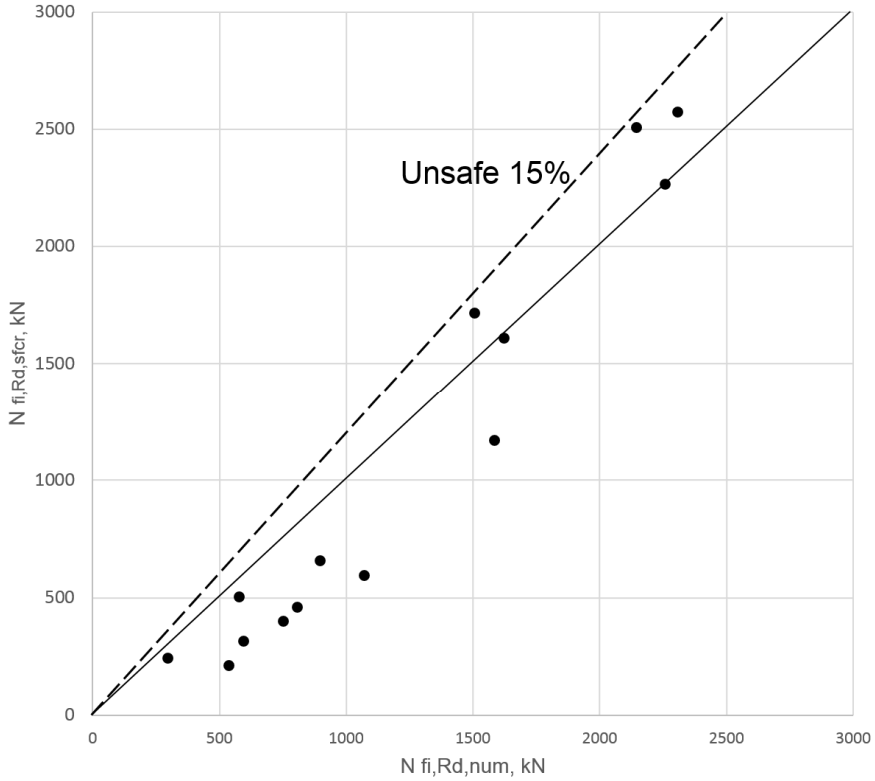

Figure 7-3 Verification of the design method for centrically loaded columns

As can be seen, safe predictions are obtained. Proposed model for flexural stiffness reduction coefficient is safe. Results meet the criteria CEN/TC250/SC4.

7.5.2. VERIFICATION OF ECCENTRICALLY LOADED SFRC CHS COLUMNS.

Based on proposed method $N_{fi,Rd,\partial,sfrc}^{pr\ 1}$ was predicted (Table 7-4).

Table 7-4 - Verification of eccentrically loaded SFRC CHS columns.

D, mm	L, mm	R_{sfrc}, min	l_θ / D	$N_{fi,Rd,\partial,sfrc}^{num}$, kN	$N_{fi,Rd,\partial,sfrc}^{pr\ 1}$, kN	$N_{fi,Rd,\partial,sfrc}^{pr\ 2}$, kN
159	750	119	4,72	149,96	37,74	37.74
159	750	78	4,72	299,91	86,16	86.16
159	750	60	4,72	449,87	127.5	127.5
159	750	105	4,72	110,42	28.79	28.79
159	750	86	4,72	220,85	42.56	42.56
159	1900	32	11,95	278,10	108.17	108.17
159	1900	32	11,95	201,76	78.47	78.47
159	3800	22	23,90	212,67	350.71	153.25
159	3800	26	23,90	152,68	170.62	74.55
324	1500	55	4,63	950,82	570.29	570.29
324	1500	53	4,63	1426,23	585.25	585.25
324	1500	46	4,63	585,12	396.40	396.40
324	1500	34	4,63	877,68	499.41	499.41
324	3750	71	11,57	424,21	323.74	323.74

D, mm	L, mm	R_{sfrc}, min	l_θ / D	$N_{fi,Rd,\partial,sfrc}^{num}$, kN	$N_{fi,Rd,\partial,sfrc}^{pr\ 1}$, kN	$N_{fi,Rd,\partial,sfrc}^{pr\ 2}$, kN
324	3750	36	11,57	848,42	423.71	423.71
324	3750	26	11,57	1272,64	592.67	592.67
324	7500	47	23,15	197,48	323.75	147.97
324	7500	30	23,15	526,61	576.81	249.95
406,4	4600	36	11,32	583,99	620.52	620.52
406,4	4600	22	11,32	1167,98	956.94	956.94
406,4	4600	18	11,32	1751,97	1148.10	1148.10
406,4	4600	24	11,32	737,67	530.32	530.32
406,4	4600	20	11,32	1106,51	624.77	624.77
406,4	9300	28	22,88	799,14	1605.26	693.58
406,4	9300	22	22,88	1198,71	1675,97	1004.88
406,4	9300	25	22,88	532,76	1284.37	524.93
406,4	9300	21	22,88	799,14	1681.32	726.44

The results shown in Fig. 7-4 were obtained by applying proposed reduction coefficient for eccentricity for SFRC to all eccentrically loaded cases $N_{fi,Rd,\partial,sfrc}^{pr\ 1}$ from the parametric studies.

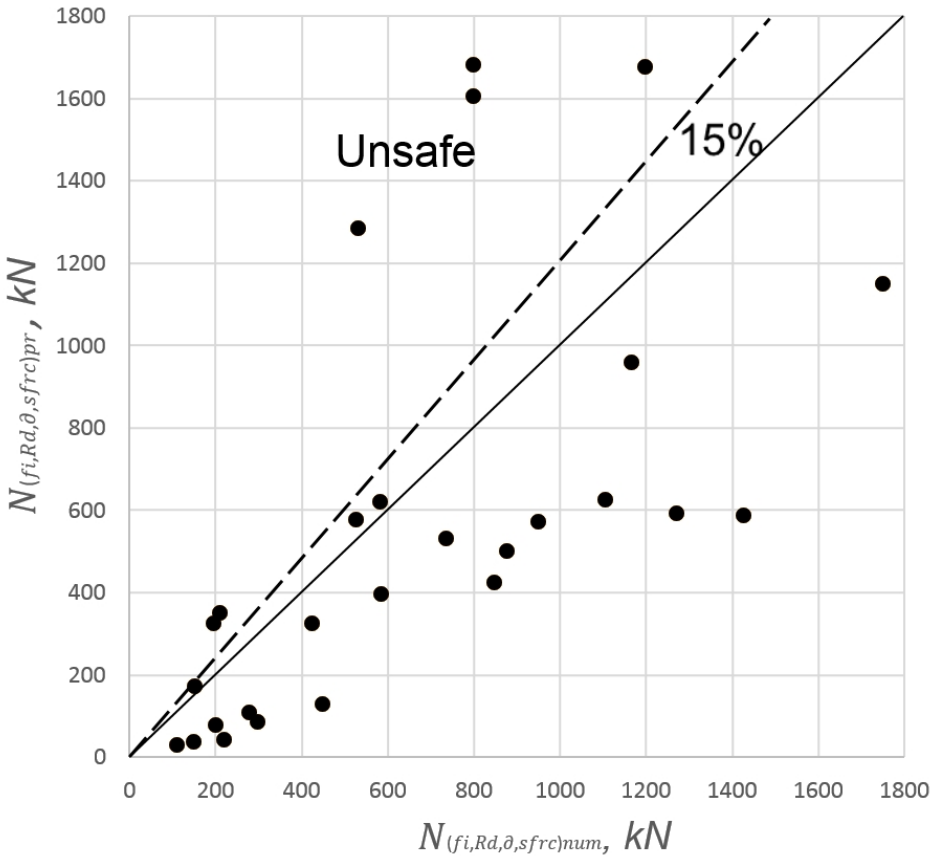

Figure 7-4 Verifying the accuracy of the developed simplified design method for eccentrically loaded columns.

It can be seen, prediction of the method is unsafe: calculation result on the unsafe side by more than 15% of the reference result. All unsafe cases occur in 22<l_θ / D<24 – slender columns. The method needs to be modified.

By the checking of the approximation function (Fig. 7-2), the predicted value of the buckling load at $(l_\theta / D) > 15$ exceeds numerical results, therefore, at $(l_\theta / D) > 15$ we take $\alpha_{f,simp} = 0{,}4$.

$$\begin{aligned} \alpha_{f,simp} &= -0{,}0102 \cdot (l_\theta / D) + 1{,}1592, \; l_\theta / D \leq 15 \\ \alpha_{f,simp} &= 0{,}4 \qquad\qquad\qquad\qquad l_\theta / D > 15 \end{aligned} \tag{43}$$

for content of fibre 0,5%.

Standard deviation $\alpha_{f,simp}$ and α_f = 0,13.

The results shown in Fig. 7-5 were obtained by applying proposed reduction coefficient for eccentricity for SFRC to all eccentrically loaded cases $N_{fi,Rd,\partial,sfrc}^{pr\ 2}$ from the parametric studies.

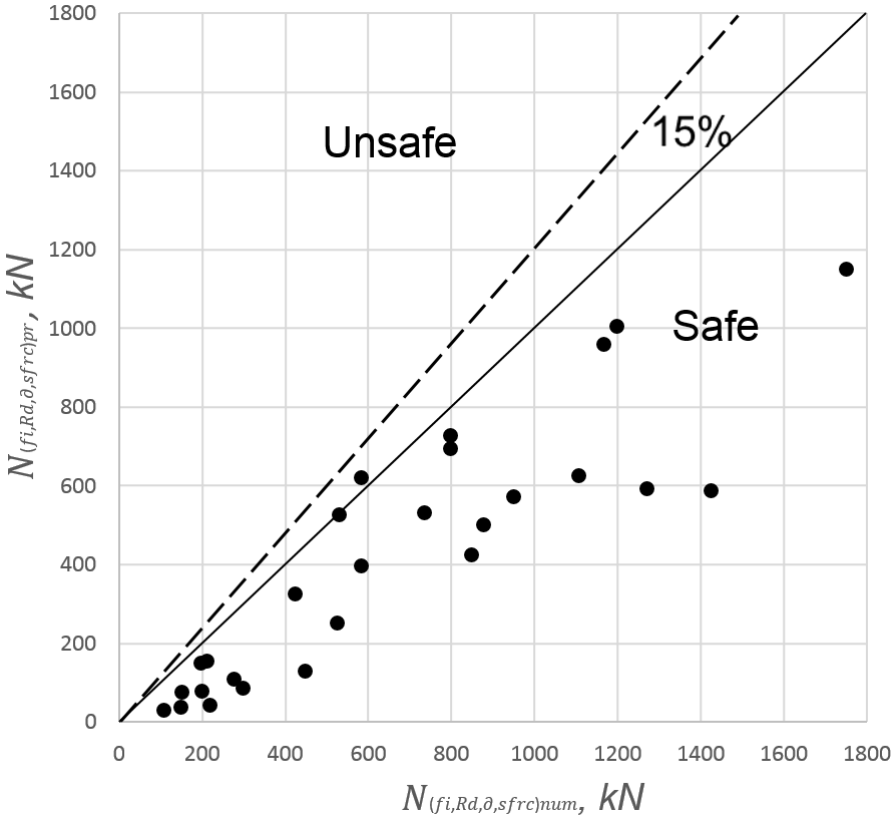

Figure 7-5 Verifying the accuracy of the developed simplified design method for eccentrically loader columns after modification.

As can be seen, safe predictions are obtained. Proposed model for reduction coefficient for eccentricity is safe.

Condition (43) ($\alpha_{f,simp} = 0{,}4, l_\theta / D > 15$) cause due to insufficient performance of 0.5% fiber content for slender columns at eccentrically load. Studies with higher fiber content are needed.

To refine the obtained formulas, it is necessary to carry out more numerical experiments to obtain not to conservative results.

7.6. RANGE OF APPLICATION OF THIS PROPOSED METHOD

The proposed design method should only be applied for CHS columns with SFRC infilling in the following conditions:

Table 7-5 - Applicability limits of the proposed method

Num	Condition
1	Section factor, cross-sectional slenderness and member slenderness: $10 \leq Am/V \leq 133$ $27 \leq D/t \leq 68$ $4{,}6 \leq l_\theta / D \leq 25$
2	Only for columns with SFRC. The percentage of SFR should not exceed 0,5%.
3	The concrete strength class should be limited between C30/37 and C50/60.
4	The relative load eccentricity e/D should not exceed 0,5.
5	The method can be used for specimens with a standard fire exposure time ranging between 15 and 150 min.
6	$0{,}2 \leq \bar{\lambda}_\theta \leq 1{,}6$
7	For SFR if $\rho = 0\%, \text{than } \alpha_s = 1$

7.7. DESIGN EXAMPLE

In this chapter, a design example is presented in order to present the application of the proposed design method for evaluating the R of SFRC CFST columns without bar reinforcement. This worked example corresponds to a standard fire period of 60 min (R60). The material and geometrical properties of the member are as follows:

Boundary conditions: P-P, $\beta = 1$.

Column length (l): 3700 mm.

Cross-sectional dimensions (CHS): D=273mm, t=8 mm

Steel yield strength: f y = 355 MPa.

Compressive concrete strength: f_c = 30 MPa.

The percentage of SFR - 0,5%.

e/D=0,25.

Firstly, the cross-sectional slenderness, section factor and member slenderness needed for the application of the method are computed:

Section factor: $A_m/V=4/D=4/273\times1000=14{,}65\ m^{-1}$.

Member slenderness in the fire situation:

$l_\theta / D = (\beta \cdot l)/D=(0{,}7\times3700)/273=13{,}55$.

Cross-sectional slenderness: D/t=273/8=34,125.

Calculation of the equivalent temperatures made following prEN1994-1-2:2024 [12]. It is out of the scope of this work.

$$\theta_{c,eq} = 457{,}68\ °C$$

$$\theta_{a,eq} = 889{,}09\ °C$$

$\theta_{s,eq}$- no reinforsment.

After the equivalent temperatures are calculated, the cross-sectional plastic resistance can be easily obtained:

$$\begin{aligned} N_{fi,pl,Rd} &= A_a f_y(\theta_{a,eq}) + A_c f_c(\theta_{c,eq}) = \\ &= 660{,}18mm^2 \cdot k_y(889{,}09\ °C) \cdot 355MPa \\ &+ 51874{,}76mm^2 \cdot k_c(457{,}68\ °C) \cdot 30MPa = \\ &= 6660{,}18mm^2 \cdot 0{,}0655 \cdot 355MPa + 51874{,}76mm^2 \\ &\cdot 0{,}6635 \cdot 30MPa = 1187{,}31\ kN. \end{aligned} \tag{44}$$

The partial factors of the materials in the fire situation $\gamma_{M,fi,i}$ have been taken as unity, as per Clause 2.3 of EN 1994-1-2 [83].

On a second stage, the flexural stiffness reduction coefficients should be calculated through the equations and tables provided in Section 7 and Folowing prEN1994-1-2:2024 [12].

$l_\theta / D = 13{,}55 > 12 \rightarrow$

$$\varphi_{a,\theta} = \varphi_{a,\theta,1}(A_m/V) \cdot \varphi_{a,\theta,2}(l_\theta/D) \cdot \varphi_{a,\theta,3}(D/t) \cdot \varphi_{a,\theta,3}(R) = 0.21$$
$$\varphi^{f}_{c,\theta,simp} = 0{,}8 + 1{,}3237(l_\theta/D)^{-0{,}94}=0{,}914 \quad (45)$$

The effective flexural stiffness of the column in the fire situation:

$$(EI)_{fi,eff} = \varphi_{a,\theta} E_a(\theta_{a,eq}) I_a + \varphi_{c,\theta} E_c(\theta_{c,eq}) I_c = \varphi_{a,\theta} \cdot E_a \cdot k_a \cdot I_a + \varphi_{c,\theta} \cdot E_{sfrc} \cdot k_c \cdot I_c = 6.32 \cdot 10^{11} N \cdot mm^2 \quad (46)$$

The Euler buckling load and the relative slenderness at elevated temperature can be calculated:

$$N_{fi,cr} = \frac{\pi^2 (EI)_{fi,eff}}{l_\theta^2} = 455.3kN \quad (47)$$

$$\bar{\lambda}_\theta = \sqrt{\frac{N_{fi,pl,Rd}}{N_{fi,cr}}} = \sqrt{\frac{1187{,}31}{502{,}57}} = \sqrt{2{,}362} = 1{,}61 \quad (48)$$

Using buckling curve ‘‘a”, corresponding to this case, a buckling coefficient $\chi = 0{,}328$ is obtained. Finally, the design value of the buckling load of the column in axial compression, after 60 min of fire exposure, is

$$N_{fi,Rd} = \chi \cdot N_{fi,pl,Rd} = 0{,}328 \cdot 1187{,}31 = 389.31 \text{ kN} \quad (49)$$

The fire resistance of the same column loaded under a relative eccentricity of e/D=0,25 is evaluated. Following the design rules in EN 1994-1-1 [109], the concentric and eccentric load of the column at room temperature are computed:

$$N_{Rd} = 3401{,}9\ kN \quad (50)$$

$$N_{Rd,\delta} = 1871\ kN \quad (51)$$

Calculation of this loads is out of the scope of this work.

Design buckling load in the fire situation in case of eccentric load can be obtained:

$$\frac{l_\theta}{D} = 13{,}55 < 15$$

$$N_{fi,Rd,\delta} = \alpha \cdot \left(\frac{N_{Rd,\delta}}{N_{Rd}}\right)_{room} \cdot N_{fi,Rd} \quad (52)$$

$\alpha_{Am/V}, \alpha_{D/t}, \alpha_R, \alpha_s$ prEN1994-1-2:2024 [12]. It is out of the scope of this work.

$$\alpha_f = -0{,}0102 \cdot (13{,}55) + 1{,}1592 = 1{,}021 \quad (53)$$

$$\alpha = \alpha_{Am/V} \cdot \alpha_{D/t} \cdot \alpha_R \cdot \alpha_s \cdot \alpha_f = 0{,}573 \cdot 0{,}375 \cdot 2{,}816 \cdot 0{,}616 = 0{,}94 \quad (54)$$

$$N_{fi,Rd,\delta} = 0{,}94 \cdot \left(\frac{1872}{3401{,}9}\right) \cdot 389{,}31 = 201{,}11\ kN \quad (55)$$

CHAPTER 8. CONCLUSIONS

8.1. SUMMARY

The thesis is dedicated to developing an analytical model for determining the fire resistance of the composite steel and fibre-reinforced centrically and eccentrically loaded SFCR columns under ISO standard fire conditions. The scope of the work was defined based on the literature review. It was shown that despite the beneficial use of SFRC infill at elevated temperature, the European standard for composite member design in the fire EN1994-1-2:2006 and prEN1993-1-2:202x didn't include an analytical method for this type of column. The work consists of data from experimental studies, verification of the numerical model, numerical experiments, and development of an analytical model based on a European standard for designing reinforced concrete elements in the fire. The proposed model determines the design buckling load in the fire situation of the composite steel and fibre-reinforced concrete columns and can be used as an appendix or supplementary technical basis in the corresponding method prepared for prEN1994-1-2:2024.

8.2. EXPERIMENTAL STUDY

Full-scale column specimens were used for experimental studies to verify the numerical model. Specimens were prepared in the hydraulic stand in the Experimental Centre of the Faculty of Civil Engineering CTU in Prague. Six pinned-pinned columns were tested in compression at an elevated temperature at the steady-state regime.

8.3. NUMERICAL MODEL AND VALIDATION

The advanced FEM model for the steady-state regime was developed in ATENA Červenka software with a GID pre-processor based on described approach. This model was validated in own experiments. The steady-state global model of the column consists of the mechanical and thermal models. The thermal model calculates heat transfer and the mechanical model calculates the response of the column from vertical force and thermal loading. Analysis of the mechanical response was designed in the ATENA Static module. ATENA Transport module was used for the calculation of heat transfer.

8.4. PARAMETRICAL STUDY

For the parametrical study was used a three-dimensional FEM fire response model of the steel fibre reinforced concrete filled tubular column in ATENA Červenka software. A parametric study is comparing fire resistance of centrally and eccentrically loaded circular hollow section columns with steel fibre-reinforced and plain concrete infill in a fire situation. Numerical experiments were provided based on prepared combinations.

8.5. ANALYTICAL MODEL

The developed analytical model determines the design buckling load in the fire situation of the composite steel and fibre-reinforced concrete centrically and eccentrically loaded column. The definition of the flexural stiffness reduction coefficient and reduction coefficient for eccentricity allows using this method in the corresponding the prepared for prEN1994-1-2:202x in the specified range of application.

8.6. FUTURE WORK

Following recommendations for future work could be made based on the findings presented in the thesis:

- Conduct experimental studies with columns with a fiber content in concrete other than 0,5 % and relative load eccentricity e/D > 0,5 to compare them with plane concrete and bar reinforced concrete.
- Further validation of the model (based on extended experimental studies) and expansion of the parametric study. This will allow to refine the analytical model and expand the applicability limits of the proposed method.

REFERENCES

[1] RICHARD LIEW, J. Y. and M. X. XIONG. Design guide for concrete filled tubular members with high strength materials to Eurocode 4, Singapore: Research Publishing, 2015.

[2] ZHAO, X. , H. HAN, and H. LU. Concrete-filled tubular members and connections , New York: Spon Press, 2010.

[3] LIN-HAI HAN, W. LI, R. BJORHOVDE. Developments and advanced applications of concrete-filled steel tubular (CFST) structures: Members. *Journal of Constructional Steel Research,* Published 1 September 2014.

[4] Concrete-Filled Hollow Structural Sections (HSS), an Unbeatable Combination, "www.continuingeducation.bnpmedia.com", November 2017. [Online]. Available: https://continuingeducation.bnpmedia.com/courses/the-steel-institute-of-new-york/concrete-filled-hollow-structural-sections-hss-an-unbeatable- combination/3/. [Accessed 27 12 2021].

[5] Concrete-filled steel tube (CFST) bridges, "www. structurae.net" 2021 [Online]. Available: https://structurae.net/en/structures/bridges/concrete-filled-steel-tube-cfst- bridges [Accessed 27 12 2021].

[6] RUSH, D., L. BISBY, A. JOWSEY and B. LANE. Structural Fire Performance of Concrete-Filled Steel Hollow Structural Sections: State-of-the-Art and Knowledge Gaps. *Proceedings of 12th International Interflam Conference. Interflam, Interscience Communications Ltd,,* p. 57-70, 2010.

[7] LAU, A. and M. ANSON. Effect of high temperatures on high performance steel fibre reinforced concrete. *Cement and Concrete Research,* vol. 36, no. 9, p. 1698-1707, 2006.

[8] KHALIQ, W. and V. KODUR. High Temperature Mechanical Properties of High-Strength Fly Ash Concrete with and without Fibers. *ACI Materials Journal,* vol. 109, no. 4, 2012.

[9] BOŠNJAK, J., S. AKANSHU and K. GRAUF. Mechanical Properties of Concrete with Steel and Polypropylene Fibres at Elevated Temperatures," *Fibres,* vol. 7, no. 9, 2019.

[10] KODUR, V. R. and T. WANG. Stress-Strain Curves for High Strength Concrete at Elevated Temperatures. *Journal of Materials in Civil Engineering,* vol. 16, no. 1, 2004.

[11] PLIYA, P., A.L. BEAUCOUR and A. NOUMOWÉ. Contribution of cocktail of polypropylene and steel fibres in improving the behaviour of high strength concrete subjected to high temperature. *Construction and Building Materials,* vol. 25, no. 4, p. 1926-1934, 2011.

[12] ALBERO, V., A. ESPINOS, M. L. ROMERO, A. HOSPITALER, G. BIHINA and C. RENAUD. Proposal of a new method in EN1994-1-2 for the fire design of concrete-filled steel tubular columns. *Engineering Structures*, vol. 128, p. 237-255, 2016.

[13] LIE, T.T. A procedure to calculate fire resistance of structural members. *Fire and materials,* vol. 8 (1), p. 40-48, 1984.

[14] TAN, K.H. and C.Y. TANG. Interaction model for unprotected concrete filled steel columns under standard fire conditions. *Journal of Structural Engineering.* (ASCE) 130(9), p. 1405-1413, 2004.

[15] WANG, Z.H. and K.H. TAN. Green's function solution for transient heat conduction in concrete-filled CHS subjected to fire. *Engineering Structures*, vol. 28, p. 1574–1585, 2006.

[16] CHIKHLADZE, E. Investigation of stress-strain and limit states of a steel concrete column subjected to force and temperature actions. *Bulletin of National University "Lvivska Politrchnika*" No. 664, p. 311-317, 2010.

[17] DING, J. and Y.C. WANG. Realistic modelling of thermal and structural behaviour of unprotected concrete filled tubular columns in fire. *Journal of Constructional Steel Research*, vol. 64, p. 1086–1102, 2008

[18] LIE, T.T. and M. CHABOT. A method to predict the fire resistance of circular concrete filled hollow steel columns. *Journal of Fire Protection Engineering*, vol. 2, p.111-126, 1990.

[19] LIE, T.T. and R.J. IRWIN. Fire resistance of rectangular steel columns filled with bar reinforced concrete. *Journal of Structural Engineering (ASCE)*, vol. 121, p. 797-805, 1995.

[20] DUSINBERRE, G.M. Heat transfer calculations by finite differences. *Scranton, Pa: International Textbook Company,* 1961.

[21] LI, L.Y and J. PURKISS. Stress-strain constitutive equations of concrete material at elevated temperatures. *Fire Safety Journal,* vol. 40, no. 7, p. 669-686, 2005

[22] ANDERBERG, Y. and S. THELANDERSSON. Stress and deformation characteristics of concrete, 2-experimental investigation and material behavior model. *Lund Institute of Technology*, Bulletin 54, 1976.

[23] SCHNEIDER, U. Concrete at high temperatures – a general review. *Fire Safety Journal*, vol. 13, p. 55–68, 1988.

[24] YOUSSEF, M.A. and M. MOFTAH. General stress-strain relationship for concrete at elevated temperatures. *Engineering Structures*, vol. 29, p. 2618–2634, 2007.

[25] KODUR, V. K. R. and T. T. LIE. Experimental Studies on the Fire Resistance of Circular Hollow Steel Columns Filled with Steel-Fibre-Reinforced Concrete. *NRC CNRC Internal Report,* no. 691, 1995.

[26] KODUR, V. K. R. and T. T. LIE. Evaluation of fire resistance of rectangular steel columns filled with fibre-reinforced concrete. *Canadian Journal of Civil Engineering,* vol. 24, 1997.

[27] KODUR, V. K. R. and J. C. LATOUR. Experimental studies on the fire resistance of hollow steel columns filled with high-strength concrete. *Institute for Research in Construction, National Research Council of Canada (NRCC) Ottawa, Canada.*, 2005.

[28] CIDECT.:Concrete filled hollow section steel columns. *Design manual, British edition,* Monograph No.1, 1970.

[29] YU, J.T., Z.D.L and Q. XIE. Nonlinear analysis of SRC columns subjected to fire. *Fire Safety Journal,* vol. 42, p. 1–10, 2007.

[30] HUI, L., ZH. XIAO-LING and H. LIN-HAI. Fire behaviour of high strength self-consolidating concrete filled steel tubular stub columns. *Journal of Constructional Steel Research*, vol. 65, p. 1995-2010, 2009.

[31] LU, H., X-L. ZHAO and L.H. FE modeling and fire resistance design of concrete filled double skin tubular columns. *Journal of Constructional Steel Research*, vol. 67 , p. 1733–1748, 2011.

[32] WANG, K.E. and B. YOUNG. Fire resistance of concrete-filled high strength steel tubular columns. *Thin-Walled Structures*, vol. 71, p. 46–56, 2013.

[33] KODUR, V., M. DWAIKAT and R. FIKE. High-Temperature Properties of Steel for Fire Resistance Modeling of Structures. Journal of Materials in Civil Engineering, vol. 22, no. 5, p. 423-434, 2010.

[34] OUTINEN, J. Mechanical properties of structural steels at high temperatures and after cooling down, Doctoral dissertation, Helsinki, Finland: Laboratory of Steel Structures Publications, Helsinki Univ. of Technology, 2007.

[35] OUTINEN, J., J. KESTI and P. MÄKELÄINEN. Fire design model for structural steel S355 based upon transient state tensile test results. *Journal of Constructional Steel Research,* vol. 42, no. 3, p. 161-169, 1997.

[36] OUTINEN, J. and P. MÄKELÄINEN. Mechanical properties of structural steel at elevated temperatures and after cooling down. *Fire and Materials,* vol. 28, p. 237-251, 2004.

[37] CEN, EN 1993-1-2, Eurocode 3:Design of steel structures - Part 1-2: General rules - Structural fire design, Brussels: CEN, 2005.

[38] ASCE. Structural fire protection. ASCE committee on fire protection, no. Manual No. 78, 1992.

[39] BARROS, J. A. and J. FIGUEIRAS. Flexural behavior of SFRC: Testing and modeling. Journal of Materials in Civil Engineering, vol. 11, no. 4, p. 0899-1561, 1999.

[40] XU, B. and H. SHI. Correlations among mechanical properties of steel fiber reinforced concrete. Construction and Building Materials, vol. 23, p. 3468-3474, 2009.

[41] ABBASS, W., M. I. KHAN and S. MOURAD. Evaluation of mechanical properties of steel fiber reinforced concrete with different strengths of concrete. Construction and Building Materials, vol. 168, p. 556-569, 2018.

[42] MARAR, K., Ö. EREN and İ. YITMEN. Compression Specific Toughness of Normal Strength Steel Fiber Reinforced Concrete (NSSFRC) and High Strength Steel Fiber Reinforced Concrete (HSSFRC). Materials Research, vol. 12, no. 2, p. 239-247, 2011.

[43] MIN, A., S. J. FOSTER and A. MUTTONI. Evaluation of the tensile strength of sfrc as derived from inverse analysis of notched bending tests. International Conference on Fracture Mechanics of Concrete and Concrete Structures, no. FraMCoS-8, Toledo, Spain, 2013.

[44] MAHASNEH, B.Z. The effect of addition of fiber reinforcement on fire resistant composite concrete material. *Journal of applied sciences*, vol. 5, p. 373–379, 2005.

[45] LAU, A. AND M. ANSON. Effect of high temperatures on high performance steel fibre reinforced concrete. *Cement and Concrete Research*, vol. 36, p. 1698-1707, 2006.

[46] BEDNÁŘ, J., F. WALD, J. VODIČKA and A. KOHOUTKOVÁ. Composite floors with steel fibre reinforced concrete slabs exposed to fire. Fire Safety Journal, vol. 59, p. 111–121, 2013.

[47] KHALIQ, W. and V. KODUR. Thermal and mechanical properties of fiber reinforced high performance self-consolidating concrete at elevated temperatures. Cement and Concrete Research, vol. 41, no. 11, p. 1112–1122, 2011.

[48] BALÁZS, G. L. and E. LUBLÓY. Post-heating strength of fiber-reinforced concretes. *Fire Safety Journal*, vol. 49, p. 100-106, 2012.

[49] KIM, D.K. , S.M. CHOI J.H. KIM, K.S. CHUNG and S.H. PARK. Experimental study on fire resistance of concrete-filled steel tube

column under constant axial loads. *International Journal of Steel Structures*, vol. 5, p. 305-313, 2015.

[50] RUSH, D., L. BISBY, A. JOWSEY, A. MELANDINOS and B. LANE. Structural performance of unprotected concrete-filled steel hollow sections in fire: A review and meta-analysis of available test data. Steel and Composite Structures, vol. 12, no. 4, p. 325–352, 2012.

[51] ČERVENKA, V., L. JENDELE and J. ČERVENKA. ATENA Program Documentation Part 1 Theory. 16 September 2020. [Online]. Available: https://www.cervenka.cz/ assets/files/atena-pdf/ATENA_Theory.pdf.

[52] International Organization for Standardization. ISO 834-1 Fire resistance tests Elements of buildings construction-Part 1: General requirements, 1999.

[53] POWELL, R. W. and R. P. TYE. High alloy steels for use as a thermal conductivity standard. British Journal of Applied Physics, vol. 11, p. 195-198, 1960.

[54] ASCE. Structural fire protection. ASCE committee on fire protection, no. Manual No. 78, 1992.

[55] REMPE, J. L. and D. L. KNUDSON. High temperature thermalproperties for metals used in LWR vessels. Journal of Nuclear Materials, vol. 372, no. 2-3, p. 350 357, 2008.

[56] Yawata Iron and Steel Co., WEL-TEN 80 material datasheet, Tokyo: 22, 1969.

[57] WEI-MING, L., T. D. LIN and J. POWERS-COUCHE. Microstructures of Fire-Damaged Concrete. Materials Journal, vol. 93, no. 3, pp. 199-205, 1996.

[58] CEN, EN 1992-1-2, Eurocode 2: Design of concrete structures - Part 1-2: General rules - Structural fire design, Brussels: CEN, 2004.

[59] LIE , T. T. and V. K. R. KODUR. Thermal and mechanical properties of steel fibre-reinforced concrete at elevated temperatures. *Canadian Journal of Civil Engineering,* vol. 23, 1996.

[60] KODUR, V. and W. KHALIQ. Effect of Temperature on Thermal Properties of Different Types of High-Strength Concrete. *Journal of materials in civil engineering,* vol. 23, no. 6, p. 793-801, 2011.

[61] XIANGWEI, L. and W. CHENGQING. Investigation on Thermal Conductivity of Steel Fiber Reinforced Concrete Using Mesoscale Modeling. *International Journal of Thermophysics,* vol. 39, no. 142, p. 1-19, 2018.

[62] DING, J. and Y.C. WANG. Realistic modelling of thermal and structural behaviour of unprotected concrete filled tubular columns in fire. *Journal of Constructional Steel Research*, vol. 64 , p. 1086–1102, 2008.

[63] HONG, S. and A.H. VARMA. Analytical modeling of the standard fire behavior of loaded CFT columns. *Journal of Constructional Steel Research,* vol. 65, p. 54-69, 2009.

[64] IDING RH, BRESLER B, NIZAMUDDIN Z. FIRES-T3. A computer program for the fires response of structures – Thermal. Report No. UCB-FRG 77-15. University of Berkeley, California, 1977.

[65] DUSINBERRE, G.M. Heat transfer calculations by finite differences. Scranton, Pa: International Textbook Company, 1961.

[66] STERNER, E. and U. WICKSTROM. TASEF – Temperature Analysis of Structures Exposed to Fire. SP Report 1990:05. Boras, Sweden: Swedish National Testing and Research Institute, 1990.

[67] FRANSSEN, J.M. SAFIR – A thermal/structural program modeling structures under fire. Proceedings of the NASCC Conference. American Institute for Steel Construction, Baltimore, 2003.

[68] LIE, T.T. and R.J. IRWIN. Fire resistance of rectangular steel columns filled with bar reinforced concrete. *Journal of Structural Engineering (ASCE)*, vol. 121, p. 797-805, 1995.

[69] HAN, L. Fire performance of concrete filled steel tubular beam-columns. *Journal of Constructional Steel Research*, vol. 57, no. 6, pp. 697-711, 2001.

[70] BIANCO, M., BILARDI, G., PESAVENTO, F., PUCCI, G. and B.A. SCHREFLER. A frontal solver tuned for fully coupled non-linear hygro-

thermo-mechanical problems. *International Journal for Numerical Methods in Engineering*, vol. 57, p.1801-1818, 2003.

[71] LIE, T. and M. CHABOT. Experimental studies on the fire resistance of hollow steel columns filled with plain concrete. Internal report No. 611, Ottawa, Canada. *Institute for Research in Construction, National Research Council of Canada (NRCC)*, 1992.

[72] CHABOT, M. and T. LIE. Experimental studies on the fire resistance of hollow steel columns filled with bar-reinforced concrete. Internal report No. 628, Ottawa, Canada. *Institute for Research in Construction, National Research Council of Canada(NRCC)*, 1992.

[73] KODUR, V. K. R. and J. C. LATOUR. Experimental studies on the fire resistance of hollow steel columns filled with high-strength concrete. *Institute for Research in Construction, National Research Council of Canada (NRCC) Ottawa, Canada.,* 2005.

[74] GRANDJEAN, G., J. GRIMAULT and L. PETIT. Détermination de la durée au feu des profiles creus remplis de béton. CIDECT Research Project 15B–80/10., Cologne, Germany: Comité International pour le Développement et l'Etude de la Construction Tubulaire, 1980.

[75] KORDINA, K. and W. KLINGSCH, Fire resistance of composite columns of concrete filled hollow sections. CIDECT Research Project 15C1/C2–83/27., Cologne, Germany: Comité International pour le Développement et l'Etude de la Construction Tubulaire, 1983.

[76] ROMERO, M. L., V. MOLINER, A. ESPINOS, C. IBAÑEZ and A. HOSPITALER. Fire behavior of axially loaded slender high strength concrete-filled tubular columns. *Journal of Constructional Steel Research,* vol. 67, no. 12, p. 1953-1965, 2011.

[77] RENAUD, C. and J. KRUPPA. Unprotected concrete filled columns fire tests - verification of 15Q. CIDECT Research Project 15R., Saint-Rémy-lès-Chevreuse, France: Centre Technique Industriel de la Construction Métallique (CTICM), 2004.

[78] RENAUD, C., D. JOYEUX and J. KRUPPA, Improvement and extension of the simple calculation method for fire resistance of unprotected

concrete filled hollow columns. CIDECT Research Project 15Q-12/03, Saint-Rémy-lès-Chevreuse, France: Centre Technique Industriel de la Construction Métallique (CTICM), 2004.

[79] HAN, L., X. ZHAO, Y. YANG and J. FENG. Experimental study and calculation of fire resistance of concrete-filled hollow steel columns. *Journal of Structural Engineering,* vol. 129, no. 3, p. 346-356, 2003.

[80] LU, H., X. L. ZHAO and L. H. HAN. Fire behaviour of high strength self-consolidating concrete filled steel tubular stub columns. *Journal of Constructional Steel Research,* vol. 65, no. 10-11, p. 1995-2010, 2009.

[81] MOLINER, V., A. ESPINOS, M. ROMERO and A. HOSPITALER. Fire behavior of eccentrically loaded slender high strength concrete-filled tubular columns. *Journal of Constructional Steel Research,* vol. 83, p. 137-146, 2013.

[82] SCHAUMANN, P., V. KODUR and O. BAHR. Fire behaviour of hollow structural section steel columns filled with high strength concrete. Journal of Constructional Steel Research, vol. 65, no. 8-9, p. 1794–1802, 2009.

[83] CEN, EN 1994-1-2, Eurocode 4: Design of composite steel and concrete structures. Part 1-2: General rules – Structural fire design., Brussels: CEN, 2005.

[84] KIM, S., K. S.YOM and S. CHOI. Evaluation of the fire resistance performance of interior anchor type CFT columns through loaded heating test. *International Journal of High-Rise Buildings*, vol. 2, no. 1, p. 39-48, 2013.

[85] KINOSHITA, T., Y. SHINTANI, T. OKAZAKI, T. NISHIMURA and R. LIEW. Effect of steel-fiber reinforced concrete on the fire resistance of concrete-filled steel tubular columns under simultaneous axial loading and double curvature bending. *SiF 2020 - The 11th International Conference on Structures in Fire*, The University of Queensland, Brisbane, Australia, 2020.

[86] WANG, Y. C. The effects of structural continuity on the fire resistance of concrete filled columns in non-sway frames. *Journal of Constructional Steel Research,* vol. 50, p. 177-197, 1999.

[87] BAILEY, C. G. Effective lengths of concrete-filled steel square hollow sections in fire. *Structures & Buildings,* vol. 140, no. 2, p. 169-178, 2000.

[88] ZHA, X. FE analysis of fire resistance of concrete filled CHS columns. *Journal of Constructional Steel Research,* vol. 59, p. 769-779, 2003.

[89] HONG, S. and A. H. VARMA. Analytical modeling of the standard fire behavior of loaded CFT columns. *Journal of Constructional Steel Research,* vol. 65, p. 54-69, 2009.

[90] POH, K. Stress–strain–temperature relationships for structural steel. *Journal of Materials in Civil Engineering,* vol. 13, no. 5, p. 371-379, 2001.

[91] SONG, T.Y. and L.H. HAN. H.X. YU. Concrete filled steel tube stub columns under combined temperature and loading. *Journal of Constructional Steel Research,* vol. 66, p. 369-384, 2010.

[92] ESPINOS, A., M. L. ROMERO and A. HOSPITALER. Advanced model for predicting the fire response of concrete filled tubular columns. *Journal of Constructional Steel Research,* vol. 66, p. 1030-1046, 2010.

[93] FELLOUH, A., A. BOUGARA and P. PILOTO. Fire resistance of partially encased composite columns subjected to eccentric loading. *Journal of Structural Fire Engineering,* vol. 09, p. 57, 2022.

[94] KINOSHITA, T., Y. SHINTANI, T. OKAZAKI, T. NISHIMURA and R. LIEW. Effect of steel-fiber reinforced concrete on the fire resistance of concrete-filled steel tubular columns under simultaneous axial loading and double curvature bending. SiF 2020 - The 11th International Conference on Structures in Fire, The University of Queensland, Brisbane, Australia, 2020.

[95] MARAR, K., Ö. EREN and İ. YITMEN. Compression Specific Toughness of Normal Strength Steel Fiber Reinforced Concrete (NSSFRC) and High

Strength Steel Fiber Reinforced Concrete (HSSFRC). Materials Research, vol. 12, no. 2, p. 239-247, 2011.

[96] LEE, S. C., J. Y. CHO and F. J. VECCHIO. Simplified Diverse Embedment Model for Steel Fiber Reinforced Concrete Elements in Tension. ACI MATERIALS JOURNAL, vol. 110, no. 4, p. 403-412, 2013.

[97] LIE, T. Fire resistance of circular steel columns filled with bar-reinforced concrete. Journal of Structural Engineering (ASCE), vol. 120, no. 5, p. 1489-1509, 1994.

[98] ESPINOS, A., M. L. ROMERO and A. HOSPITALER. Advanced model for predicting the fire response of concrete filled tubular columns. Journal of Constructional Steel Research, vol. 66, p. 1030-1046, 2010.

[99] HICKS, H. D. Confinement of Fire in Buildings. Fire Protection Handbook, 19th ed., National Fire Protection Association, Quincy, MA, p. 12-93 – 12-112, 2003.

[100] BSI. BS5400, PART 5: Code of practice for design of composite bridges. London, 2005.

[101] DBJ13-51. Technical specification for concrete-filled steel tubular structures. *Fuzhou,* 2003.

[102] KODUR, V. K. R. Performance-based fire resistance design of concrete-filled steel columns. *Journal of Constructional Steel Research,* vol. 51, no. 1, p. 21-26, 1999.

[103] WANG, Y.C. Some Considerations in the Design of Unprotected Concrete-Filled Steel Tubular Columns Under Fire Conditions. *Journal of Constructional Steel Research*, vol.44, p. 203–223, 1997.

[104] HAN, L-H. and J-S. HUO. Concrete-filled hollow structural steel columns after exposure to ISO-834 fire standard. *Journal of Structural Engineering (ASCE)*, vol. 129, p. 68-78, 2003.

[105] KODUR, V.K.R. and D.H. MACKINNON. Simplified design of concrete-filled hollow structural steel columns for fire endurance. *Journal of Constructional Steel Research*, vol. 46, p. 298–301, 1998.

[106] ASCE/SFPE 29-99: Standard Calculation Method for Structural Fire Protection. Reston, USA: American Society of Civil Engineers, 1999.

[107] ACI 216.16-07: Standard Method for Determining Fire Resistance of Concrete and Masonry Construction Assemblies. Detroit, USA: American Concrete Institute, 2007.

[108] PARK, S., S. CHOI and K. CHUNG. A study on the fire-resistance of concrete-filled steel square tube columns without fire protection under constant central axial loads. *Steel and Composite Structures*, vol. 8, p. 491-510, 2008.

[109] CEN, EN 1994-1-1, Eurocode 4: Design of composite steel and concrete structures - Part 1-1: General rules and rules for buildings, Brussels: CEN, 2004.

[110] WANG, R., C. ZHANG AND G. LI. Simple approach for performance-based fire safety design of circular CFT columns in large enclosure. Advanced Steel Construction, vol.12, No.1, p.32-43, 2016.

[111] ESPINÓS, A. Numerical analysis of the fire resistance of circular and elliptical slender concrete filled tubular columns, Ph.D. Thesis, Valencia (Spain): Universitat Politecnica de Valencia, 2013.

[112] CEN, EN 1993-1-1, Eurocode 3: Design of steel structures - Part 1-1: General rules and rules for buildings, Brussels: CEN, 2005.

[113] PRYL, D. and J. ČERVENKA. ATENA Program Documentation Part 11 Troubleshooting Manual. 23 9 2020. [Online]. Available: https://www.cervenka.cz/ assets/files/atena-pdf/ATENA-Troubleshooting.pdf. [Accessed 25 06 2022].

AUTHOR‘S PUBLICATIONS RELATED TO THE THESIS

Journal papers

[114] TRETYAKOV, A., I. TKALENKO, and F. WALD. Fire response model of the steel fibre reinforced concrete filled tubular column. Journal of Constructional Steel Research. 2021, 186, p 1 18. ISSN 1873-5983. DOI 10.1016/j.jcsr.2021.106884.

[115] TKALENKO I., A. TRETYAKOV, and F. WALD. Analytical model of the mechanical behaviour of the steel fibre reinforced concrete filled tubular

column in fire. *Journal of Constructional Steel Research*. Completed, 2022.

Conference papers

[116] TKALENKO, I. Experimental and numerical study of behaviour of steel and fibre concrete columns at elevated temperature. In: Studnička, J. and J. Fíla, eds*. Sborník semináře doktorandů katedry ocelových a dřevěných konstrukcí 13.2. a 20.9. 2018*. Praha: ČVUT, Fakulta stavební, Katedra ocelových a dřevěných konstrukcí, 2018. p. 51-56. ISBN 978-80-01-06448-1.

[117] ARHA, T., V. KŘÍSTEK, A. TRETYAKOV, BLESÁK L., TKALENKO, F. WALD, J. NOVÁK, R. ŠTEFAN and A. KOHOUTKOVÁ. To shear failure of steel and fibre-reinforced concrete circular hollow section composite column at elevated temperature. In: *12th international conference on 'Advances in Steel-Concrete Composite Structures' - ASCCS 2018*. Valencia, 2018-06-27/2018-06-29. Valencia: Editorial Universitat Politècnica de València, 2018. p. 863-869. ISBN 9788490486016.

[118] TKALENKO, I., A. TRETYAKOV, F. WALD, T. ARHA, J. NOVÁK, R. ŠTEFAN and A. KOHOUTKOVÁ. Bending Resistance of the Steel and Fibre-Reinforced Concrete Circular Hollow Section Composite Column in Fire. In: *3rd R N Raikar Conference*. Mumbai: India Chapter of American Concrete Institute, 2018. p. 546-553.

[119] TKALENKO, I., A. TRETYAKOV, F. WALD, J. NOVÁK, R. ŠTEFAN and A. KOHOUTKOVÁ. The steel and fibre-reinforced concrete circular hollow section composite column exposed to fire. In: Eurosteel 2017. Eurosteel 2017, Copenhagen, Copenhagen, 2017-09-13/2017-09-15. Berlin: Ernst & Sohn, 2017. p. 2678-2687. ISSN 2509-7075. DOI 10.1002/cepa.317.

[120] TKALENKO, I. Experimental study on behaviour of composite steel and fibre-concrete columns at elevated temperature. In: Studnička, J. and J. Fíla, eds*. Sborník semináře doktorandů katedry ocelových a dřevěných konstrukcí 16.2. a 26.9. 2017.* Praha: ČVUT, Fakulta stavební, Katedra ocelových a dřevěných konstrukcí, 2017. p. 31-34. ISBN 978-80-01-06167-1.

[121] TRETYAKOV, A., I. TKALENKO, F. WALD, J. NOVÁK, R. ŠTEFAN and A. KOHOUTKOVÁ. Flexural stiffness of the composite steel and fibre-reinforced concrete circular hollow section column. In: Broukalová, I., et al., eds. *Fibre Concrete 2017*. Praha, 2017-09-13/2017-09-16. Bristol: IOP Publishing Ltd, 2017. IOP Conference Series: Materials Science and Engineering. vol. 246. ISSN 1757-899X. DOI 10.1088/1757-899X/246/1/012021.

[122] TRETYAKOV, A., I. TKALENKO, F. WALD, J. NOVÁK, R. ŠTEFAN and A. KOHOUTKOVÁ. To fire resistance of the steel and fibre-reinforced concrete circular hollow section column. In: GILLIE, M and Y WANG, eds. *Applications of Fire Engineering. Applications of Structural Fire Engineering*, Manchester, 2017-09-07/2017-09-08. Leiden: CRC Press/Balkema, 2017. p.73-79.ISBN978-1-138-09291-4.

[123] TKALENKO, I. Behaviour of Composite Steel and Fibre-concrete Columns at Elevated Temperature. In: Studnička, J. and J. Fíla, eds*. Sborník semináře doktorandů katedry ocelových a dřevěných konstrukcí 18.2. a 22.9. 2016.* Praha: ČVUT, Fakulta stavební, Katedra ocelových a dřevěných konstrukcí, 2016. pp. 15-16. ISBN 978-80-01-05963-0.